Lawrence Berkeley National Laboratory
Recent Work

Title
APPLIED BATTERY AND ELECTROCHEMICAL RESEARCH PROGRAM REPORT FOR 1981

Permalink
https://escholarship.org/uc/item/7v8038dq

Author
Cairns, E.

Publication Date
1982-06-01

Lawrence Berkeley Laboratory

UNIVERSITY OF CALIFORNIA

ENERGY & ENVIRONMENT DIVISION

APPLIED BATTERY AND ELECTROCHEMICAL RESEARCH PROGRAM
REPORT FOR 1981

Elton Cairns, Lutgard DeJonghe, James Evans,
Rolf Muller, John Newman, Philip Ross,
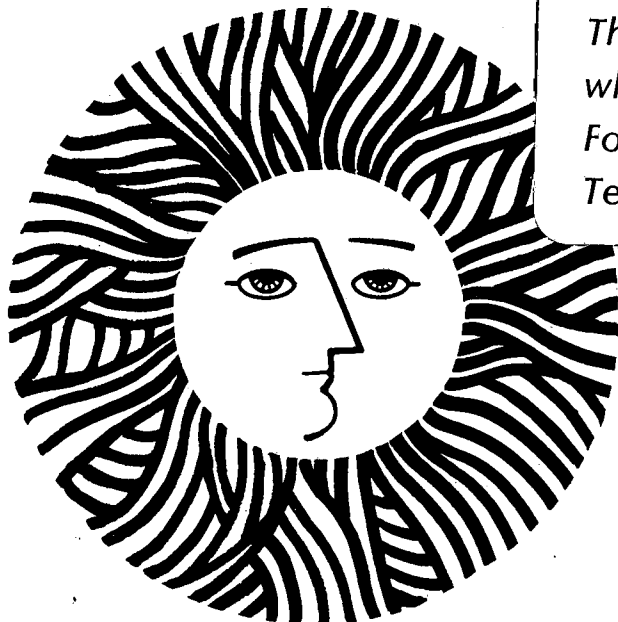Charles Tobias and Frank McLarnon

June 1982

DISCLAIMER

APPLIED BATTERY AND ELECTROCHEMICAL RESEARCH PROGRAM

REPORT FOR 1981

Energy & Environment Division
Lawrence Berkeley Laboratory
University of California
Berkeley, California 94720

Prepared by Frank McLarnon, Program Manager

Program Participants:

Elton Cairns[1]
Lutgard DeJonghe[2]
James Evans[2]
Rolf Muller[2]
John Newman[2]
Philip Ross[2]
Charles Tobias[2]

June 1, 1982

[1] Head, Energy & Environment Division

[2] Materials and Molecular Research Division, Alan Searcy, Division Head

CONTENTS

Lawrence Berkeley Laboratory (LBL) is a lead laboratory for management of the Applied Battery and Electrochemical Research Program, which provides supporting research for the Department of Energy (DOE) Electrochemical Systems research programs. The general objective of this program is to help provide advanced electrochemical systems that can satisfy stringent performance and economic requirements for electric vehicle and stationary energy storage applications. The specific goal of the program is to identify the most promising electrochemical technologies and transfer them to industry and/or another DOE program for further development and scale-up.

General problem areas addressed by the program include identification of new electrochemical couples for advanced batteries, determination of technical feasibility of new couples, improvements in battery components, and establishment of engineering principles applicable to batteries and electrochemical processes. Major emphasis is given to applied research that will lead to superior performance and lower life-cycle costs. The program is divided into four major areas: Exploratory Battery R & D, Engineering-Science Research, Materials Research, and Electrolytic Processes.

ACCOMPLISHMENTS DURING 1981

LBL monitored 35 research subcontracts during Fiscal Year 1981 and conducted a vigorous in-house research program on Electrochemical Energy Storage, also summarized in this report.

Exploratory Battery R & D

The objective of this program element is to identify, evaluate, and initiate development of new electrochemical couples with the potential to meet or exceed advanced system performance goals. Efforts are focused on systems that promise high specific energy, high specific power, and extended lifetime. Also included are studies on molten-salt cells that operate at temperatures lower than certain high-performance systems, such as Na/S and Li/FeS_x.

1. Management responsibility for the ambient-temperature $Zn/NaOH/Fe(CN)_6^{3-}$ hybrid redox system, which offers energy and power densities superior to those of other redox systems, was transferred to Sandia National Laboratories for further development and scale-up.

2. The high-temperature $Ca/molten\ salt/FeS_2$ system was shown to have adequate (but not superior) performance, and no further development work is planned at this time. This work demonstrated the feasibility of substituting abundant Ca for Li in the Li/FeS_x battery.

3. Work continued on the ambinet-temperature $Li/SO_2/C$ system, which promises specific energy and power values comparable to those of high-temperature batteries. Reversible chemistry for the $Li/SO_2/C$ cell was established.

3

4. Exploration of the new intermediate-temperature Na/β''-Al$_2$O$_3$/NaNO$_3$ system was initiated. This cell, like the Na/β''-Al$_2$O$_3$/SCl$_4$-AlCl$_3$-NaCl cell, may operate at approximately 200°C and exhibit corrosion problems less severe than those in the 300°C Na/S battery.

Engineering-Science Research

The aim of this program element is to establish an electrochemical scientific and engineering base that will lead to improvements in battery and electrochemical system performance lifetime and costs.

1. Structural, optical, thermodynamic, and electrical studies of battery electrodes continued. These efforts are providing improved understanding of the chemical and physical changes that occur in operating Zn/NiOOH, Fe/NiOOH, Al/air, and redox systems.

2. Investigations of new electrode/electrolyte formulations and novel separators for the Zn/NiOOH battery continued. The primary aim is to identify practical means of improving the lifetime of this promising battery.

3. Studies of transport processes and measurements of transport properties in Zn/halogen flow systems were initiated. These investigations will provide the data necessary to optimize Zn/halogen system designs.

4. Calorimetry provided extremely accurate measurements of thermal energy generation rates in high-temperature Li/FeS cells, and the resulting information will lead to a workable strategy for thermal management of this high-temperature system.

5. Measurements of composition profiles in Li/FeS and Zn/NiOOH systems lacked sufficient accuracy to warrant continuing efforts.

6. Investigations of new components for photoelectrochemical energy storage cells were initiated. Amorphous boron photoelectrodes, photointercalation compounds, and antimony redox couples are being studied.

Materials Research

The goal of this program element is to identify, characterize, and improve materials and components for use in batteries and electrochemical processes.

1. NASICON ($Na_{1+x}Zr_2Si_xP_{3-x}O_{12}$) ceramic electrolyte was originally considered to offer great promise as an easily fabricated alternative to β''-Al$_2$O$_3$, the electrolyte employed in Na/S batteries. However, it was shown to be unstable in molten Na at 300°C, and no further development work for high-temperature applications is planned. Rather, efforts will be focused on materials research and electrochemical compatibility of new compositions.

2. A novel technique to fabricate thin-walled β''-Al_2O_3 tubes by a tape-wrapping process was shown to be feasible and potentially competitive with conventional methods.

3. Electrical properties of fast lithium-ion-conducting glasses ($\sigma_{300} \approx 10^{-2}$ ohm^{-1} cm^{-1}) in the Li_2O-$(LiCl)_2$-B_2O_3 system have been measured and correlated with glass composition and structure. Several of these glasses may be suitable as electrolytes for extremely high performance Li/S cells.

4. New ceramic systems, including several NASICON-like structures, have been found to display fast ion conduction. It is hoped that one or more of these structures will be an attractive alternative to β''-Al_2O_3.

5. Work on intermediate-temperature $LiNO_3$-KNO_3 molten salt electrolytes, novel all-solid composite microstructure electrodes (e.g., Li alloy dispersed in a metallic matrix), and ternary lithium-metal oxide positive electrodes has continued. These components promise stability superior to those presently employed in Li/FeS_x batteries.

6. It was demonstrated that the polymer film polyethylene oxide-lithium trifluoracetate is, in fact, a solid electrolyte that conducts Li ions ($\sigma_{140} \approx 10^{-4}$ ohm^{-1} cm^{-1}). Small quantitites of water vapor absorbed by the films increase their ionic conductivities by 2 orders of magnitude to values in agreement with prior measurements. This material is a candidate electrolyte for rechargeable ambient-temperature Li/TiS_2 cells.

7. Work on novel Li- and Na-ion-conducting membranes continued.

Management Activities

1. An annual LBL Electrochemical Contractors' Meeting was held in Berkeley, California, on December 15 - 16, 1981. The agenda is included as an Appendix.

2. A workshop addressing the research needs of the zinc/nickel oxide battery was held in Emeryville, California, on December 17, 1981.

3. A review of the Applied Battery and Electrochemical Research Program was held in Washington, D.C., on October 6, 1981.

PLANNED ACTIVITIES FOR FY 1982

The scope of LBL's management responsibilities will be expanded to the role of Lead Center for the Technology Base Research (TBR) project. The TBR Project includes four major elements:

1. Electrochemical Systems Research
   a. Exploratory Battery R & D*
   b. Metal/Air Systems
      (managed by Lawrence Livermore National Laboratory)

2. Supporting Research
   a. Engineering-Science Research*
   b. Materials Research*
   c. Molten Salt Cell Research
   d. Systems Analysis

3. Fuel Cells for Transportation Application
   (managed by Los Alamos National Laboratory)

4. Electrochemical Processes

A TBR Project summary for calendar year 1981 (LBL-14305) has been compiled and is available from the Program Manager.

New research projects planned for FY 1982 include:

1. Research on rechargeable ambient-temperature lithium cells.

2. Application of transformation toughening to improve the stability of β''-Al_2O_3 ceramic electrolytes.

3. Investigation of transition metal macrocyclic complexes as catalysts for fuel cell air electrodes.

The LBL scientists who participate in the program are: E. J. Cairns, L. C. DeJonghe,[†] J. W. Evans,[†] F. R. McLarnon, R. H. Muller,[†] J. S. Newman,[†] P. N. Ross,[†] and C. W. Tobias.[†]

---

*Included in FY 1981 responsibilities.

[†]Materials and Molecular Research Division of the Lawrence Berkeley Laboratory.

II. EXPLORATORY BATTERY RESEARCH
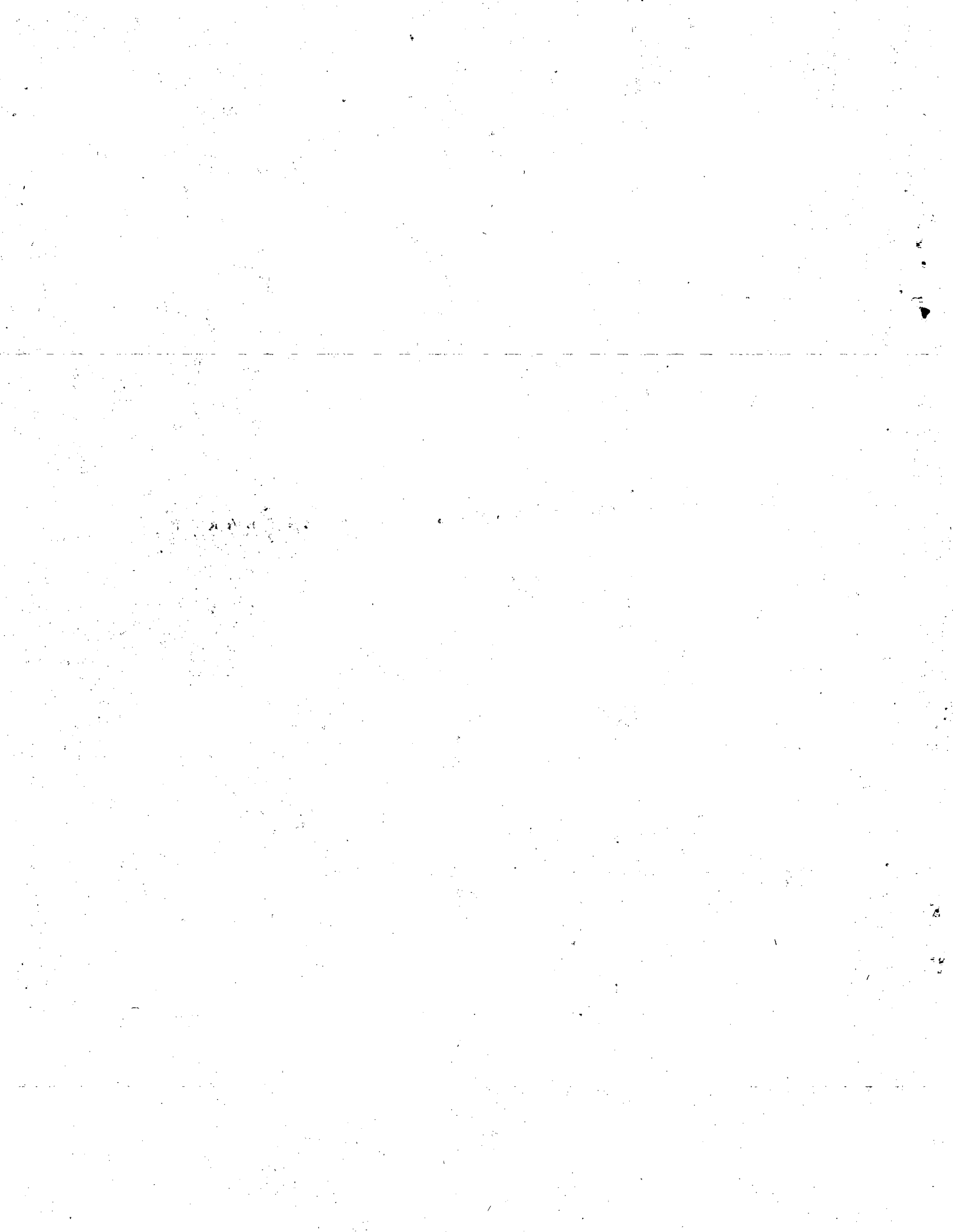
A. STUDY OF HIGH-ENERGY CATHODES AND ANODES FOR MOLTEN SALT BATTERIES

DOE Program Manager • A. R. Landgrebe

LBL Project Manager • E. Cairns

LBL Subcontractor • University of Tennessee (G. Mamantov)

B&R Number • AL-05-10-05

Contract Value • 74K

Contract Number • 4502810

Contract Term • October 1, 1980 – September 30, 1981

Reporting Period • October 1, 1980 – September 30, 1981

Objectives • Investigate electrochemical and chemical processes that determine the operation of the Na/S(IV) cell in molten $AlCl_3-NaCl$

• Evaluate this cell as an intermediate-temperature alternative to the Na/S battery

This program is concerned with the research and development of a rechargeable low-temperature molten salt cell:

$$Na/Na^+ \text{ conductor}/SCl_3^+ \text{ in molten chloroaluminates.}$$

The cell operates at 180-250°C (the lower temperature limit is primarily determined by the resistance of β''-alumina, the usual Na^+ conductor) and has an open circuit voltage of 4.2 V.

Studies during the past year have involved laboratory cell (both glass and metal) development, Raman spectroscopic studies of a cell during discharge and charge, a study of polarization at the sodium/β''-alumina and molten salt/β''-alumina interfaces, and an examination of the electro-oxidation of sulfur in chloroaluminate melts of intermediate pCl.

In some of the cells, the positive electrode was placed inside the β''-alumina tube and the sodium metal was placed outside. The performance of one of these cells, operated at 225°C using current densities of 30 and 15 mA/cm^2 for discharge and charge, respectively, is illustrated in Figs. 1 and 2. The operation of this cell was interrupted three times, and the cell was frozen each time; no appreciable change in performance was observed after the interruptions. A shift in the charge curves toward higher voltage was
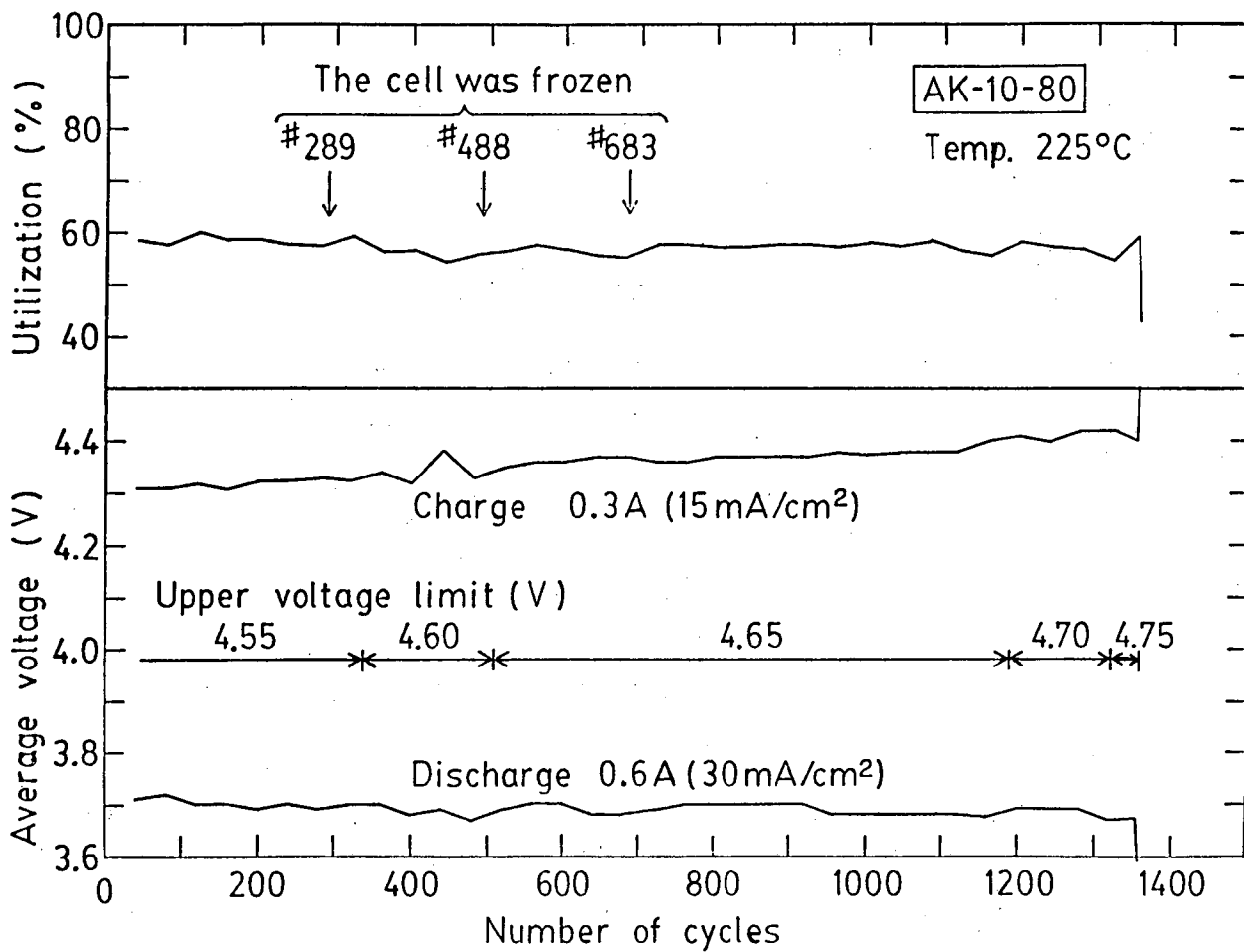
Fig. 1. Performance of a rechargeable molten salt cell operated at 225°C. Current densities were 15 mA/cm² for charge and 30 mA/cm² for discharge.
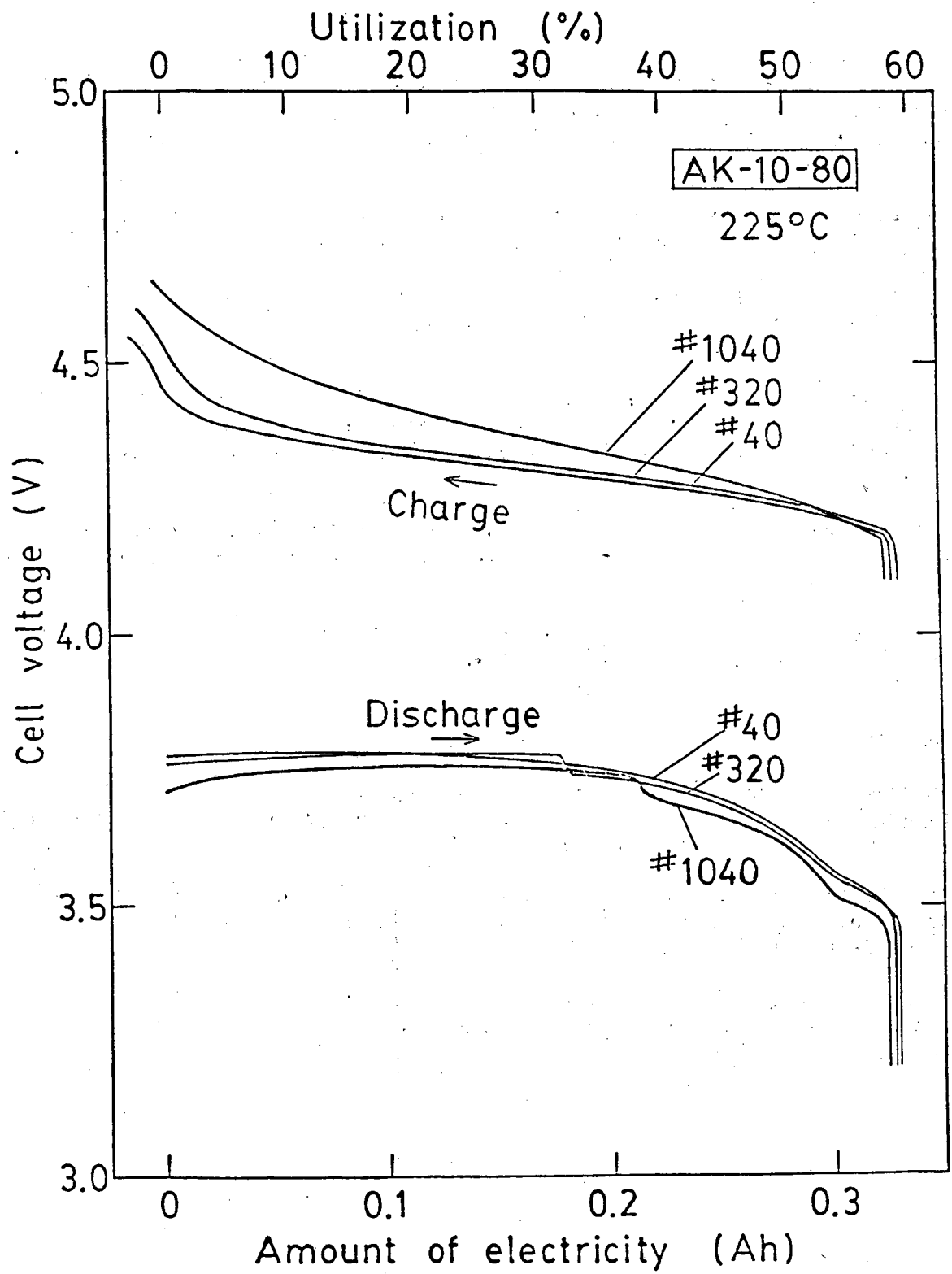
Fig. 2. Performance of same cell as in Fig. 1: utilization and amount of electricity plotted against cell voltage. Operating temperature 225°C.

observed as the number of cycles increased, although the discharge curves remained almost unchanged. This cell was terminated after 1376 cycles because of a leak in the tungsten current collector (positive electrode) - glass seal. The same leakage problem has caused the termination of most previous laboratory cells.

Another cell, equipped with a reticulated vitreous carbon current collector and rich in SCl_3AlCl_4, was used to study both discharge steps ($S(IV) \rightleftarrows S(0)$ and $S(0) \rightleftarrows S^{2-}$). The reversibility of the second step was much better than that obtained in prior cells. An overall energy density of 457 Wh/kg (at 21 mA/cm^2 and 200°C) was obtained (the theoretical energy density for this cell is 703 Wh/kg).

Raman spectroscopic studies performed on a cell undergoing discharge and charge have provided excellent evidence for the presence of SCl_3^+, S_8, $(AlSCl)_n$, and $(AlSCl_2)_n^{n-}$. Assignment of several other bands must await additional studies.

We have recently demonstrated that the main source of polarization in this cell is at the β''-alumina/molten salt interface. Further polarization studies are in progress.

A paper on the oxidation of sulfur in chloroaluminate melts of intermediate pCl has been submitted to the Journal of the Electrochemical Society.

PUBLICATIONS

G. Mamantov, R. Marassi, M. Matsunaga, Y. Ogata, J. P. Wiaux, and E. J. Frazer, "The Use of Tetravalent Sulfur in Molten Chloroaluminate Secondary Batteries," J. Electrochem. Soc., <u>137</u>, 2319 (1980).

G. Mamantov, "Molten Salt Electrolytes in Secondary Batteries," in <u>Materials for Advanced Batteries</u>, D. W. Murphy, J. Broadhead, and B.C.H. Steele, eds., Plenum Press, 1980, pp. 111-122.

V. E. Norvell, K. Tanemoto, G. Mamantov, and L. Klatt, "UV-Visible and Electron Spin Resonance Spectroelectrochemical Studies of Sulfur Oxidation in $AlCl_3$-NaCl (63/37 Mole %) Melt," J. Electrochem. Soc., <u>128</u>, 1254 (1981).

B. SODIUM/ALKALI NITRATE AND CALCIUM/IRON DISULFIDE SECONDARY CELLS

DOE Program Manager • P. N. Ross

LBL Subcontractor • Argonne National Laboratory (M. F. Roche)

B&R Number • AL-05-10-05

Contract Value • 370K

Contract Number • 4505310

Contract Term • October 1, 1980 - September 30, 1981

Reporting Period • November 1, 1980 - November 1, 1981

Objectives • Evaluate inexpensive, high-performance
molten salt batteries

• Complete the evaluation of Ca/FeS_2
cells as a low-cost alternative to the
Li/FeS_x battery

• Evaluate sodium/alkali nitrate cells as
an intermediate-temperature alternative
to the Na/S battery

The objective of this program is to determine the technical feasibility of new electrochemical couples for advanced secondary batteries. At present, we are concluding studies of the calcium/iron disulfide cell, and we have begun an investigation of alkali-nitrate positive electrodes for sodium cells.

The calcium/iron disulfide cell[1,2] employs $CaAl_{1.2}Si_{0.4}$ negative electrodes, $Fe_{0.93}Co_{0.07}S_2$ positive electrodes, and $LiCl-NaCl-CaCl_2-BaCl_2$ (mp 383°C) electrolyte. The electrodes are separated by layers of BN felt, and the current collectors are iron (negative electrode) and molybdenum (positive electrode). This cell, which is operated at 475°C, has been shown to be capable of high specific energy and power[2]; multiplate cells containing 33 wt% active material will yield over 120 Wh/kg and 170 W/kg. However, declining coulombic efficiency presently limits the cell cycle life to about 300 cycles (one-half year of accelerated testing). This coulombic efficiency problem is caused by contamination of the BN felt separator by the electrode materials, which become very finely divided (less than 10 microns diameter) during extended cycling. To retain such materials in the electrodes, it will be necessary to develop a separator having a less open structure than the BN felt currently available. Powder separators such as MgO offer one possible solution to this problem.

The sodium/alkali nitrate cells employ molten sodium negative electrodes, β''-alumina electrolytes (Ceramatec), and molten alkali-nitrate positive electrodes. The overall cell reaction can be represented as:

$$2Na + MNO_3 \longrightarrow Na_2O + MNO_3 \quad ,$$
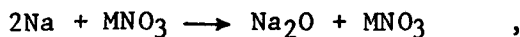
where MNO_3 is the alkali nitrate and MNO_2 is the corresponding nitrite. We have conducted preliminary cycling tests with MNO_3 being $NaNO_3$ (mp 307°C), $LiNO_3$ (mp 256°C), or the $NaNO_3$ – $LiNo_3$ eutectic (mp 196°C). In these tests, the $NaNO_3$ electrode has been cycled at 330°C for 14 cycles (500 h) with an average utilization of about 40% per cycle. The type 304 stainless steel current collector in this 1.75-V cell was severely corroded; Na_3CrO_4 and Na_4CrO_4 were afterwards detected by x-ray diffraction of the $NaNO_3$. Similarly, the $NaNO_3$–$LiNO_3$ eutectic electrode was cycled at 206°C for 14 cycles (700 h) with an average utilization of about 25%. The nickel screen current collector in this 1.62-V cell was oxidized to some extent, but it continued to function well. The $LiNO_3$ electrodes, using the Ni screen current collector and a temperature of 260°C, have generally failed within one cycle because of fracture of the β'' tubes. Ion microprobe profiles have revealed a significant increase in the ratio of lithium to sodium in the fracture areas of these tubes.

These preliminary tests have demonstrated the rechargeability of certain alkali nitrate electrodes, but they have also indicated the need for detailed fundamental studies directed toward optimization of the alkali nitrate mixture and the current collector.

REFERENCES

1. D. L. Barney, M. F. Roche, S. K. Preto, L. E. Ross, N. C. Otto, and F. J. Martino, "Calcium/Metal Sulfide Battery Development Program, Progress Report for October 1979 – September 1980," Argonne National Laboratory Report ANL-81-14 (March 1981).

2. S. K. Preto, L. E. Ross, N. C. Otto, J. F. Lomax, and M. F. Roche, in Proceedings of the 16th Intersociety Energy Conversion Engineering Conference, American Society of Mechanical Engineers, New York, 1981, pp. 765-768.

C. PERFORMANCE CHARACTERIZATION OF A SOLID-STATE STORAGE BATTERY

DOE Program Manager • A. R. Landgrebe

LBL Project Manager • P. N. Ross

LBL Subcontractor • Duracell, Inc. (A. N. Dey)

B&R Number • AL-05-10-05

Contract Value • 199K

Contract Number • 4504310

Contract Term • April 1, 1980 – May 1, 1981

Reporting Period • April 1, 1980 – May 1, 1981

Objective • Fundamental investigation of the
electrode materials, electrolyte and
electrode/electrolyte interfaces in a
solid-state storage battery based on the
systems Li alloy/LiI·Al_2O_3/metal
sulfides

The performance of the totally solid Li-alloy/LiI(Al_2O_3)/metal sulfides energy storage system was improved. Limited positive-electrode cells, of 400 mAh and 1 Ah capacity, were used to study the charge/discharge characteristics of sulfide-based systems. Cycle life was lengthened to nearly 500 deep discharge cycles at 50-65% of stoichiometric capacity. High coulombic efficiency, 99-100%, was demonstrated throughout cycle life, at energy efficiencies of 84-87% at a current density of 5 mA/cm^2 or C/10 rate. Negative electrode modification enabled 45-55% capacity utilization at a current density of 10 mA/cm^2 or C/5 rate of discharge. Peak power density observed was 220-340 W/kg (without packaging) at full charge and 100-200 W/kg at half charge.

Major improvements in the performance of a second positive-electrode system were made as well. Capacity utilization in excess of 50% of stoichiometric was attained at the 5 mA/cm^2 rate. The operating temperature range for this cell type was extended to 400°C, where stability was demonstrated for almost 200 cycles. Limited energy density data for unoptimized cells have exceeded that previously observed (120 Wh/kg versus 110 Wh/kg, packaging not included).

D. ALL-INORGANIC AMBIENT-TEMPERATURE LITHIUM BATTERY

DOE Program Manager • A. R. Landgrebe

LBL Project Manager • P. N. Ross

LBL Subcontractor • Duracell, Inc. (A. N. Dey)

B&R Number • AL-05-10-05

Contract Value • 59K

Contract Number • 4507410

Contract Term • June 1, 1980 - November 30, 1980

Reporting Period • June 1, 1980 - November 30, 1980

Objectives • Evaluate the all-inorganic Li/SO_2 rechargeable battery for energy storage applications

• Investigate alternate cathode materials to extend cell lifetime, and search for alternate electrolytes lower in cost than the $Li_2B_{10}Cl_{10}-SO_2$ presently employed

We made all-inorganic Li/SO_2 prototype rechargeable D cells with reference electrodes and demonstrated that SO_2 is deposited quantitatively in the catalytic carbon cathode as lithium dithionite ($Li_2S_2O_4$) during cell discharge. We demonstrated that the $Li_2S_2O_4$ is then quantitatively oxidized to SO_2 during the recharge portion of the cell cycle, according to the overall reaction

$$2Li + 2SO_2 \rightleftharpoons Li_2S_2O_4 \quad .$$

We found that the electrolyte salt $Li_2B_{10}Cl_{10}$ is oxidized in solution at slightly over the recharge potential of Li/SO_2 to give a one-electron oxidation product. The oxidation product undergoes a further one-electron oxidation to give a second product at potentials greater than those attained in cell recharge.

E. STUDIES OF LITHIUM ANODES IN NONAQUEOUS ELECTROLYTES FOR AMBIENT-TEMPERATURE LITHIUM BATTERIES

DOE Program Manager • A. R. Landgrebe

LBL Project Manager • P. N. Ross

LBL Subcontractor • Electrochimica Corporation (M. Eisenberg)

B&R Number • AL-05-10-05

Contract Value • 82K

Contract Number • 4507210

Contract Term • May 30, 1980 – February 28, 1981

Reporting Period • May 30, 1980 – February 28, 1981

Objective • Determine the rechargeability of the lithium electrode in newly developed organic electrolytes

The objective of this eight-month program was a preliminary study of the electrochemical and morphological aspects of lithium anode rechargeability in organic-electrolyte ambient-temperature systems. It is increasingly recognized that the limited rechargeability of lithium anodes may have a serious effect on the future development and capabilities of ambient-temperature, high-energy secondary lithium batteries.

To provide a basis for future reliable evaluation of electrolyte systems, it was necessary to examine the technique of stripping efficiency studies for lithium with particular reference to the effect of substrates, amount of charge passed, current density, and other conditions. Next was a development of a technique for preparing lithium electrodes for electrodeposition for scanning electron microscopy (SEM) studies. With these techniques, a number of basic electrolyte systems were examined in order to elucidate the directions in which future efforts should be emphasized. Two additional techniques, capillary cells for microscopic observation of electrocrystallization of lithium and an apparatus for the analytical determination of the metallic lithium content on electrode surfaces, have been designed and worked on, but were not ready for employment at the conclusion of this effort.

PUBLICATION

M. Eisenberg, "Study of the Secondary Li Electrode in Organic Electrolyte," Lawrence Berkeley Laboratory report LBL-13263, 1981.

F. RECHARGEABLE ALKALINE ZINC/FERRICYANIDE HYBRID REDOX BATTERY

DOE Program Manager • A. R. Landgrebe

LBL Project Manager • F. R. McLarnon

LBL Subcontractor • Lockheed Missiles & Space Company
(R. Hollandsworth)

B&R Number • AL-05-10-05

Contract Value • 120K

Contract Number • 4503710

Contract Term • April 1, 1980 - July 31, 1981

Reporting Period • November 1, 1980 - July 31, 1981

Objectives • Investigate the performance of cost-effective electrode substrates and separator materials

• Study the stability of the redox electrolyte

• Continue cell cyclic testing with improved instrumentation

This project was directed primarily at the technical advancement of key, economically-sensitive battery components for the alkaline zinc/ferricyanide rechargeable battery. The project should help assess the feasibility of using this battery for utility load leveling and other bulk electrical energy storage applications. During this second year of the contract (Phase 2), the problems of ferro-ferricyanide redox substrate selection, alternative zinc/zincate substrate evaluation, alternative low-cost separator selection, and methods for attaining zinc capacities of 300 mA h/cm^2 were studied in detail. In addition, the decomposition rate of alkaline ferricyanide was measured, and a preliminary mathematical model was developed. Cyclic cell test results indicate that by utilizing low-cost cell components, the performance of the alkaline zinc/ferricyanide system exceeds by 5 to 10% the originally proposed goal of 70% for turnaround energy efficiency.

Specifically, the following accomplishments are highlighted:

1. In full cell testing with graphite felt substrates for the ferro/ferricyanide couple, overall energy efficiency is 75% in 5N NaOH electrolyte at 40°C. Voltaic and coulombic efficiencies at 35 mA/cm^2 were 85 and 88%, respectively.

2. In full cell testing in 2$\underline{N}$ NaOH at 40°C, the mean energy efficiency is 79%, with voltaic and coulombic efficiencies each at 89%.

3. Cadmium, copper, and brass substrates for the zinc/zincate couple each demonstrate efficient operation (95-100% coulombic efficiency) in 2$\underline{N}$ and 5$\underline{N}$ NaOH electrolyte.

4. The cadmium substrate is best suited for the zinc/zincate half-cell based upon its resistance to anodic dissolution under conditions of cell reversal or deep discharge.

5. Zinc charge capacity of 300 mA·h/cm^2 has been demonstrated with over 240 four-hour cycles with a mean coulombic efficiency of 97.8 ± 1.8%. Tests at a capacity of 200 mA h/cm^2 over 260 cycles demonmstrated a mean coulombic efficiency of 97.4 ± 4.4%.

6. A moderately priced ($3.25/ft^2) separator (P-1010) from RAI Research Corporation has been selected for further evaluation. A full cell with the P-1010 separator displays a mean energy efficiency of 79%, with voltaic and coulombic efficiencies of 90 and 87%, respectively.

7. Current cycle life of the 1.5-mil-thick Teflon-based P-1010 separator is 120 four-hour cycles.

8. Seventeen separators ranging from microporous polyvinyl-chloride-based materials to cationic Teflon materials were evaluated, and critical resistivity and transference rates were identified.

9. The rate of ferricyanide decomposition in static testing in 5$\underline{N}$ sodium hydroxide electrolyte at 50°C in darkness was found to be less than 4% per year of the initial ferrocyanide capacity. On this basis, religation with cyanide to recover full capacity could be an annual maintenance procedure.

10. The microcomputer system to control and monitor battery testing was completely restructured to comprise two microcomputer systems operating in a master/slave configuration. The slave, programmed in assembly language, controls all battery-cycle functions via 12-bit analog data input and digital relay control output. The master computer, operating in BASIC, performs all data reduction, using floating-point math, and logs the reduced data to an HP-1000 mainframe computer for storage and graphics display.

11. A preliminary mathematical model developed for the battery system indicates that key areas for detailed investigation are optimization of mass transport at the porous redox electrode and dissolution/crystallization kinetics of the redox reactant/product.

PUBLICATION

G. B. Adams, R. P. Hollandsworth, and E. L. Littauer, "Rechargeable Alkaline Zinc/Ferricyanide Hybrid Redox Battery," Proceedings of the 16th Intersociety Energy Conversion Engineering Conference, Paper 819384, American Institute of Mechanical Engineers, New York, 1981, pp. 812-816.

III. ENGINEERING-SCIENCE RESEARCH

A. ELECTROCHEMICAL ENERGY STORAGE

DOE Program Manager	● A. R. Landgrebe
LBL Principal Investigators	● E. Cairns, L. DeJonghe, J. Evans, ● R. Muller, J. Newman, P. Ross, and C. Tobias
B&R Number	● AL-05-10-10
Contract Value	● 1220K
Contract Number	● DE-AC03-76SF00098
Contract Term	● October 1, 1980 - September 30, 1981
Reporting Period	● October 1, 1980 - September 30, 1981
Objective	● Improve the performance and durability and lower the costs of batteries and electrochemical processes employed in energy storage technologies
Progress	● Summaries for nine partially interdependent projects follow:

A.1 Surface Morphology of Metals in Electrodeposition

A.2 Metal Couples in Nonaqueous Solvents

A.3 Surface Layers on Battery Materials

A.4 Analysis and Simulation of Electrochemical Systems

A.5 Electrode Kinetics and Electrocatalysis

A.6 Electrochemical Properties of NASICON

A.7 Improvements in Efficiency of Aluminum Reduction Cells

A.8 Engineering Analysis of Gas Evolution in Electrolysis

A.9 Battery Electrode Studies

A.1 SURFACE MORPHOLOGY OF METALS IN ELECTRODEPOSITION

C. W. Tobias, Investigator

The objective of this project is to develop a pragmatic understanding of the partial processes governing the macrocrystallization of metals. This understanding is necessary for the design and optimization of metal deposition processes, including those in rechargeable galvanic cells. Current projects include: (a) the effect of hydrodynamic flow on the surface morphology of copper and zinc, and (b) dynamic modeling of surface profiles in electro-deposition and dissolution.

A.1.1 THE INFLUENCE OF LEAD IONS ON THE MACROMORPHOLOGY OF ELECTRODEPOSITED ZINC

T. Tsuda and C. W. Tobias

The morphology of zinc as it is electrodeposited from acid solutions demonstrates a remarkable imprint of electrolyte flow conditions. The development of macromorphology of zinc deposits under galvanostatic conditions on a rotating platinum disk electrode has been investigated by photomacrography, scanning electron microscopy (SEM), electron probe microanalysis, and Auger microprobe analysis.[1] Logarithmic spiral markings, which reflect the hydrodynamic flow on a rotating disk, appear in a certain region of current density well below the limiting current density (Fig. 1). Morphological observations revealed the major influence of trace lead ions on the amplification of surface roughness through coalescence and preferred growth of initial protrusions. Results obtained from ultrapure electrolyte suggest preferred crystal growth towards well-mixed regions of the concentration field caused by slight differences in crystallization overpotential. The spiral striations (Fig. 2) form by the following sequence: (1) nucleation and growth of nuclei; (2) coalescence of nuclei into larger protrusions; (3) preferential growth of larger protrusions; and (4) successive coalescence and consumption of smaller protrusions by larger ones.

The concentration field is disturbed by these protrusions acting as distributed roughness elements. Eventually, well-established secondary flows occur. Local eddy mixing is originated by protrusions, the heights of which reach a certain portion of the thickness of the diffusion boundary layer. Slight differences in zinc concentration result in slight differences in crystallization overpotential, causing enhanced crystal growth in well-mixed locations. Thus, connection of protrusions along spiral lines occur. Secondary flow occurs as connection of protrusions proceeds. Spiral ridges become more pronounced owing to mass transfer onto ridges rather than into recesses.

The role of major species (lead or hydrogen ions) may be summarized as follows: they (1) decrease the number of initial nucleation sites for zinc; (2) poison the platinum surface for hydrogen evolution, so that the whole
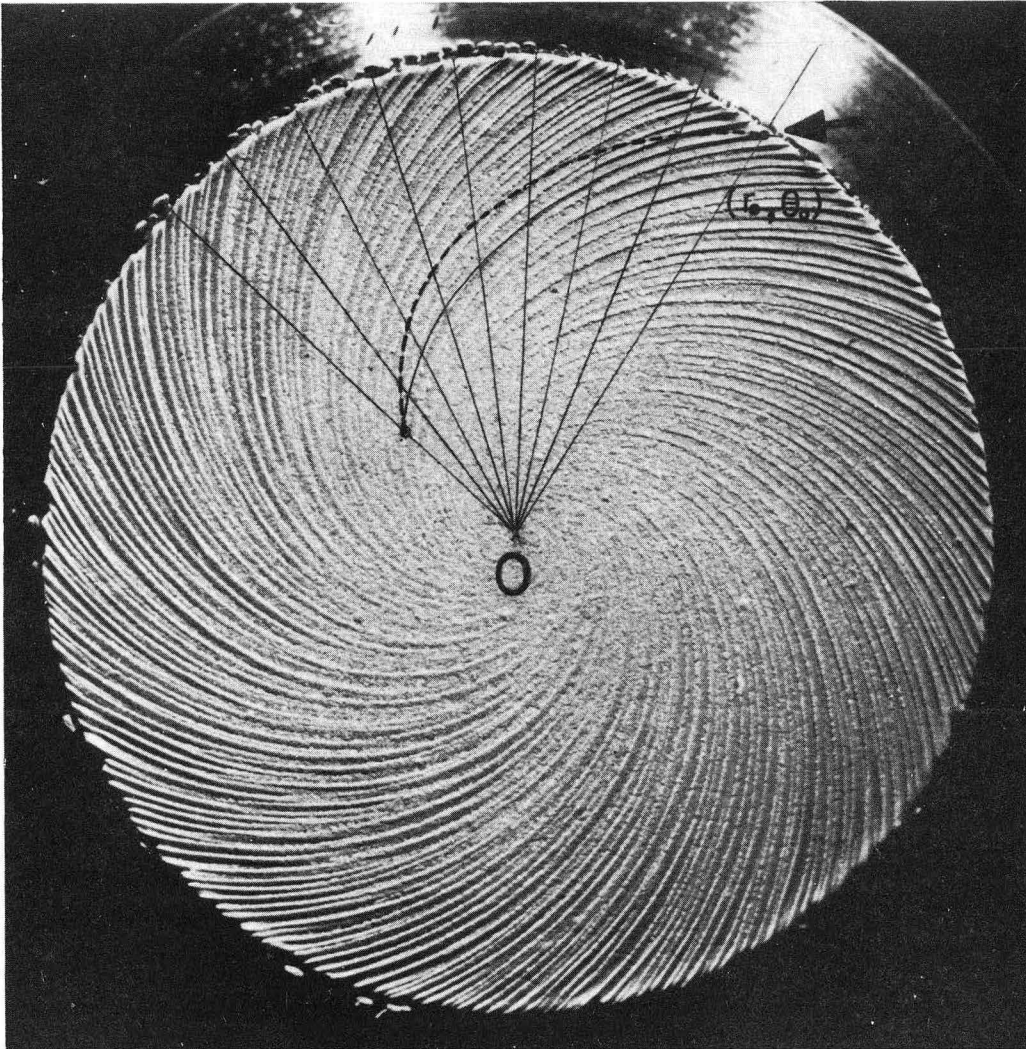
Fig. 1.   The dotted line is an Archimedes spiral described by $\theta - \theta_0 = 0.0304 \ (r - r_0)$.   The fine solid curve is a logarithmic spiral described by $\theta - \theta_0 = 1.25 \ \ln r/r_0$.   Note that the Archimedes spiral deviates greatly from the striation.

25
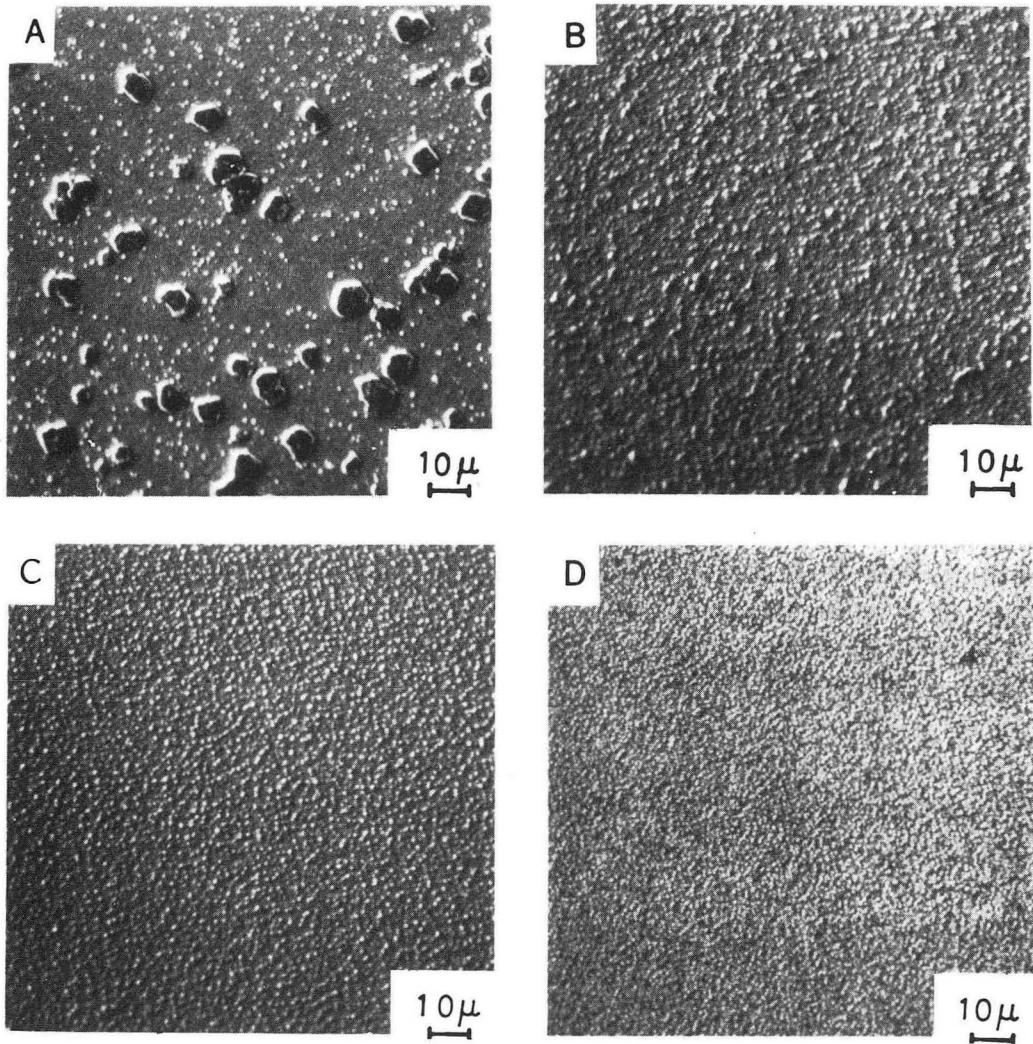
XBB 817-6791A

Fig. 2. Effect of current density on the numbers and size of initial
protrusions. (a) 10 mA/cm^2 x 1.5 min; (b) 30 mA/cm^2 x 0.5 min;
(c) 60 mA/cm^2 x 15 sec; (d) 120 mA/cm^2 x 5 sec. 1$\underline{M}$ ZnCl$_2$ with
4.8 x 10^{-5} $\underline{M}$ Pb, 800 rpm.

surface can be covered by a thin layer of zinc-platinum alloy from the very beginning of deposition; (3) enhance successive coalescence and preferential growth of protrusions; and (4) deform the crystalline structure to a rounded shape.

H^+ ions seem not to affect either the initial nucleation or successive coalescence of protrusions, but instead change the crystalline structure to a rounded shape with decreasing pH values.

A.1.2 THE MORPHOLOGY OF ELECTRODEPOSITED COPPER

A. Kindler and C. W. Tobias

When a metal is electrodeposited, the developing surface morphology determines surface properties such as brightness, smoothness, and hardness, and, indirectly, compactness, strength, and ductility. This investigation deals with the surface morphology of copper produced under well-defined conditions of mass transfer and uniform current distribution in the absence of inhibitors.

Morphology was investigated with SEM after electrodeposition from an aqueous $CuSO_4-H_2SO_4$ solution in a flow cell with a plane-parallel electrode. Uniform current distribution and well defined mass transfer conditions present during turbulent forced convection made investigation of three regimes possible: (1) direct-current deposition at the limiting current; (2) direct-current deposition below the limiting current; and (3) pulsed-current deposition below the limiting current.

In Regime 1, nodular powder deposits are due to transformation from a dendritic structure to a coherent one when the mass transfer boundary layer at the growing dendrite tip thins out. The coherent portion of the structure caps the dendrite, giving it a mushroom-like appearance in photomicrographs of the deposit cross section. In Regime 2, the roughness generated during electro-deposition results from the growth of a few large protruding crystals embedded in a very fine flat polycrystalline deposit resembling sand. These large crystals originate mostly near the electrode/deposit interface. After their growth ends, coverage by the "sandy" deposit gives the crystals a deceptively nodular and amorphous appearance (Fig. 3). The number of large crystals decreased with increasing interfacial $CuSO_4$ concentration and decreasing current density. Average crystal size decreases as the number of crystals and/or the interfacial concentration increases. The number of smaller crystals in the fine structure depends on current density (Fig. 4) and similarly on concentration; the average size is inversely related to the number density.

Further observations demonstrate that: (1) the electrode preparation influences the number of crystals (large and small) because the energy of the surface is linked to its pretreatment, and (2) increased roughness found in thicker deposits is generated by preferential deposition of fine structure on the large crystals. In Regime 3 the growth of the large crystals can be inhibited with pulsed current instead of with organic inhibitors. The

27
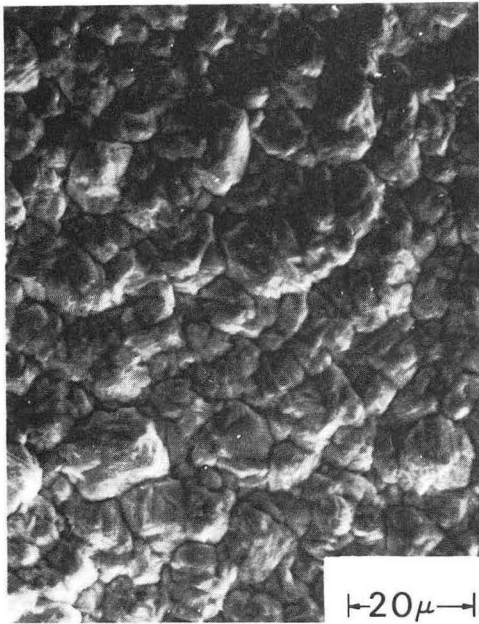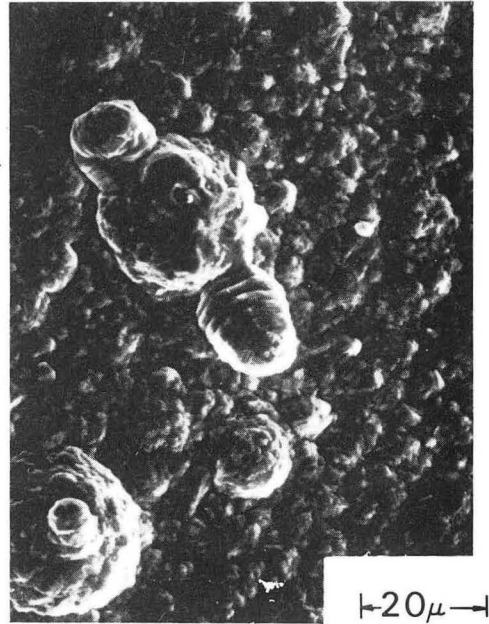
9.59 MA/CM^2 24.02 MA/CM^2

40% I_L
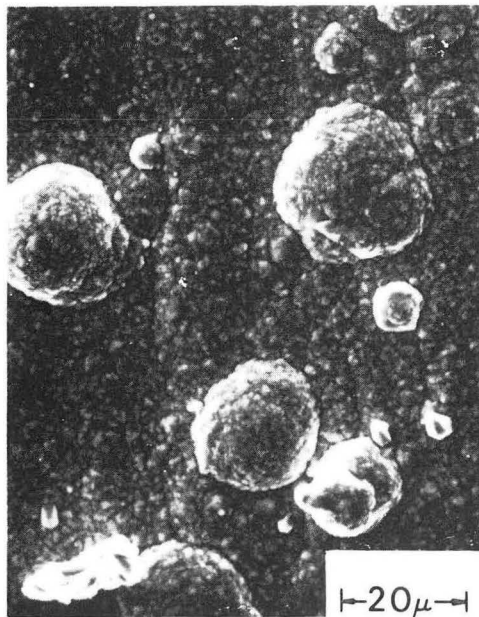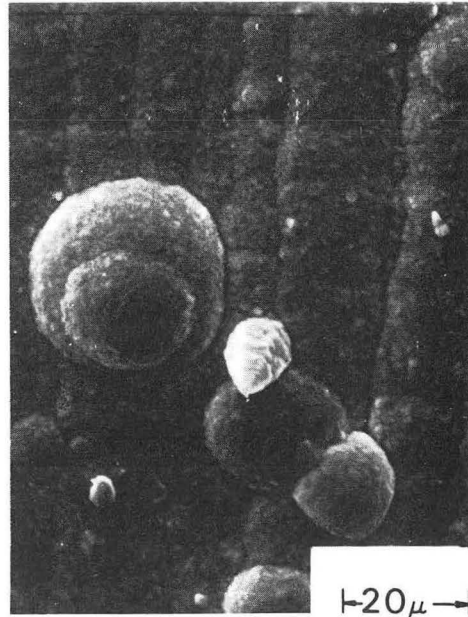
90.25 MA/CM^2 111 MA/CM^2

40% I_L XBB 812-1783

Fig. 3. Grain size of fine structure decreases with increasing current.
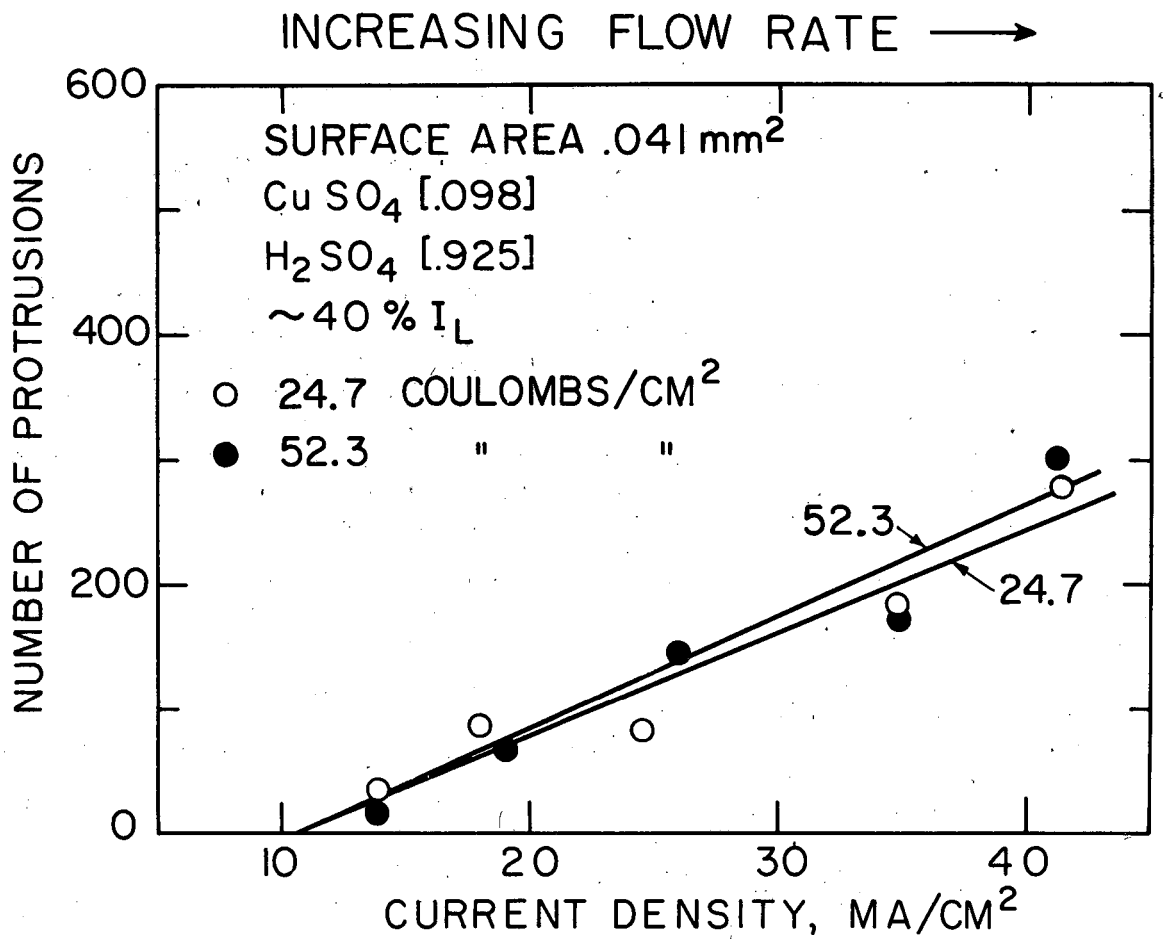
Fig. 4.   Effect of current density on the number of protrusions.

off-time between the pulses is demonstrated to be the cause of this phenomenon. It is proposed that during this period, passivation of crystal growth sites occurs.

WORK IN PROGRESS

The effects of current density, time of metal deposition, hydrodynamic conditions, and substrate conditions on the zinc electrodeposition process are being studied in a channel-flow cell with planar electrodes. The morphology of zinc deposited under galvanostatic conditons from $1\underline{M}$ $ZnCl_2$ acidified solution is evaluated well below the limiting current.

A finite-element model is under development for modeling electrodes that exhibit passivity. In particular we focus on the coexistence of active and passive regions on the same surface. The finite-element technique, relatively new to current-distribution modeling, is generally regarded as superior to the finite-difference method for accommodating singularities and irregular geometries. To evaluate the validity of the assumptions made in setting up the model, the current distribution and the location of the "boundary" corresponding to active-passive transition will be measured on a rotating cylinder experiment using a segmented nickel anode.

REFERENCE

1. T. Tsuda (with C. W. Tobias), "The Influence of Lead Ions on the Macromorphology of Electrodeposited Zinc" (M. S. Thesis), Lawrence Berkeley Laboratory, LBL-13057, 1981.

A.2 METAL COUPLES IN NONAQUEOUS SOLVENTS

C. W. Tobias, Investigator

The objective of this project is to develop practical alternatives to aqueous or high-temperature molten-salt systems for the efficient electrochemical reduction and oxidation of reactive metals. Past accomplishments include the efficient reduction of potassium metal from $KAlCl_4$ dissolved in propylene carbonate. The thickness and chemical nature of surface films on lithium in propylene carbonate electrolytes are under study. This project is carried out as part of efforts devoted to the identification of novel solvent-electrode combinations of potential interest for use in electrolysis and in batteries.

The use of a benzophenone-alkali-metal ketal either as an effective drying agent of nonaqueous electrolytes or, in combination with an inert electron collector, as an alkali metal electrode, is being investigated. Solubilities of selected salts and of potassium metal are being determined with and without added co-solvents. Results to date indicate that the ketal mixtures are stable, under dry nitrogen, over periods of weeks. However, solubilities of

potassium (less than 1 g/100 g solvent) and conductivities measured so far
$(1\text{-}2000 \times 10^{-6}$ ohm cm$^{-1})$ are too low for application in batteries and
electrosynthesis.

PUBLICATIONS

Refereed Journals

1. C. W. Tobias, "The Coming of Age of Electrochemical Engineering," AIChE
   Symposium Series, 204, 77 (1981).

2. C. W. Tobias and H. H. Law, "The Morphology of Potassium Deposited from
   Propylene Carbonate Electrolyte," Proceedings of the Symposium on
   Electrocrystallization, Rolf Weil, ed., Vol. 81-6, the Electrochemical
   Society, June, 1981.

LBL Reports

A. Kindler (with C. W. Tobias), "The Morphology of Electrodeposited-Copper"
   (Ph.D. Dissertation), University of California, Berkeley, LBL-12838, 1981.

G. A. Prentice, "Modeling of Changing Electrode Profiles" (Ph.D. Dissertation),
   University of California, Berkeley, LBL-11694, 1980.

G. A. Prentice and C. W. Tobias, "A Survey of Numerical Methods and Solu-
   tions of Current Distribution Problems," accepted for publication in the
   Journal of the Electrochemical Society. LBL-12191, 1981.

G. A. Prentice and C. W. Tobias, "Finite Difference Calculation of Current
   Distributions at Polarized Electrodes," accepted for publication in the
   AIChE Journal. LBL-11058, in press.

G. A. Prentice and C. W. Tobias, "Deposition and Dissolution on Sinusoidal
   Electrode," accepted for publication in the Journal of the Electrochemical
   Society, LBL-12167, 1981.

G. A. Prentice and C. W. Tobias, "Simulation of Changing Electron Profiles,"
   accepted for publicaton in the Journal of the Electrochemical Society,
   LBL-12192, 1981.

Other Publications

H. Gerischer and C. W. Tobias, eds., Advances in Electrochemistry and
   Electrochemical Engineering, Vol. 12, Wiley-Interscience, New York, 1981.

Invited Talks

R. T. Atanasoski, H. H. Law, and C. W. Tobias, "Determination of Water in
   Propylene Carbonate Electrolytes by Cyclic Voltametry," Meeting of the
   Electrochemical Society, Minneapolis, Minn., May 10-15, 1981; Extended
   Abstracts, 81-1, (392), p. 985-986 (based on LBL-11847).

H. H. Law and C. W. Tobias, "The Cathodic Overpotential of Potassium in KAlCl-
   Propylene Carbonate Electrolyte," Meeting of the Electrochemical Society,
   Denver, Colorado, October 11-16, 1981; Extended Abstracts, 81-2, (585), p.
   1403 (based on LBL-11487).

C. W. Tobias, "Electrochemical Engineering of Batteries," short course,
   Continuing Education Institute, Cherry Hill, New Jersey, June 22-26, 1981.

C. W. Tobias, "Prospects of the Electrochemical Technology," W. R. Grace
   Research Center, Columbia, Maryland, September 18, 1981.

A.3   SURFACE LAYERS ON BATTERY MATERIALS

R. H. Muller, Investigator

   The purpose of this work is to provide direct experimental information
about formation and properties of surface layers on battery-electrode
materials.

A.3.1   ELECTROCHEMICAL STUDIES OF THE FILM FORMATION ON LITHIUM IN PROPYLENE CARBONATE SOLUTIONS UNDER OPEN CIRCUIT CONDITIONS

Y. Geronov, F. Schwager, and R. H. Muller

   Lithium is thermodynamically unstable in contact with most nonaqueous
battery electrolytes and can be used only because of the formation of
protective surface layers on the metal. The properties of these layers are
important for the current delivery, the shelf-life, and the rechargeability of
lithium electrodes. The aim of this study is to determine the mode of
formation and the properties of films that spontaneously form on lithium in
propylene carbonate solutions of $LiClO_4$ and $LiAsF_6$ in order to identify
means to improve electrode performance.

   Film-formation under open circuit conditions was followed by use of the
galvanostatic pulse polarization technique. For the measurement of electrode
capacitance, pulses of typically 0.1 mA/cm^2 amplitude and 5 μs duration were
employed. For polarization measurements, pulse amplitude was 1-20 mA/cm^2
and duration 10 ms.

   The kinetic behavior of the Li electrodes is found to be controlled by the
field-assisted ion conduction through an insulating surface layer. The thick-
ness of this layer, as derived from capacitance measurements, increases with

time according to a parabolic rate law, with the rate increasing with water content of the solution. The exchange current density of 5.5 mA/cm^2 determined here on a smooth surface at the beginning of immersion in 1$\underline{M}$ $LiClO_4$, when the surface layer is only about 20 Å thick, agrees with the value of 12 mA/cm^2 reported for an anodically cleaned rough electrode. The results are consistent with the fast formation of a compact protective film by reaction with residual water. This layer acts as a solid ionic conductor. Li_2O is the thermodynamically favored reaction product. Capacitance measurements are sensitive to this layer, which faces the electrode. A nonprotective porous overlayer, which faces the solution and is formed by electrode corrosion or solvent decomposition, has little electrical effect. It is visible in scanning electron micrographs and found by ellipsometry. Future efforts will be directed toward increasing the ionic conductivity of the compact surface layer.

A.3.2 ELLIPSOMETRIC STUDIES OF SURFACE LAYERS ON LITHIUM

F. Schwager, Y. Geronov, and R. H. Muller

Protective surface layers are necessary for the use of lithium in batteries with nonaqueous solvents but have been implicated in the poor rechargeability of lithium electrodes. The purpose of this study, conducted in parallel with electrochemical measurements reported in the preceding section, was to provide independent optical data on the thickness, structure, and composition of surface layers formed on lithium in $LiClO_4$ and $LiAsF_6$ solutions in propylene carbonate solvent. Ellipsometry is particularly well suited for the in situ observation of electrochemical film formation because of its great sensitivity and minimum disturbance to the surface.

Ellipsometric and electrochemical measurements were conducted in a hermetically sealed polypropylene cell consisting of an electrode compartment with two strain-free quartz windows arranged for a 75° angle of incidence of the light beam. A solution compartment was located above the electrode compartment and connected with it by internal valves. This configuration enables one to take measurements very soon after the electrode is brought in contact with the solution. The ellipsometer used was of the self-compensating type in the polarizer/quarter-wave plate/sample-analyzer configuration.[1] A mercury lamp for a wavelength of 5461 Å and an argon-ion laser at a wavelength of 5145 Å were used as light sources. The cell was assembled in an inert atmosphere box with recirculating helium (<0.5 ppm O_2, H_2O, 5 ppm N_2). After the experiment, the working electrode was washed with pure propylene carbonate, dried, and transferred to vacuum for scanning electron microscopy, Auger spectroscopy, or ellipsometry of the dry film.

This work has shown that the growth of surface layers on lithium in propylene carbonate solutions can be followed by ellipsometry, although the refractive indices of many potential film materials are close to those of the electrolyte. Film thicknesses calculated from ellipsometer measurements increase linearly over periods of several days at open circuit; thicknesses are several times larger than those derived from galvanostatic pulse measurements.

Films are found to be inhomogeneous with properties varying as a linear function of thickness; compact regions are located adjacent to the metal and porous regions adjacent to the solution. The compact region is responsible for the electrode capacitance and can also be generated by reaction with water in the vapor phase. The porous region is primarily responsible for the ellipsometer measurements. It may be formed by the precipitation of decomposition products of the solution.

WORK IN PROGRESS

Electrical impedance measurements are being conducted to further characterize surface layers on lithium in propylene carbonate solutions and to determine the effect of anodic and cathodic electrode polarization.

REFERENCE

1. H. J. Mathieu, D. E. McClure, and R. H. Muller, Rev. Sci. Instrum. <u>45</u>, 798 (1974).

PUBLICATIONS

LBL Reports

Y. Geronov, F. Schwager, and R. H. Muller, "Electrochemical Studies of the Film Formation on Lithium in Propylene Carbonate Solutions under Open Circuit Conditions," LBL-12102, 12102-Rev., 12102-Rev. 2, 1981.

Felix Schwager, "Operation of Inert Atmosphere Glove Box," LBL-13774, 1981.

Felix Schwager, "Operating Procedure for Combined Auger- and UHV System, LBL-13609, 1981.

Invited Talk

Rolf H. Muller, "Highlights of In-House Research Programs, Development of Electrochemical Synthesis and Energy Storage," Annual Program Managers Meeting, Division of Energy Storage, DOE, Washington, D.C., October 6, 1981.

A.4   ANALYSIS AND SIMULATION OF ELECTROCHEMICAL SYSTEMS

J. S. Newman, Investigator

This program includes the investigation of efficient and economical methods for electrical energy conversion and storage, development of mathematical models to predict the behavior of electrochemical systems and to identify important process parameters, and experiments to verify of the completeness and accuracy of the models. Specific projects include analysis of flow-through

porous electrodes for metal-ion removal from waste streams and for energy storage, and development of an electrochemical impregnation method of preparing porous Ni electrodes for high-energy battery applications.

WORK IN PROGRESS

An alternating voltage impedance method will be used to study the anodic behavior of zinc in an acidic aqueous medium. This work will have practical applications ranging from the study of corrosion of underground and underwater pipelines to the prevention of battery discharge due to the formation of pits within the electrodes. In this investigation, impedance measurements will be performed on both a rotating disk and rotating hemispherical zinc electrode. The advantage of a rotating hemispherical electrode is that the metal dissolution does not interfere with the fluid flow, as it would with a rotating disk electrode.

Theoretical work has begun on the frequency response of current and potential to high-frequency sinusoidal speed modulation on a rotating-disk electrode. The unsteady state Navier-Stokes equations, coupled with the convective diffusion equation, were solved numerically to give velocity and concentration profiles at high modulation frequencies. This work is useful for studying the mass transfer characteristics of corrosion processes because accurate diffusion coefficients can be obtained by combining the theoretical predictions with experimental impedance measurements. Excellent agreement between the theory and experiment has been found with the $Fe(CN)_6^{3-}/Fe(CN_6^{4-}$ system at the half-wave potential in galvanostatic regulation.

Theoretical work examining the feasibility of several proposed battery systems will begin. Among these, the polyacetylene battery recently appearing in the literature will be examined. Emphasis will be on developing general design criteria for such prospective battery systems.

Many electrochemical systems use channel flow between two-plane parallel electrodes. For example, this configuration can be used in $Fe^0-Fe^{2+}-Fe^{3+}$ energy storage cells or in electro-organic synthesis. A mathematical model, useful in the design of such systems, is being developed to calculate the concentration, potential, and current distribution in a thin-gap flow cell. While previous models have assumed that the interelectrode gap is much larger than the diffusion boundary layer thickness, the present model allows the gap to be thin enough for the diffusion boundary layers to interact. The model also can take into account multiple reactions at the electrodes.

An electrochemical impregnation method of preparing porous Ni electrodes for high-energy battery applications is being investigated. The method used currently involves electroprecipitation of $Ni(OH)_2$. An understanding of the electroprecipitation is necessary to develop an improved preparation process for producing Ni battery electrodes. Preliminary experiments have shown that the $Ni(OH)_2$ deposit becomes less adherent as the temperature of the acidic nickel nitrate bath decreases.

Molten sodium sulfide and sodium polysulfides are involved in a number of practical enginering applications. In particular, the use of sulfur and associated sodium polysulfides as the cathode in a sodium-sulfur secondary cell seems especially promising. Sodium-sulfur batteries are expected to possess a high specific energy greater than 150 W-hr/kg and a cycle life greater than 1000 cycles. These characteristics, combined with the abundant availability and low price of sulfur, make the sulfur electrode and the sodium-sulfur battery attractive for both vehicle propulsion and utility load-leveling applications. It has been determined that the rate-limiting process occurring at the sulfur cathode is the diffusion of charged species within the poly-sulfide melt. Since the performance of sodium-sulfur cells is strongly influenced by the diffusion of anions and cations through the melt, optimal design of sulfur electrodes will depend upon the availability and accuracy of diffusion coefficient data for polysulfide melts. An experimental apparatus has been designed to measure the diffusion coefficient of sodium ions in melts of sodium polysulfides, using the method of restricted diffusion. The advantage of this method is that the current densities will be low enough to eliminate the problem of electrode blockage by insoluble polysulfide or sulfur phases.

In many practical electrochemical applications, the formation and growth of dendrites can be critical to the operation and performance of the system. In zinc batteries the metal deposition and subsequent dendritic growth can pierce separators and cause internal shorting. In plating operations, the formation of dendrites can give a rough, unattractive finish to the final product. At present, the physics of initiation and growth of dendrites is not well understood. A theoretical stability analysis will be undertaken to examine the effects of plating additives, current density, flow hydrodynamics, and electrode materials on dendrite initiation.

The effects of process variables on the removal of lead from dilute sulfuric waste streams is being investigated in a high-pressure electrochemical reactor. In particular, the effect of pressure on the current efficiency of the process is being determined through current-potential measurements and effluent analysis. Higher reactor pressures thermodynamically reduce the amount of hydrogen discharged and further inhibit hydrogen nucleation, which would increase the ohmic potential drop through the reactor.

PUBLICATIONS

Refereed Journals

R. Pollard and J. S. Newman, "Mathematical Modeling of the Lithium-Aluminum, Iron Sulfide Battery. I. Galvanostatic Discharge Behavior," J. Electro-chem. Soc., 128, 491-502 (1981).

R. Pollard and J. S. Newman, "Mathematical Modeling of Lithium-Aluminum, Iron Sulfide Battery. II. The Influence of Relaxation Time on the Charging Characteristics," J. Electrochem. Soc., 128, 503-507 (1981).

J. A. Trainham and J. S. Newman, "A Comparison between Flow-through and Flow-by Porous Electrodes for Redox Energy Storage," Electrochim. Acta, 26, 455-469 (1981).

LBL Report

P. S. Fedkiw and J. S. Newman, "Mass-Transfer Coefficients in Packed Beds at Very Low Reynolds Numbers," LBL-12497, 1981.

Invited Talks

J. S. Newman, "Thermodynamics and Cell Potential, Mass Transfers, and Mathematical Modeling of Battery Systems," three lectures for Electrochemical Engineering of Batteries, a national short course, Cherry Hill, New Jersey, June 22-26, 1981.

W. Tiedemann and J. S. Newman, "Simulation of Electric Vehicle Driving Profiles Based on Mathematical Models of the Lead-Acid Battery System," Detroit Meeting of the American Institute of Chemical Engineers, August 16-19, 1981.

A.5 ELECTRODE KINETICS AND ELECTROCATALYSIS

P. N. Ross, Investigator

Complex electrochemical reactions in which chemical bonds are broken and/or formed are invariably catalytic, with electrode kinetics varying by many orders of magnitude for different electrode materials. Catalytic electrode materials are essential to technologies like fuel cells, metal-air batteries, electrolyzers, and electro-organic synthesis. Air electrodes constitute a major technology in themselves. In addition to being integral parts of fuel cells, air batteries, and water electrolyzers, air electrodes are being used increasingly in metal electrorefining and in air-depolarized electrolytic cells. Alkaline fuel cells (e.g., Zn-air, Al-air and H_2-air) are receiving renewed attention for use in transportaton applications and for on-site plant electricity generation from waste hydrogen. Interest in electrochemical processes for synthesis of organics has been increasing in recent years due to new classes of catalysts, e.g., alloys and organometallics.

A.5.1 CHARACTERISTICS OF AN NH_3-AIR ALKALINE FUEL CELL FOR VEHICLES

P. N. Ross and V. Kopytov*

The use of hydrogen-air alkaline fuel cells in a consumer vehicle application was examined. Liquid anhydrous ammonia was found to be an excellent storage medium for hydrogen, even though the endothermicity of the NH_3 cracking reaction results in some efficiency penalty. In the system developed here, hydrogen is supplied to a fuel cell by the catalytic cracking of liquid anhydrous ammonia, making the total system an indirect NH_3-air fuel cell. The advantages of the alkaline fuel cell relative to any acid fuel cell are higher power density (factor of 2-3) and lower cost (factor of 2) resulting in significantly lower total cost (factor of 4-6).

Laboratory-scale examinations were made of the ammonia-cracking reaction and the power characteristics of an alkaline fuel cell running on cracked ammonia and air. Single-cell testing indicated that system thermal efficiencies of 34-44% (based on H.H.V. of NH_3) can be achieved at power densities of 2600-1000 W/m^2, respectively, using currently known electrode technology that does not require a precious-metal catalyst (e.g., Pt). Computer simulations of vehicle characteristics were developed in cooperation with the LLNL electric and hybrid vehicle program. The vehicle chosen was a fuel cell-Zn/NiOOH battery hybrid, with the fuel cell sized for sustained cruising at 55 mph and the battery providing all peak power requirements. The fuel consumptions for the simulated SAE J227a "D" driving cycle with different power plant configurations are summarized in Table 1. Diesel ICE-equivalent (33 W/kg) vehicle performance can be achieved in a fuel cell-battery hybrid vehicle that yields an NH_3 consumption rate of 10-20 km/l (2-seater urban car to 5-seater Volkswagen Rabbit type). A full-performance ICE-equivalent (49 W/kg) vehicle could be achieved with only a small penalty in fuel efficiency. For NH_3 produced from coal, the energy yield is slightly lower than for methanol from coal, but the ammonia fuel-cell vehicle is more than twice as efficient as the methanol ICE vehicle for the same performance. The result is a primary energy consumption one-half that of the ICE-powered vehicle.

---

*Lawrence Livermore National Laboratory

Table 1. NH_3 consumption rates for fuel cell-battery powered hybrid vehicles of varying performance and cost (current density).

Intermediate Performance			Power-to-Mass Ratio: 33 W/kg		Range: 240 km	
2 seater vehicle		----------component masses [kg]----------				
design option	curb wt.	fuel cell	Ni-Zn bat	full tank	fuel consumed[a] km/l	
0.40 A/cm^2	332	46	20	13.3	18.2	
0.15 A/cm^2	372	81	22	9.9	20.6	
5 seater vehicle						
0.40 A/cm^2	893	71	52	24.2	10.0	
0.15 A/cm^2	976	127	58	21.4	11.3	
Equivalent Performance			Power-to-Mass Ratio: 49 W/kg		Range: 400 km	
2 seater vehicle		----------component masses [kg]----------				
design option	curb wt.	fuel cell	Ni-Zn bat	full tank	fuel consumed[a] km/l	
0.40 A/cm^2	401	48	44	24.0	16.8	
0.15 A/cm^2	464	85	50	21.5	18.8	
5 seater vehicle						
0.40 A/cm^2	1057	76	110	44.7	9.0	
0.15 A/cm^2	1153	136	120	39.6	10.2	

[a] Divide into 9.606 to obtain primary energy in kWh/km.

A.5.2 METAL-OXIDE-DOPED ACTIVE CARBONS AS OXYGEN REDUCTION CATALYSTS IN ALKALINE ELECTROLYTE

P. N. Ross

It is well-known that activated carbon blacks and certain transition metal oxides are catalysts for oxygen reduction. These two materials are felt to have very different catalytic action. Carbon blacks appear to catalyze oxygen reduction via a peroxide sequence,

$$O_2 + 2H_2O + 2e^- \rightleftarrows HO_2^- + 2OH^- \quad \text{(fast)}$$

$$HO_2^- + H_2O + 2e^- \rightleftarrows 3OH^- \quad \text{(slow)}$$
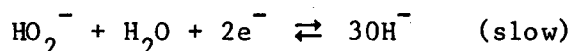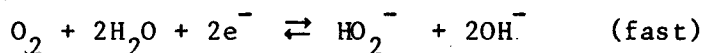
with the peroxide-elimination step being rate-limiting. This type of catalytic action limits the potential that can be achieved in air electrodes to about -0.25 V (versus Hg/HgO). Transition metal oxides appear to catalyze via a four-electron sequence not involving an HO_2^- species in solution. In addition, some transition metal oxides are very effective HO_2^- reduction catalysts. It is therefore of considerable interest to discover whether the combination of a transition metal oxide with an activated carbon support would give rise to a synergistic effect between the two. The metal oxide is dispersed into carbons of variable activity. A synergistic effect would appear as an increase in the specific activity relative to that of the oxide on an inert substrate.

An example of this analysis is shown in Fig. 1 for carbon black impregnated with Co_3O_4. In our study, Co_3O_4 was the most active non-Pt group transition metal oxide for oxygen reduction in alkali. Shawinigan actate black is a nearly inert substrate, having an activity level 2 orders of magnitude below that for the most active carbon investigated, designated EMC in Fig. 1. Co_3O_4/EMC carbon had 5 times the activity of Co_3O_4/acetylene black in the potential region above -0.1 V (vs. Hg/HgO), or about 3 times the specific activity of unsupported oxide of the same nominal surface area. The explanation of this synergistic effect we favor at present is a "peroxide spillover" mechanism in which HO_2^- formed on the carbon surface migrates via surface diffusion to the Co_3O_4, where reduction occurs to OH^-. In addition, O_2 is reduced directly to OH^- on the Co_3O_4 clusters as if the carbon were not present.

A.5.3 BIFUNCTIONAL AIR-ELECTRODE STUDIES

P. N. Ross and L. R. Johnson

These studies provide supporting research in air-electrode technology for DOE metal-air battery projects. Metal-air systems have, in principle, the highest energy and power densities (>100 Wh/kg, >100 W/kg) of all ambient temperature systems. This is because one of the electroactive species (oxygen)
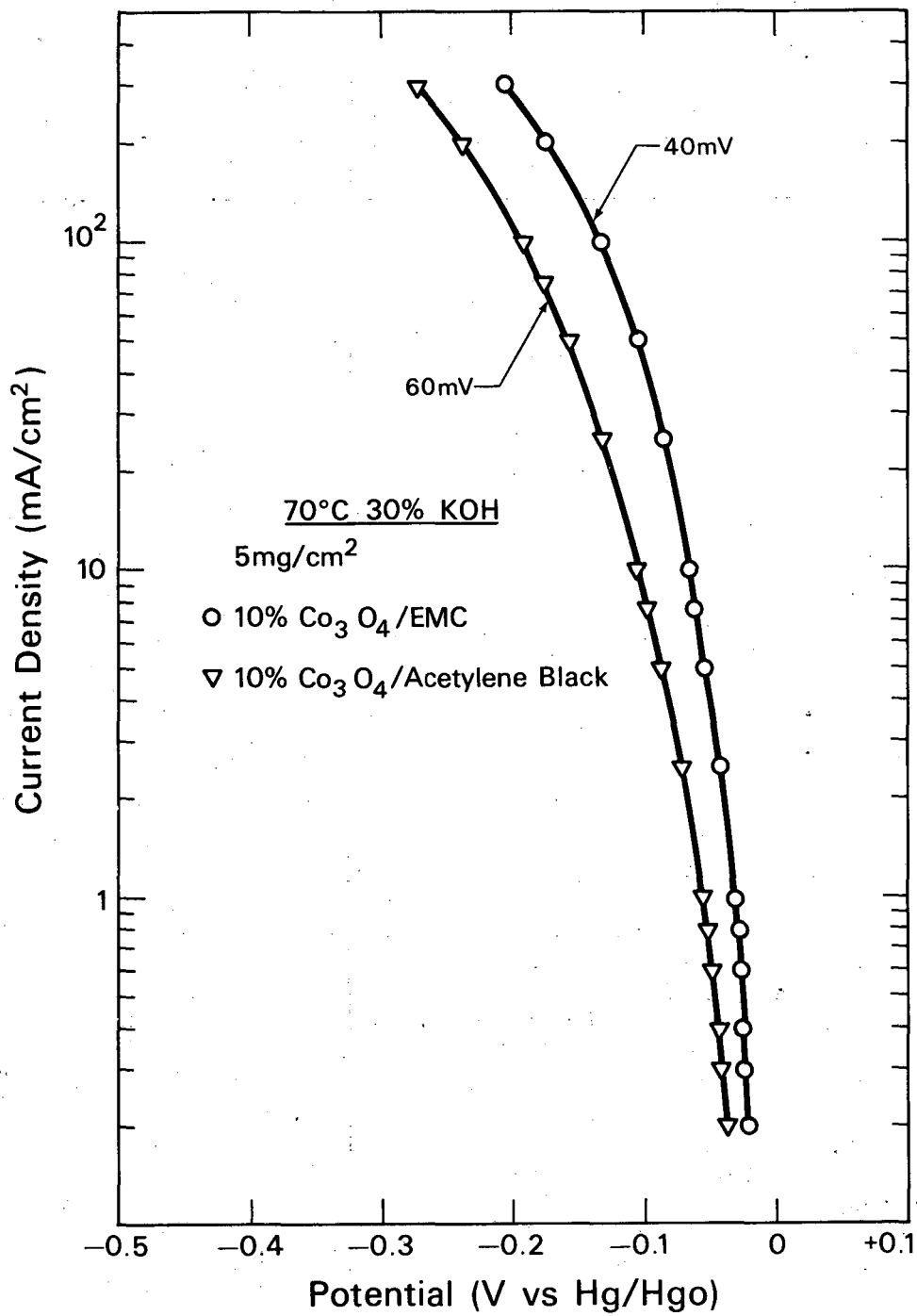
Fig. 1. Polarization curve for the reduction of pure O_2 with gas diffusion electrodes using Co_3O_4 impregnated carbon black.

need not be contained within the battery. However, practical development of this technology has been slow, owing to problems in developing suitable air-electrode materials. In electrically rechargeable metal-air batteries, the positive electrode must be bifunctional, both evolving and consuming oxygen. Few materials are stable at the potentials required for oxygen evolution; of these, fewer still are catalytically active for oxygen reduction and evolution. A number of metals and/or metal oxides have been examined for their stability and catalytic activity. In virtually every material examined, the polarization was greater in one direction than the other. Qualitatively the results were:

Unstable (dissolution): Ag, Pd, Fe_3O_4, MnO_2

Reduction activity: Pt > Ru > Co_3O_4 ≈ Rh ≈ Ir > NiO

Evolution activity: Ir ≈ Ru > Co_3O_4 > NiO > Pt

Co_3O_4 was the most cost effective catalyst of those studied so far and was very stable in the potential range of interest for air electrodes (+ 0.6 V to -0.2 V vs. Hg/HgO); e.g., less than 2 ppm Co detected in solution after 100 cycles. We have therefore concentrated on bifunctional electrodes based on Co_3O_4 as the catalytic material.

In order to prepare Co_3O_4 of the highest possible surface area, the oxide was impregnated into a carbon black support material and carefully heat-treated to produce the Co_3O_4 phase. Analysis by x-ray diffraction and electron microscopy indicated that the characteristic size of oxide particles was 100-200 Å (equivalent to about 50 m^2/g) when the carbon black used was Shawinigan acetylene black. This material is used by Westinghouse in its developmental air electrode. To determine the stability of the carbon phase, we have developed a ^{14}C tracer method that produces in situ determination of carbon loss from the electrode. The characteristic cycling behavior of an Fe-air battery using a standard Westinghouse 100 mAh/cm^2 iron electrode and an air electrode fabricated from the Co_3O_4 catalyst is summarized in Fig. 2. Carbon loss was appreciable; after the loss reached 15%, the gas pores in the catalyst layer became progressively filled with electrolyte, resulting in rapidly increasing polarization. Analysis of the electrolyte and of the electrode revealed no loss of cobalt from the electrode. The failure of the electrode was attributed directly to the carbon corrosion.

Corrosion of acetylene black in the potential region for oxygen evolution was studied using the ^{14}C tracer method. The results are summarized in Fig. 3. The corrosion rate showed a strong dependence on both potential and temperature, 140 mV per decade and 23 kcal/gmol, respectively. The corrosion current was calculated from the mass rate of carbon loss, assuming 6 e^- per atom, equivalent to oxidation to CO_3^{2-}. Chemical analysis of the electrolyte has, however, indicated that the principal corrosion product is not
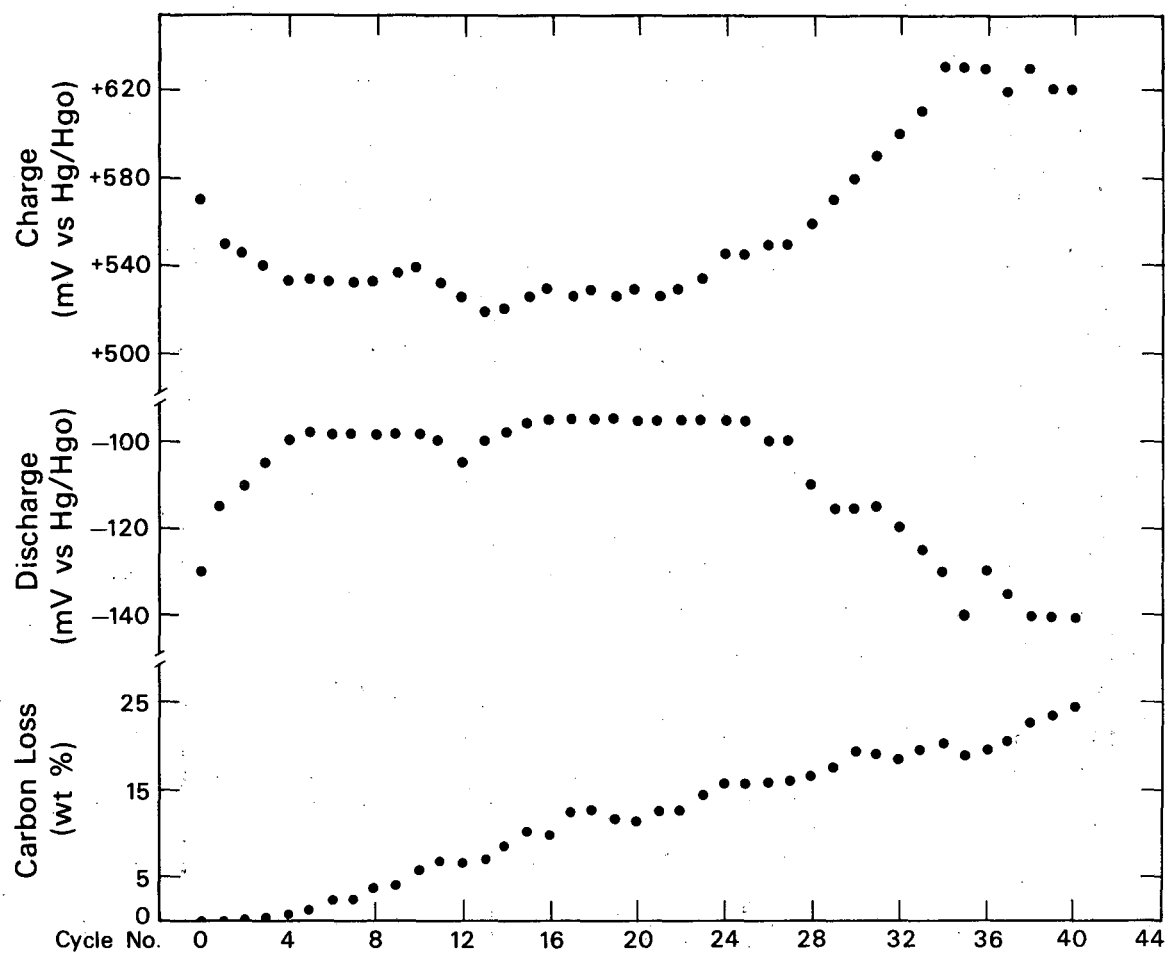
Fig. 2. Cycling behavior of a Co_3O_4 impregnated acetylene black air electrode. Galvanostatic at $I = 10$ mA/cm^2. 25 mg/cm^2. 45°C, 10^{-4} Hz.
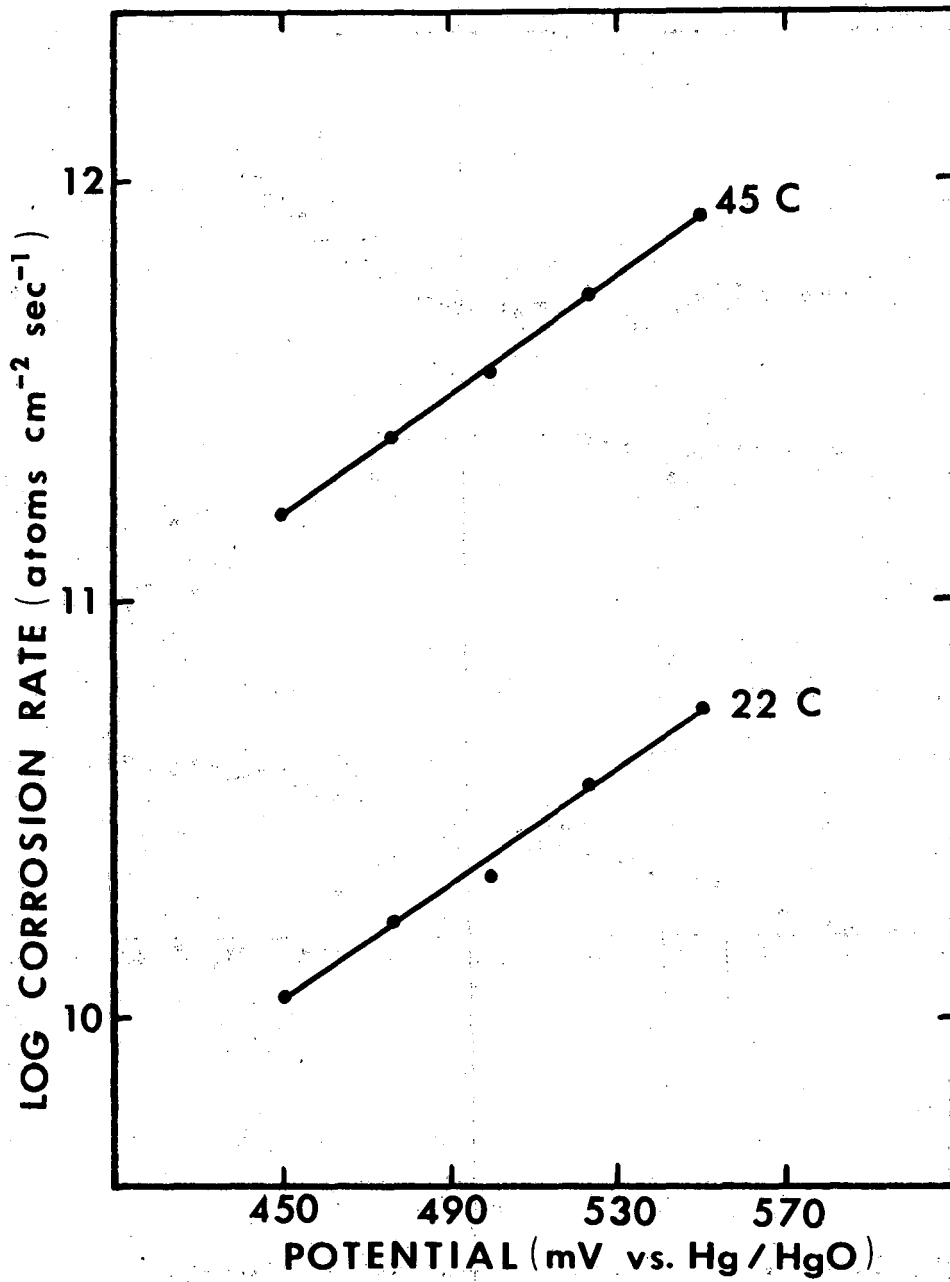
Fig. 3. Tafel plots for acetylene black corrosion at oxygen evolution potentials.

XBL 822-7826

44

CO_3^{2-}. These corrosion rates indicate that, at 23°C, a charging potential of +500 mV vs. Hg/HgO would extend the cycle life relative to the test conditions by a factor of 30 (to about 900 cycles). To reduce the charging potential to +500 mV will require a substantial improvement in oxygen evolution catalysis relative to that achieved with Co_3O_4.

PUBLICATIONS

Proceedings

P. N. Ross, "Characteristics of an NH_3-Air Fuel Cell for Vehicle Applications," Proceedings of the 16th Intersociety Energy Conversion Engineering Conference, vol. 1, pp. 726-733, American Society of Mechanical Engineers, New York, 1981.

P. N. Ross, F. Will, and W. O'Grady, eds., Proceedings of the Symposium on Electrocatalysis, Electrochem. Soc. Proc., PV81-6 (1981).

LBL Reports

P. N. Ross, "Characteristics of an NH_3-Air Fuel Cell for Vehicle Applications," LBL-12754, 1981.

P. N. Ross, "Oxygen Reduction with Carbon Supported Metallic Cluster Catalysts in Alkaline Electrolyte," LBL-11891, 1981.

Invited Talks

P. N. Ross, "Oxygen Reduction with Carbon Supported Metallic Cluster Catalysts in Alkaline Electrolyte," Occidental Research, Irvine, California, February 1981.

P. N. Ross, "Oxygen Reduction with Carbon Supported Metallic Cluster Catalysts in Alkaline Electrolyte," Diamond Shamrock, Cleveland, Ohio, March 1981.

P. N. Ross, "Characteristics of an NH_3-Air Fuel Cell for Vehicle Applications," General Motors Research Center, Warren, Michigan, June 1981.

P. N. Ross, "Oxygen Reduction with Carbon Supported Metallic Cluster Catalysts in Alkaline Electrolyte," Electrochemical Society meeting, Minneapolis, Minnesota, May 10-15, 1981.

P. N. Ross, "Characteristics of an NH_3-Air Fuel Cell for Vehicle Applications," 16th Intersociety Energy Conversion Engineering Conference, Atlanta, Georgia, August 15-18, 1981.

A.6 ELECTROCHEMICAL PROPERTIES OF NASICON

L. C. De Jonghe, Investigator

A.6.1 CHEMICAL STABILITY OF NASICON

H. Schmid, L. C. De Jonghe, and C. Cameron

NASICON compounds, $Na_{1+x}Si_xZr_2P_{3-x}O_{12}$, were identified by Hong et al.[1] as possible alternatives to sodium-β and β'' solid electrolytes. One important requirement of these ceramic electrolytes is that they be chemically stable toward the battery electrodes. It has been noted that while ionic resistivities of a few ohm-centimeters can be readily achieved, many NASICONs appear to degrade and crack rapidly when in contact with molten sodium at temperatures around 300°C. The rate at which the degradation occurs depends on both the chemical composition of the NASICON and the presence of impurities. Since there appears to be some question whether NASICONs are chemically stable in contact with sodium, some other applications were explored as well.

NASICON powders with $x = 2$ and with the recently proposed new composition[2] of $Na_{3.1}Zr_{1.55}Si_{2.3}P_{0.7}O_{11}$ were fabricated by a sol-gel method and sintered for 24 hours at 1220°C in air. Densities of around 95% of theoretical maximum were achieved. The specimens were then immersed in sodium at 300°C for a period of up to 2 weeks. Analysis with x-rays showed that the lattices of both electrolytes had undergone changes as a result of chemical reaction with the sodium. The x-ray diffractograms from as-prepared and immersed material could be fitted to a monoclinic and a rhombohedral unit cell. Figure 1 compares the diffractograms of as-prepared (a) and immersed (b) electrolytes, illustrating the shifts in the lattice parameters. The data indicated that the samples were actually a mixture of rhombohedral and monoclinic phases. The data also indicated that the reaction with metallic sodium increased the sodium content of the NASICON electrolytes. The lattice parameter changes were sufficiently large to produce stresses that fractured the electrolytes.

Minor alumina contamination was found to lead to the formation of a sodium alumino-silicate intergranular phase that was rapidly attacked by the sodium. Elimination of contamination by alumina dramatically increased the resistance to chemical degradation of the electrolytes. Nevertheless, after about 10 weeks of immersion at 300°C, the electrolytes again showed the same type of degradation that was observed in the more rapidly degrading electrolytes containing some alumina. Experiments are continuing to explore the dependence of the susceptibility to chemical attack by sodium for electrolytes of different composition.

Indications are that NASICONs containing less phosphorous have increased stability towards sodium at higher temperatures. NASICONs are currently being tested for use in different environments; one potentially important application is as thin membranes in chlor-alkali cells. NASICONs have been found to be far more resistant to degradation by water than the sodium-beta aluminas, making them potentially suitable for applications involving aqueous electrolytes. In
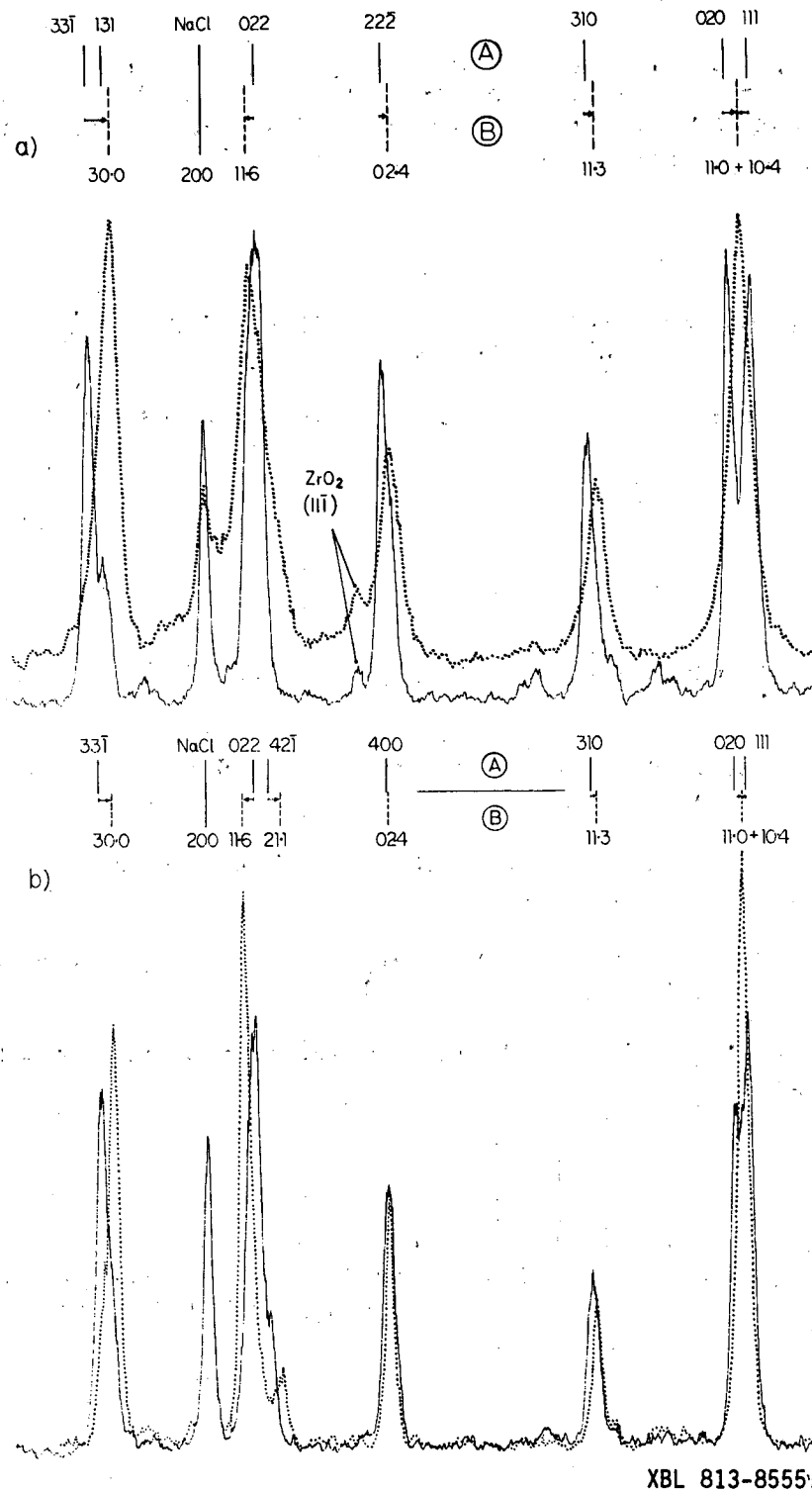
Fig. 1. Comparison of as-prepared (a) and sodium immersed (b) electrolyte
diffraction patterns. NaCl was used as a standard.
(a) $Na_3Si_2ZrPO_{12}$. (b) $Na_{3.1}Zr_{1.55}Si_{2.3}P_{0.7}O_{11}$.
Solid lines: as prepared; dotted lines: after immersion in Na, for
16 days at 300°C.

XBL 813-8555A

47

preliminary tests, NASICON membranes were subjected to current densities of up to 1 A/cm^2 for about 2 hours in a chlor-alkali cell, at 80°C. Static tests have shown that NASICONs are stable in saturated sodium chloride solutions and in sodium hydroxide solutions containing more than 30 wt% of sodium hydroxide.

REFERENCES

1. H. Y-P. Hong, Mat. Res. Bull. 11, 173, (1976); and M. B. Goodenough, H. Y-P. Hong, and J. A. Kafalas, Mat. Res. Bull. 11, 203 (1976).

2. U. Von Alpen, M. F. Bell, and W. Wichelhouse, Mat. Res. Bull. 14, 1317 (1979).

PUBLICATIONS

LBL Reports

H. Schmid, L. C. De Jonghe, and C. Cameron, "Chemical Stability of NASICON," LBL-12460, 1981.

L. C. De Jonghe, "The Transport Number Gradients in Solid Electrolyte Degradation," LBL-12070 Rev., 1981.

L. C. De Jonghe, L. Feldman, and A. Buechele, "Failure Modes of Sodium Beta Alumina," LBL-12445, 1981.

L. Feldman and L. C. De Jonghe, "Initiation of Mode I Degradation in Sodium Beta Alumina Electrolytes," LBL-12194, 1981.

L. C. De Jonghe and A. Buechele, "Chemical Coloration of Sodium Beta Alumina," LBL-12440, 1981.

Other Reports

L. C. De Jonghe, "Performance of Sodium Beta Alumina Solid Electrolytes in Na/S Cells," Proceedings of the 16th Intersociety Energy Conversion Engineering Conference, vol. 1, American Society of Mechanical Engineers, New York, 1981, p. 826.

Invited Talks

L. C. De Jonghe, "Factors Affecting the Performance of Solid Electrolytes," 4th US-DOE Battery and Electrochemical Contractors Conference, June 2-4, 1981, Washington, D.C.

L. C. De Jonghe, "Solid Electrolyte Batteries," American Ceramics Society, Berkeley, California, August 1981.

A.7 IMPROVEMENTS IN EFFICIENCY OF ALUMINUM REDUCTION CELLS

J. W. Evans, Investigator

The purpose of this investigation is to reduce the energy consumed in the electrolytic production of aluminum. Approximately 11 gigawatts of electrical energy are consumed in the U.S. in aluminum production; there is, therefore, considerable incentive to develop new technology that will minimize such energy consumption. We have developed a mathematical model that will predict the performance of an electrolytic cell producing aluminum. The model is based on the design of the cell and on operating parameters under the control of the cell user. By means of the model, rapid screening of alternative cell designs or operating practices can be carried out, promoting the development of cells consuming less electrical energy.

A.7.1 DEVELOPMENT AND TESTING OF THE MATHEMATICAL MODEL FOR THE HALL-HEROULT CELL

S. Lympany, H-C. Lee, and J. W. Evans

The major consumer of energy in the production of aluminum is the Hall-Heroult cell wherein electrical energy is used to electrolytically reduce aluminum oxide to metal. A mathematical model for the cell has been under development for some years, and has now reached the point of testing and refinement. Two performance parameters of interest from an energy consumption viewpoint are the current efficiency of the cell and the flatness of the interface between the two liquid layers in the cell (molten aluminum and the molten salt electrolyte). The former has an obvious connection with energy consumed per unit mass of product; the latter variable is important because "bowing" of this interface prevents the shortening of the anode-interface distance (shortening this distance reduces energy consumption by reducing resistive losses in the electrolyte).

Both the current efficiency and flatness of the interface are primarily dependent on electromagnetic forces that arise within the cell from the interaction of cell currents with magnetic fields. The magnetic fields arise from the currents flowing within the cell, surrounding conductors ("bus bars"), and surrounding cells. The current efficiency is less than 100% because the aluminum product has a slight solubility in the electrolyte, and this dissolved aluminum is transported to the anode, where it re-oxidizes. This transport of aluminum is due to turbulent convection in the electrolyte, and is, therefore, a function of the electrolyte flow, a flow driven by the electromagnetic forces. The model computes the current distribution in the cell, the magnetic field, the electromagnetic stirring forces, the velocity field of the electrolyte and aluminum, the bowing of the interface, and the current efficiency.

Figure 1 is typical of results recently generated by the model. It depicts the conductors for six cells (the cell of interest, two adjacent cells in the same line of cells, and the three closest cells in an adjacent line). The cell

NOVEL CELL (50-50)
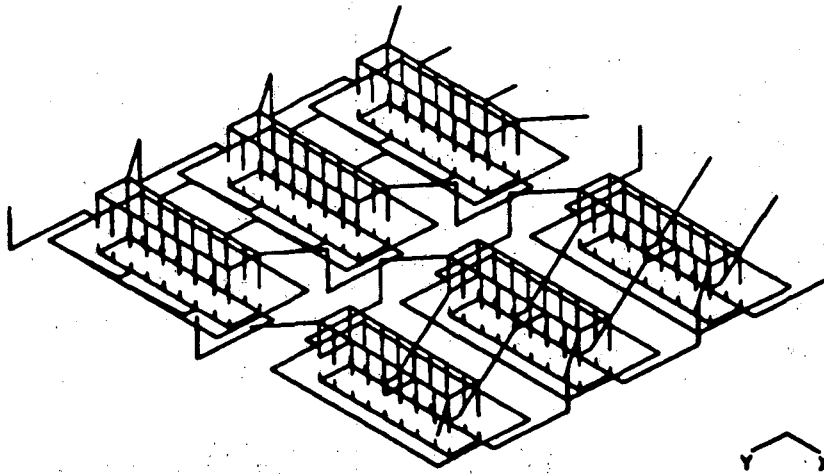
94.3% EFFICIENT
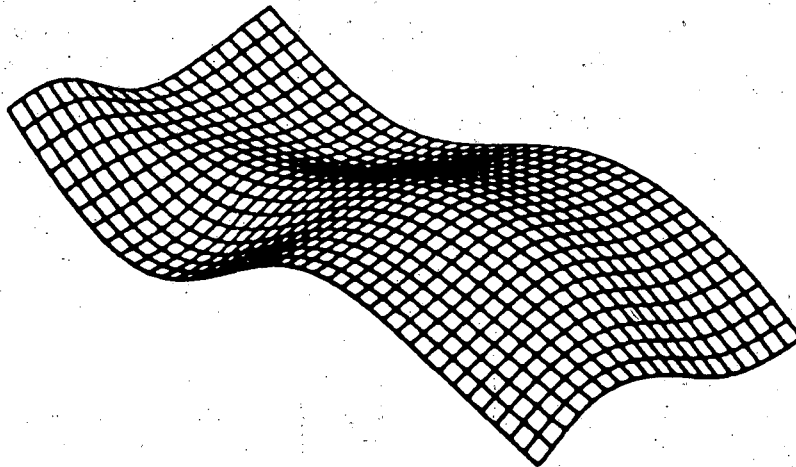
TROUGH-PEAK DISTANCE = 4.6 CM.
INTERFACE TOPOLOGY

XBL 823-8492

Fig. 1. A novel conductor arrangement for six Hall-Héroult cells and its
current efficiency. The lower half of the figure depicts the
computed shape of the interface between molten metal and salt
(vertical scale exaggerated for effect).

is different from the usual Hall-Héroult cell in that the current is taken out of the cell by conductors ("collector bars") passing out through the bottom of the cell; the usual cell has conductors passing out through the side. The computed current efficiency is 93.1% versus a best computed current efficiency of 91.7 for a comparable cell of conventional design. The aluminum-electrolyte for the novel cell is depicted in the lower half of Fig. 1. and is flatter than that of a comparable conventional cell (4.6 cm trough-to-peak distance versus 7.0 cm for the conventional cell).

WORK IN PROGRESS

The refinement of the mathematical model is continuing. An example of such refinement would be incorporation of vertical electromagnetic forces into the model. These forces are less important than the horizontal forces presently included. A second refinement that is being attempted is the incorporation of the effect of gas bubbles. These bubbles, generated at the anode, are thought to affect the circulation of electrolyte and, thereby, the current efficiency. An attempt is also being made to compare the predictions of the model with experimental measurements. Measurements on actual cells are not available, either because it is too difficult to make them in the cell environment (960°C with molten aluminum and salt present) or because information is retained by cell operators on proprietary grounds. A "cold" physical model of the cell is, therefore, being built. The model--approximately one-tenth the scale of a real cell--is to contain a low-melting-point alloy. Measurements of the velocity of the metal in the cold model can then be compared with computer predictions for the model.

PUBLICATIONS

Refereed Journals

J. W. Evans, Y. Zundelevich, and D. Sharma, "A Mathematical Model for Prediction of Currents, Magnetic Fields, Melt Velocities, Melt Topography and Current Efficiency in Hall-Héroult Cells," Metallurgical Transactions, 12B, 353 (1981).

D. P. Ziegler, M. Dubrovsky, and J. W. Evans, "A Preliminary Investigation of Some Anodes for Use in Fluidized Bed Electrodeposition of Metals," J. Appl. Electrochem., 11, 625 (1981).

LBL Reports

D. J. Coates, J. W. Evans, and S. S. Pollack, "Identification of the Origin of TiO_2 Deposits on Hydrodesulfurizaton Catalysts," LBL-13244.

D. J. Coates, J. W. Evans, and K. H. Westmacott, "Defects in Antiferromagnetic Nickel Oxide," LBL-13704.

Other Publications

M. Dubrovsky and J. W. Evans, "Fluidized Bed Electrowinning of Cobalt," in
Processes and Fundamental Considerations of Selected Hydrometallurgical
Systems, M. C. Kuhn, ed., AIME, New York, 1981.

J. W. Evans, S. Lympany, and D. Sharma, "A Mathematical Model of the Hall-
Heroult Cell and Calculations for Some Improved Cell Designs," Proceedings
of the 2nd World Congress of Chemical Engineering, Montreal, Canada, vol.
6, p. 211, 1981.

M. Dubrovsky, D. P. Ziegler, I. F. Masterson, and J. W. Evans, "Electro-
winning of Copper and Cobalt Using Fluidized Bed Cathodes," Proceedings of
Extraction Metallurgy '81, London, England, Institution of Mining and
Metallurgy, London, 1981.

Papers Presented at Meetings

J. W. Evans and M. H. Abbasi, "Diffusion and Radiation Heat Transport in Porous
Solids or Packed Beds," AIME Annual Meeting, Chicago, February, 1981.

J. W. Evans and M. Dubrovsky, "The Use of a Fluidized Bed Cathode for Selective
Deposition of Metals from Aqueous Solutions," AIME Annual Meeting,
Chicago, February, 1981.

A.8. ENGINEERING ANALYSIS OF GAS EVOLUTION IN ELECTROLYSIS

C. W. Tobias, Investigator

Gas evolution by electrolysis is one of the most common reaction types in
electrosynthesis. Electrically rechargeable batteries that also develop gases
on charge are now under development. This project is directed toward the
physical description and correlation of the behavior of electrochemically
generated gas-electrolyte emulsions, including the effect bubble streams have
on mass transport at electrode surfaces. Liberation of hydrogen, oxygen, or
chlorine from various substrates situated in a flow channel is observed under
intense illumination over broad ranges of current densities and flow rates.
The ohmic component of overpotential is measured and correlated to process
conditions. Understanding the behavior of bubble streams should lead to
improvements in the energy efficiency of gas-generating processes.

A.8.1 BUBBLE DYNAMICS AT ELECTRODE SURFACES

Philippe Cettou and C. W. Tobias

Gas evolution is usually accompanied by two effects brought on by the bubbles: an increase in mass transfer rate and a rise in ohmic losses. With the rising cost of energy, the latter has received growing attention. In a gas-evolving cell the bubbles responsible for the losses can be classified into two categories: bubbles in the bulk, which do not interact with the electrode surface, and bubbles in the vicinity of the surface, referred to as the bubble layer. Practical improvements of cell and electrode design have largely eliminated the resistance caused by bubbles in the bulk, but the bubble layer, with its characteristics not well known, remains a problem. The aim of this work is to advance the fundamental understanding of this bubble layer to stimulate improvements in cell performance.

We have chosen to study the first generation of bubbles at the electrode, which evolves just after the current is turned on. During this initial period of gas evolution, there are no bubbles in the bulk, and the events occurring at the electrode surface are easily observed. Also, we can measure the contribution of the bubble layer to the total cell resistance.[1] The evolution of hydrogen and oxygen was observed on three different electrode materials (gold, nickel, and stainless steel) and with three electrolytes (sodium hyroxide, sodium sulfate, and sulfuric acid). The influence of current density is also considered. The events associated with gas evolution-- nucleation, growth by diffusion and by coalescence, and departure from the electrode--occur rapidly and on a small scale. To reveal details of these events, high speed cinematography through a microscope is required.

The results of the motion picture studies are qualitative, but they reveal striking differences in nucleation density, residence time, and surface coverage from case to case, depending on conditions. For example, the residence time of bubbles at the electrode surface is always higher for oxygen than for hydrogen (Fig. 1). The average size of the bubbles depends strongly on the frequency of coalescence, which is in turn very sensitive to the nature of the electrolyte (Fig. 2). We have experimentally determined the dependence of electrical resistance upon electrode coverage; this compared favorably with predictions from established theoretical models. To minimize the resistance of a gas-evolving cell, both the electrode coverage and the bubble layer thickness should be lowered. Our studies show that strong coalescence achieves both of these desired effects. Thus, it is advantageous to operate under conditions in which coalescence readily occurs, as in our experiments with sulfuric acid. It appears worthwile to conduct further studies on bubble dynamics, particularly on coalescence phenomena.
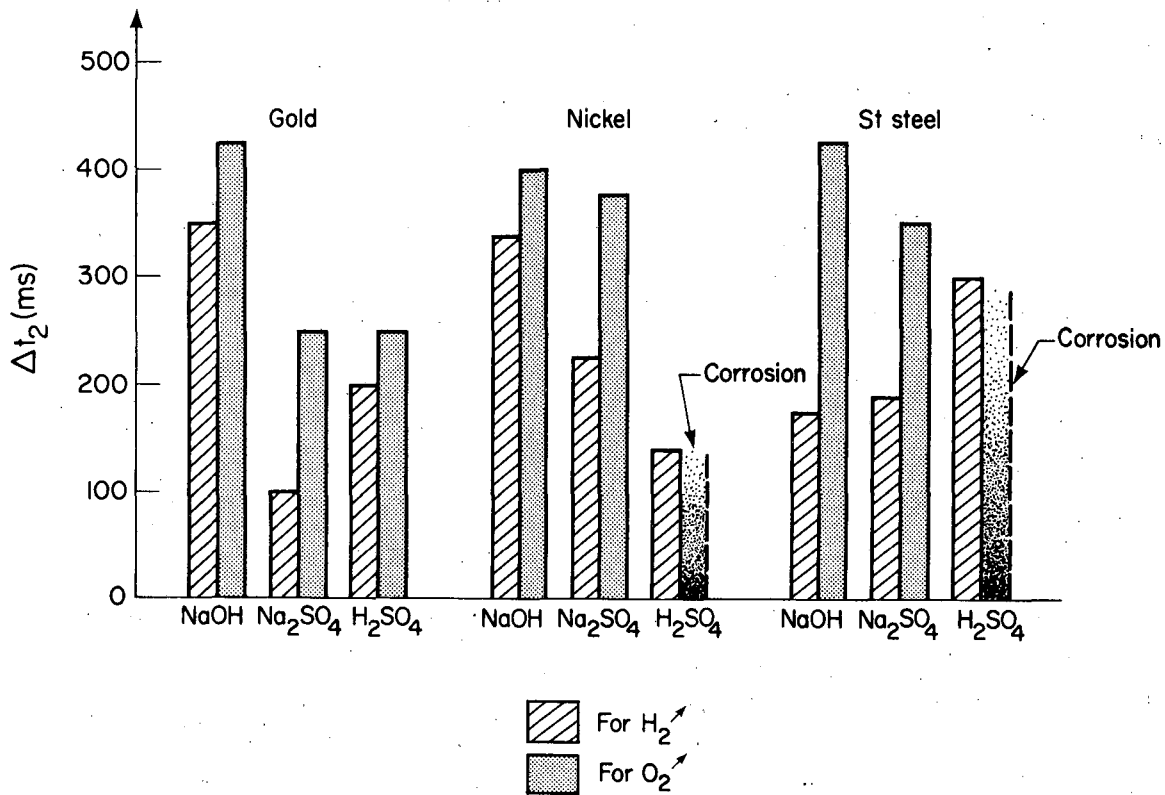
Fig. 1. Bubble residence times at the electrode surface. 1.25 cm³/cm²/ min.

Bubble Average Diameter

$G = 1.25 \, cm^3/cm^2 \, min$
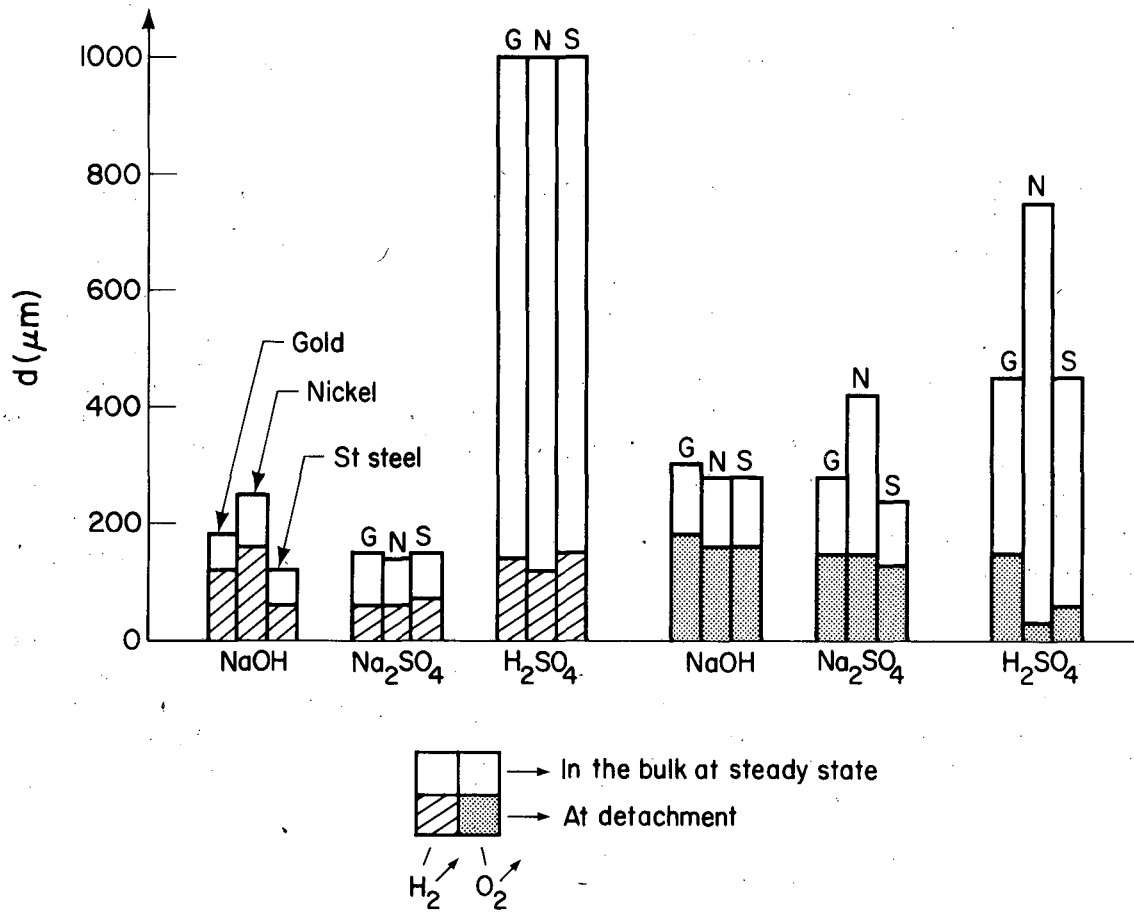
Fig. 2. Average bubble diameters at detachment and at steady state. $G = 1.25 \, cm^3/cm^2/min$.

XBL 819-1313

A.8.2 STUDIES OF BUBBLE DYNAMICS ON A MOSAIC ELECTRODE

D. Dees and C. W. Tobias

Electrochemically generated gas bubbles have a significant effect on mass transport at electrode surfaces. This effect is a result of the convection generated by bubble phenomena occurring at the electrode, which include growth, coalescence, disengagement, and ascension of the bubbles. Previous work[2] done in this laboratory has demonstrated that each of these phenomena can be produced separately and their effect on the mass transport measured. To obtain quantitative measurements of the change in mass transport, a novel mosaic electrode has been produced jointly by this laboratory and Hewlett-Packard Co. The electrode has been prepared on a silicon chip by integrated circuit technology. It consists of a 10 by 10 matrix of square platinum segments on 100-micron centers electrically isolated from each other (Fig. 3). The matrix is surrounded by 12 specially positioned segments and a relatively large buffer segment, all coated with platinum. The matrix simulates a continuous surface, but at the same time, one can control and measure the current and/or potential for each segment.

Changes in mass transfer rates as a result of a single bubble disengagement were studied with the mosaic electrode. All of the electrode segments were polarized cathodically in the mass transfer limiting region to reduce ferric- to ferrous-ion, just above the potential for hydrogen evolution. By reducing the potential of an individual segment approximately 300 mV below the other segments, a single bubble could be nucleated and grown. The change in mass transfer when the bubble disengaged was measured by monitoring the current at a segment where only the redox couple reaction was occurring. A typical plot is given in Fig. 4.

The rise time of the current is on the order of tenths of seconds. The initial rise is due to the collapse of the bubble contact area. There is a decrease in the current after the maximum below the baseline current. Theoretical results indicate that the decrease is caused by the convection generated by the ascension of the bubble from the horizontal plane.

REFERENCES

1. Philippe Cettou and Charles W. Tobias, "Bubble Dynamics at Electrode Surfaces," LBL-13632, in press.

2. Dennis Dees and Charles W. Tobias, "Mass Transfer Studies with a Micro-Segmented Electrode," MMRD Annual Report 1980, LBL-12000, 1981.

PUBLICATIONS

Refereed Journals

C. W. Tobias, "The Coming of Age of Electrochemical Engineering," AIChE Symposium Series, 204, 77 (1981).

P. C. Foller and C. W. Tobias, "The Effect of Electrolyte Anion Adsorption on Current Efficiencies for the Evolution of Ozone," J. Phys. Chem., 85, 3238 (1981). [Joel H. Hildebrand Centennial Issue].
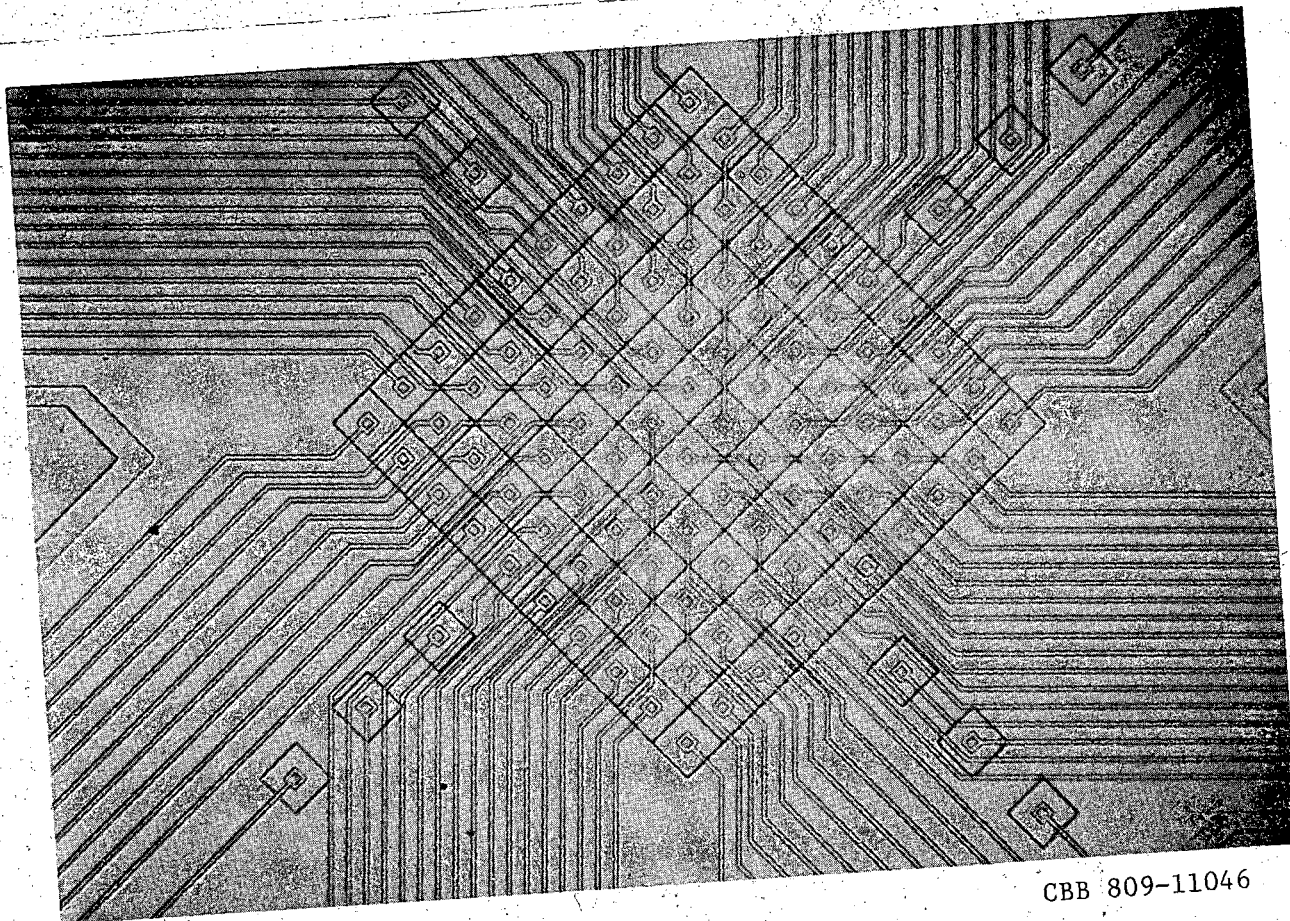
CBB 809-11046

Fig. 3. 10 x 10 matrix of electrically isolated platinum coated segments on 100-micron centers; produced on a silicon wafer in collaboration with Hewlett Packard Co.
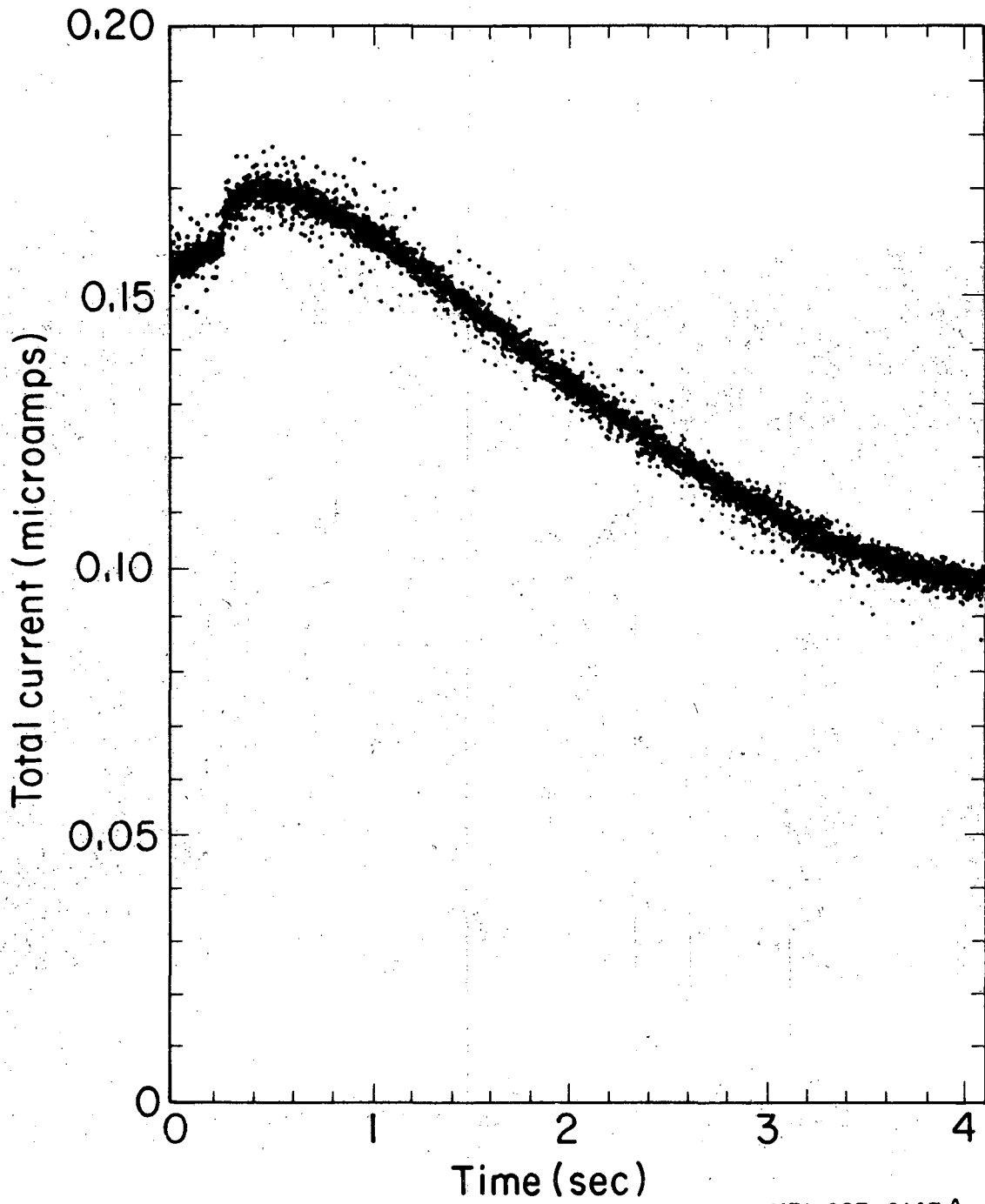
Fig. 4. Current to a segment 400 microns from the center of a disengaging
1485-micron diameter bubble.

58

LBL Reports

P. J. Sides (with C. W. Tobias), "Bubble Dynamics at Gas Evolving Electrodes"
    (Ph.D. Dissertation), University of California, Berkeley, LBL-11849.

C. W. Tobias and P. J. Sides, "Resistance of a Planar Array of Spheres; Gas
    Bubbles on an Electrode," submitted to the Journal of the Electrochemical
    Society.

P. Cettour and C. W. Tobias, "Bubble Dynamics at Electrode Surfaces,"
    LBL-13632, 1981.

Other Publications

H. Gerischer and C. W. Tobias, eds., Advances in Electrochemistry and
    Electrochemical Engineering, Wiley-Interscience, New York, vol. 13, 1981.

Invited Talks

P. J. Sides and C. W. Tobias, "A Close View of Gas Evolution," meeting of the
Electrochemical Society, Minneapolis, Minnesota, May 10-15, 1981; Extended
Abstracts, 81-1 (392), 985-986 (based on LBL-11849).

P. C. Foller and C. W. Tobias, "The Effect of Electrolyte Anion Adsorption
    on Current Efficiences for the Evolution of Ozone," meeting of the
    Electrochemical Society, Minneapolis, Minnesota, May 10-15, 1981; Extended
    Abstracts, 81-1 (478), 1182-83.

C. W. Tobias, "Electrochemical Engineering of Batteries," short course,
    Continuing Education Institute, Cherry Hill, New Jersey, June 22-26, 1981.

C. W. Tobias, "Prospects of the Electrochemical Technology," W. R. Grace
    Research Center, Columbia, Maryland, September 18, 1981.

Philippe Cettou and C. W. Tobias, "The First Generation of Bubbles on Gas-
    Evolving Electrodes," meeting of the Electrochemical Society, Denver,
    Colorado, October 11-16, 1981; Extended Abstracts, 81-2 (584), 1401 (based
    on LBL-13632).

C. W. Tobias, "On the Nature of Electrolytic Gas Evolution," Department of
    Chemical Engineering, University of Houston, November 6, 1981.

A.9 BATTERY ELECTRODE STUDIES

E. J. Cairns, Investigator

The purpose of this research is to study the behavior of electrodes used in secondary batteries and to investigate practical means for improving their performance and lifetime. Systems of current interest include ambient-temperature rechargeable cells with zinc electrodes ($Zn/NiOOH$, Zn/AgO, Zn/Cl_2, Zn/Br_2, Zn/Air and $Zn/Fe(CN)$) and rechargeable molten salt cells ($Li-Al/FeS$, $Li-Al/FeS_2$, $Li-Si/FeS$, $Li-Si/FeS_2$, and $Na/\beta''-Al_2O_3/NaCl-AlCl_3-SCl_4$). Life- and performance-limiting phenomena are studied under realistic cell operating conditions.

ACCOMPLISHMENTS DURING 1981

Investigations have centered on the zinc electrode, which exhibits satisfactory performance in rechargeable alkaline cells ($Zn/NiOOH$, Zn/AgO) but has an inadequate cycle life. The short lifetime and continual capacity loss of the zinc electrode are closely related to a phenomenon known as shape change, the redistribution of active material over the face of the electrode as the cell is cycled.

A.9.1 COMPUTER CONTROL OF ELECTRODE PERFORMANCE EXPERIMENTS

M. Katz, E. Cairns, and F. McLarnon

A computer-controlled testing system[1] for cycle-life testing of battery electrodes has been implemented. Eight modular-design current controllers were built and tested to verify independent control of up to eight channels from a single power supply. A variety of cycling regimes, including constant-current, constant-potential, constant-power, pulsed-power, etc., have been tested, and extensive data treatment and display capabilities are available.

Experiments have been planned to establish the effect of various charging techniques on the behavior of $Zn/NiOOH$ cells discharged under EPA urban driving profiles, an example of which is shown in Fig. 1. Typical test data for a 2.3 Ah $Zn/NiOOH$ cell cycled under a 10 Hz (9/1 off/on) pulsed charging regime are displayed in Fig. 2.

A.9.2 ZINC ELECTRODE RESEARCH

J. Nichols, E. Cairns, and F. McLarnon

Researchers have recognized[2] the need for reduced solubility of the zinc species in alkaline electrolyte to reduce shape change and improve the lifetime of $Zn/NiOOH$ cells. The focus of this project is to identify candidate electrolytes and characterize the effect of lowered zinc solubility on the cycle-life performance of $Zn/NiOOH$ cells.
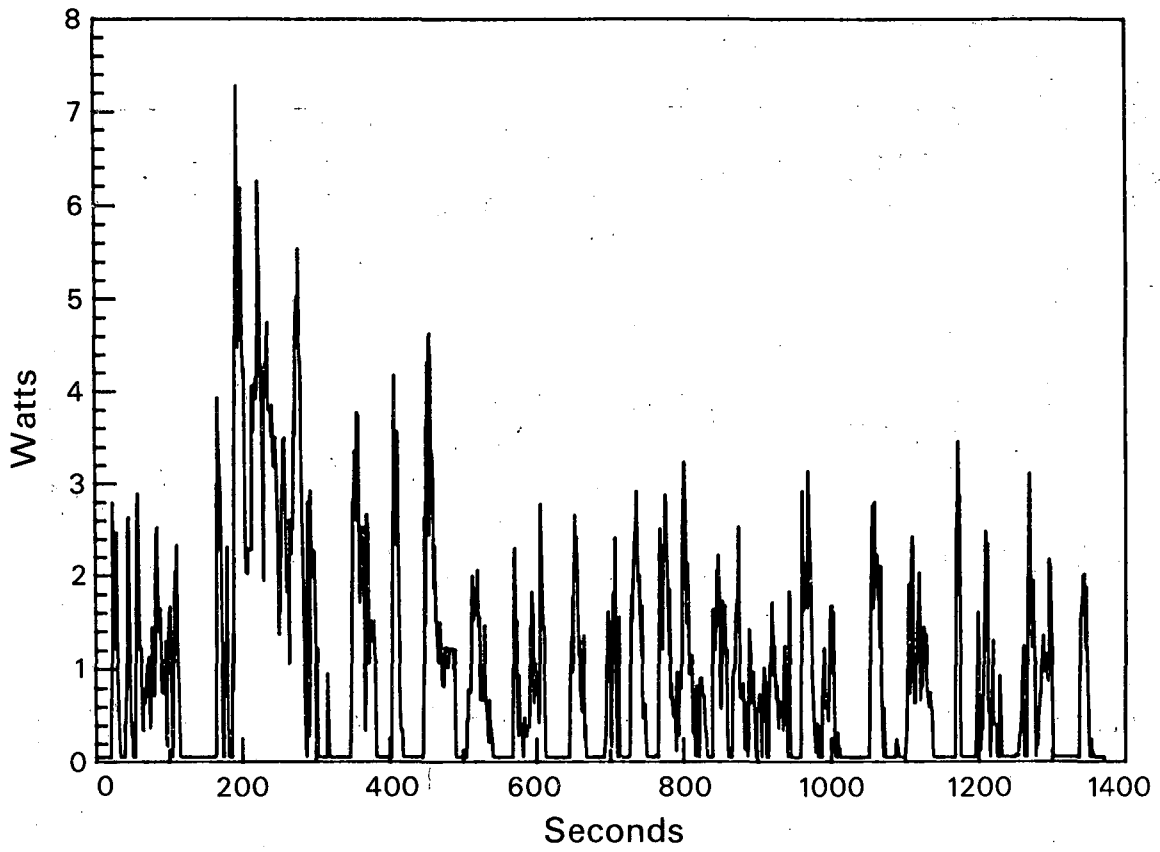
EPA URBAN DRIVING PROFILE: POWER

Fig. 1.   EPA urban driving profile with power requirement scaled to a 2.3 Ah cell.
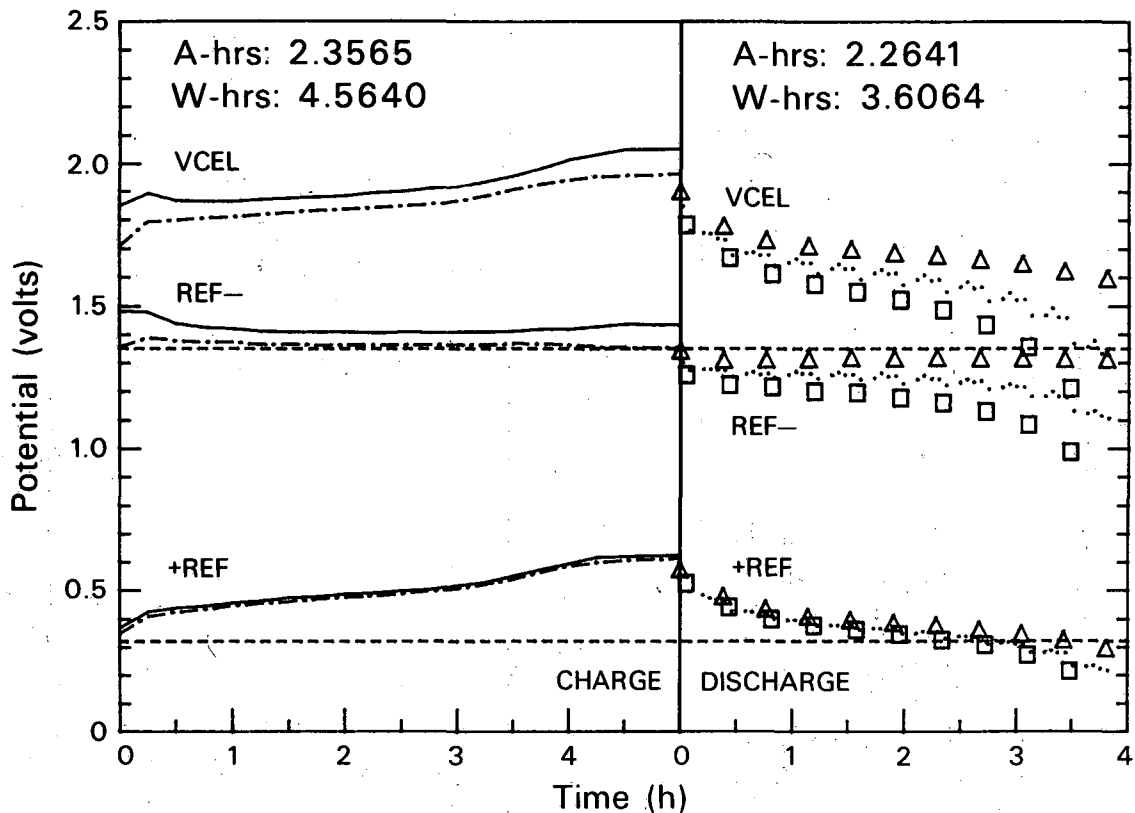
CELL VOLTAGE AND REFERENCE VOLTAGES FOR CYCLE 6 CELL 3A

Fig. 2. Charge/discharge curves for a 2.3 Ah Zn/NiOOH cell cycled with 10 Hz pulsed-current charging (9/1 off/on) and EPA power-profile discharging (Fig. 1).

CHARGE: Solid curves: measurements at current-on time.

Dotted-dashed curves: Measurements at current-off time

VCEL: NiOOH electrode vs. Zn electrode
REF-: Hg/HgO reference electrode vs. Zn electrode
+REF: NiOOH electrode vs. Hg/HgO reference electrode
Dashed lines: open-circuit values of REF- and +REF

DISCHARGE: Triangles: at base load (0.049 W)
Squares: at peak load (7.28 W)
Dots: at intermediate load (2.90 W)
Other notation as in charge portion of this figure.

The tri-electrode cell case[1] was redesigned to reduce machining costs and assure uniform electrode spacing (<2% thickness variation across the electrode). Cells were cycled to test Zn electrode fabrication techniques and practical cycling regimes. These electrodes were successfully photographed by x-ray transmission at 60 keV, and geometric distribution was then measured to calculate shape change rates, ranging from 0.6 to 1.0%/cycle, over 87 and 25 cycles, respectively. Five-hour charge rates and three-hour discharge rates were employed; typical charge/discharge curves are shown in Fig. 3.

Capacity loss of the zinc electrode is shown to correlate with the loss of ZnO material that occurs each cycle, as shown in Fig. 4. It is necessary to overcharge the Zn electrode each cycle to accommodate the inefficiency of the NiOOH electrode, and the repeated overcharging results in a gradual conversion of excess ZnO material to Zn metal.

A literature search has revealed several electrolytes with reduced hydroxyl-ion concentration, reduced zinc species solubility, and sufficient conductivity to warrant cycle testing to measure the shape-change rates. SAM, SEM, and electron microprobe analyses are underway to elucidate Zn electrode morphology and determine the distribution of various elemental species in the electrode.

A.9.3 MATHEMATICAL MODELING OF THE ZINC ELECTRODE

K. Miller, E. Cairns, and F. McLarnon

It has been found that two factors limiting cycle life of zinc batteries are shape change,[3-5] the redistribution of active material over the face of the electrode, and passivation,[6-7] caused by the formation of an oxide layer on the surface of the electrode. Two one-dimensional models have been proposed to account for these phenomena.[4-5] The purpose of the present study is to develop a two-dimensional mathematical model to account for changes in current density, electrode overpotential, and species concentrations both parallel to and normal to the electrode surface. The aim is to predict the degree of shape change and passivation as the electrode is cycled.

Experiments will be designed to test and verify the modeling results. Preliminary work is under way.

PLANNED ACTIVITIES FOR 1982

Cycle-life testing of Zn/NiOOH cells will be continued, and work on rechargeable molten-salt cells will begin.

REFERENCES

1. Energy and Environment Division Annual Report FY 1980, LBL-11990, 1981, pp. 3-40.
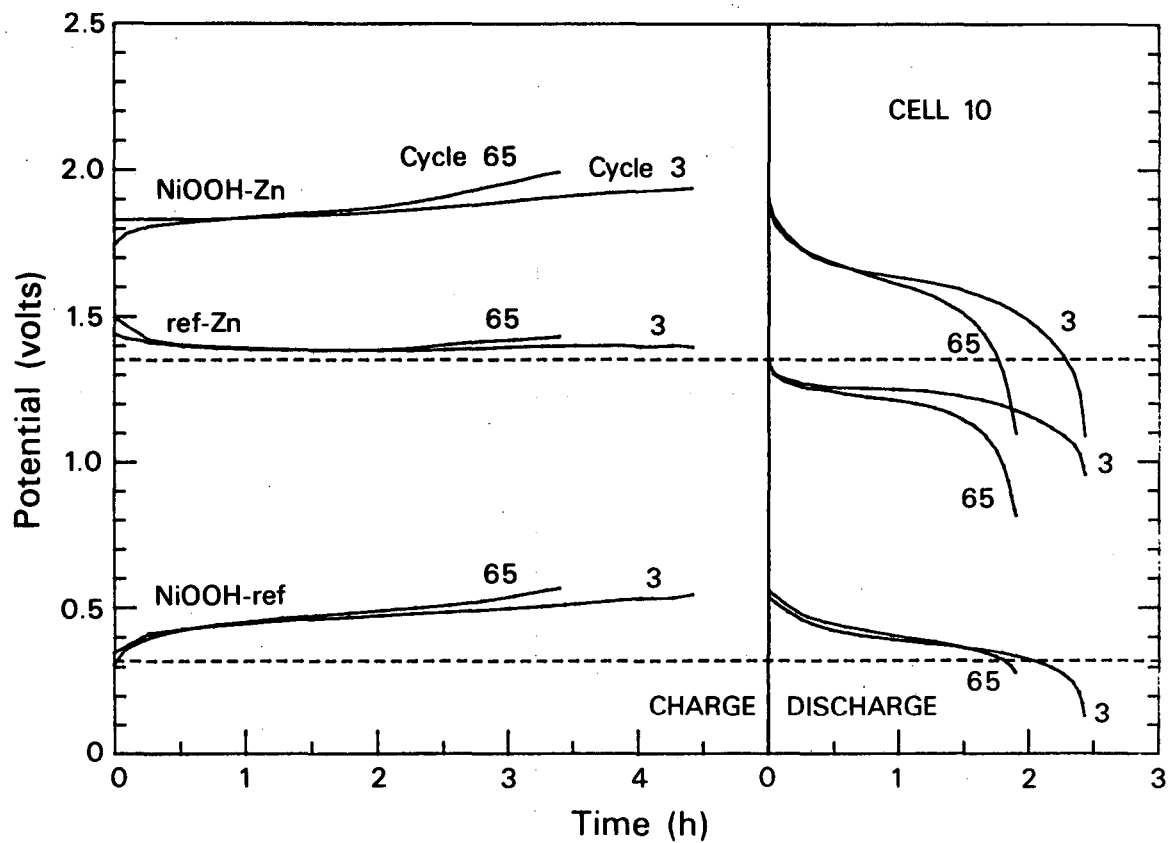
CONSTANT-CURRENT CHARGE/DISCHARGE CURVES

XBL 821-1767

Fig. 3. Charge/discharge curves for a 2.3 Ah Zn/NiOOH cell cycled under constant-current conditions.
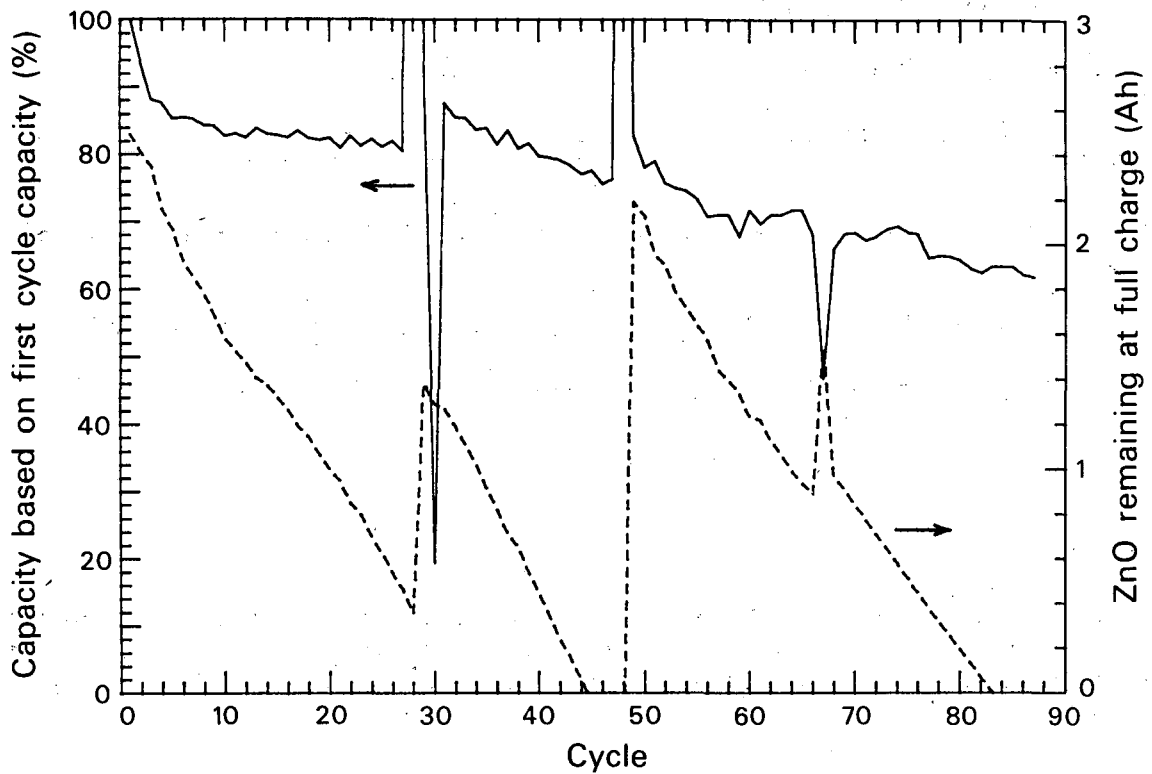
CELL CAPACITY AND ZINC OXIDE RESERVE

Fig. 4. Capacity degradation of a 2.3 Ah Zn NiOOH cell during cycling.

      ——— Cell capacity (percent of cycle 1 capacity)
      – – – ZnO reserve

2. J. McBreen and E. J. Cairns, in <u>Advances in Electrochemistry and Electrochemical Engineering</u>, H. Gerisher and C. W. Tobias, eds., vol. 11, Wiley-Interscience, pp. 273-353 (1978).

3. J. McBreen, J. Electrochem. Soc. <u>119</u>, 1620 (1972).

4. K. W. Choi, D. N. Bennion, and J. Newman, J. Electrochem. Soc. <u>123</u>, 1616 (1976).

5. K. W. Choi, D. N. Bennion, and J. Newman, J. Electrochem. Soc. <u>123</u>, 1628 (1976).

6. W. G. Sunu and D. N. Bennion, J. Electrochem. Soc. <u>127</u>, 2007 (1980).

7. W. G. Sunu and D. N. Bennion, J. Electrochem. Soc. <u>127</u>, 2017 (1980).

PUBLICATIONS

LBL Report

E. J. Cairns, "Batteries of the Future for Vehicle Applications," International Symposium on Electrochemistry in Industry--New Directions, Case Institute of Technology Centennial Celebration, Case Western Reserve University, Cleveland, Ohio, October 20-22, 1980. LBL-13108.

Other Publications

E. J. Cairns, "Requirements of Battery Systems," in <u>Materials for Advanced Batteries</u>, vol. 2, Murphy, Broadhead, and Steele, eds., Plenum Press, New York, 1980, pp. 3-27. (See also LBL-13576.)

E. J. Cairns, "Rechargeable Molten-Salt Cells," in <u>Proceedings of the Third International Symposium on Molten Salts</u>, vol. 81-9, Mamantov, Blander, and Smith, eds., The Electrochemical Society, 1981, pp. 138-157A. (See also LBL-11090.)

E. J. Cairns, "Secondary Batteries--New Batteries: High Temperature," in <u>Comprehensive Treatise of Electrochemistry</u>, vol. 3, Bockris, Conway, and Yeager, eds., Plenum Publishing Corporation, New York, 1981, pp. 421-504. (See also LBL-12031.)

E. J. Cairns and E. H. Hietbrink, "Electrochemical Power for Transportation," in <u>Comprehensive Treatise of Electrochemistry</u>, vol. 3, Bockris, Conway, and Yeager, eds., Plenum Publishing Corporation, New York, 1981, pp. 421-504. (See also LBL-12031.)

E. J. Cairns, "Molten Salt Batteries," in <u>Molten Salt Technology</u>, Lovering, ed., Plenum Publishing Corporation, New York (in press). (See also LBL-13641.)

Invited Talks

E. J. Cairns, "The Future of Conservation and Solar Programs under Reagan's DOE: A Panel Discussion," Energy & Environment Division Seminar Series, Lawrence Berkeley Laboratory, Berkeley, California, March 17, 1981.

E. J. Cairns, "Electrochemical Energy Storage," Energy & Chemistry Symposium, Annual Chemical Congress of the Royal Society of Chemistry, University of Surrey, Guildford, England, April 7-9, 1981. (See LBL-13199.)

E. J. Cairns, "Molten Salt Cells," "Solid Electrolyte Cells," and "Materials for Batteries," Electrochemical Engineering of Batteries Short Course, Cherry Hill, New Jersey, June 22-24, 1981.

E. J. Cairns, "ELectrochemical Energy Conversion--Batteries and Fuel Cells," panel at National Research Strategy Session, 16th Intersociety Energy Conversion Engineering Conference, Atlanta, Georgia, August 9-14, 1981.

E. J. Cairns, "Molten Salt Batteries," Molten Salt Battery Development Session, Gordon Conference on Molten Salts and Metals, Brewster Academy, Wolfeboro, New Hampshire, August 17-21, 1081.

E. J. Cairns, "Recent Research on Advanced Rechargeable Batteries," keynote lecture at 32nd Meeting of the International Society of Electrochemistry, Dubrovnik/Cavtat, Yugoslavia, September 13-20, 1981.

E. J. Cairns, "Advanced Batteries: A Step Toward Energy Independence," "What Physicists Do" Lecture Series, Sonoma State University, Rohnert Park, California, November 16, 1981.

E. J. Cairns, "The Electrochemistry of Zinc in Aqueous Electrolytes," meeting of Bay Area Electrochemists, Cupertino, California, November 24, 1981.

E. J. Cairns, "Thermally Regenerative Bimetallic Cells," DOE Thermally Regenerative Electrochemical Systems Workshop, Alexandria, Virginia, December 4, 1981.

B. INVESTIGATION OF THE NATURE AND STRUCTURE OF DEPOSITS ON LITHIUM AND
    ALUMINUM ANODES

DOE Program Manager	● A. R. Landgrebe
LBL Project Manager	● R. Muller
LBL Subcontractor	● University of Southampton (M. Fleischmann)
B&R Number	● AL-05-10-10
Contract Value	● 28K
Contract Number	● 4504410
Contract Term	● March 1, 1980 - February 28, 1981
Reporting Period	● March 1, 1980 - February 28, 1981
Objectives	● Study the interfaces between metal anodes and electrolytes using in situ Raman spectroscopy
	● Identify anodic oxidation products formed in metal/air cells

The objectives of this project were:

1. To carry out an in situ analysis of the interface between aluminum electrodes and aqueous alkaline electrolytes.

2. To extend the study to lithium electrodes and organic solvent/electrolytes.

3. To study the action of corrosion inhibitors in Al/concentrated alkali systems (the inhibitors reduce capacity losses). Similar studies on Li systems were also envisaged.

4. To investigate the surfaces of layers of alloy constituents on which the performance of aluminum is known to depend.

The methods of study, some of which were unique and all of which were pioneered at Southampton, were:

1. Laser Raman vibrational spectroscopy on dry and specifically on in situ electrode surfaces.

2. In situ infrared vibrational spectroscopy, using external modulated reflectance facilities and expertise provided by A. Bewick and colleagues.

3. The recently developed in situ x-ray diffraction system at Southampton.

4. Photocurrent spectroscopy as developed by L. Peter.

Initial studies focused on aluminum oxides and aluminum aqueous electrolyte interfaces, using laser Raman methods. We assembled background data, experimental methods, and expertise in the examination of thin aluminum oxide films over the pure metal and on some alloys. We confirmed, with spectroscopic evidence, the presence of γ-like alumina on electrode surfaces. It is worthy of note that, from a Raman spectroscopic viewpoint, these measurements are very difficult to make, the most sophisticated equipment and procedures being absolutely essential.

A detailed study is in hand on the nature of the oxide layers over alloys of aluminum. Currently, the alloy 98% Al/1% Si/1% other is of principal interest. We are fairly sure the oxides are somewhat mixed and may contain incorporated anions and probably sorbed or chemically combined water.

In addition to these basic steps, we concerned ourselves with the environment surrounding OH groups in or on the oxide surface. This proved rewarding, and we feel our recently developed electrochemical step/Raman data accumulation techniques will continue to be fruitful.

It is too early to conclude whether systematic results on the correlation of structural data with electrode polarization will be forthcoming. In particular, we were not able, at the time of writing, to use our multiplex laser Raman spectrometer because of its late delivery.

C. BIBLIOGRAPHY OF CONVECTIVE TRANSPORT CORRELATIONS

DOE Program Manager   • A. R. Landgrebe

LBL Project Manager   • C. Tobias

LBL Subcontractor   • Illinois Institute of Technology
(J. R. Selman)

B&R Number   • AL-05-10-10

Contract Value   • 36K

Contract Number   • 4511610

Contract Term   • April 1, 1981 – September 30, 1982

Reporting Period   • April 1, 1981 – November 1, 1981

Objectives   • Search the scientific and technical
literature for references on experi-
mentally established convective mass
transfer and heat transfer correlations

• Abstract, index, review, and publish as
a bibliography essential information
useful for the detailed analysis of
convective transport phenomena in energy
storage systems

A preliminary search of the most prominent electrochemical and chemical engineering journals since 1970 has been made with the specific objective of supplementing the available store of convective mass transfer correlations obtained by the limiting current method.[1] This search has resulted in 70 publications not previously recorded. A beginning has been made with a computer search convering a wide spectrum of journals, using the Lockheed DIALOG on-line bibliographic retrieval system.

The information in the publications collected thus far has been recorded on a disk file using the following nine-digit classification code: (1) flow containment (9 categories); (2) flow regime and phase (10 categories); (3) flow geometry (9 categories); (4) type of convection (10 categories); (5) electrode movement (6 categories); (6) electrode geometry, if single element (9 categories); (7) electrode geometry, if multiple element (6 categories); (8) reactant (10 categories); and (9) supporting electrolyte (8 categories).

The MIDASFILE system of Prime, Inc., has been adopted for index-sequential processing; some difficulties have been encountered in using this economical system, but we are trying to resolve them. It is expected that data filing can

resume in January, 1982, in time to accommodate the results of the extended search presently under way.

Preliminary contacts have been made to establish a panel of experts to advise on search procedures and to review the draft report (due March 1, 1982). Those contacted expressed a willingness to participate, but on a correspondence basis rather than as traveling consultants. Accordingly, the permission of DOE-LBL is being requested to organize the review on this basis. The final composition of the panel is expected to be complete by January 1, and a review of the search procedures used thus far will then be requested, to be followed by the review of the draft report in March.

REFERENCE

1. J. R. Selman and C. W. Tobias, Adv. Chem. Eng. 10, 211 (1978).

D. RESEARCH ON LEAD-ACID BATTERY ELECTRODES

DOE Program Manager	• A. R. Landgrebe
LBL Project Manager	• P. N. Ross
LBL Subcontractor	• Naval Research Laboratory (S. M. Caulder and A. C. Simon)
B&R Number	• AL-05-05-05
Contract Value	• 125K
Contract Number	• 4505710
Contract Term	• March 1, 1980 – February 28, 1981
Reporting Period	• March 1, 1980 – February 28, 1981
Objectives	• Continue investigation of the atomic structure of PbO_2
	• Study electrolyte stratification and its effect on cell performance
	• Investigate the effect of electrolyte concentration and current density on electrode reaction and microstructure
	• Study the coralloid structure that forms during cell cycling

For successful electric vehicle application, lead acid batteries require improved energy density and extended deep-discharge cycle life. Improved energy density can come from increased use of the active plate (electrode) material, which even in the latest batteries seldom exceeds 35-40%. Cycle life is also principally determined by the active plate material, i.e., by the reactions and physical changes that occur in the active material with cycling and cause it to lose capacity to accept charge. Rational approaches to significantly improving lead-acid battery performance must rely heavily, therefore, on understanding the reactions of this material.

This report describes several investigations to elucidate important reactions or transformations occurring in active plate material that are relevant to electric vehicle operation.

Formation of electrochemically inactive PbO_2 (i.e., a form of PbO_2 not reduced in plate discharge) is a substantial cause of positive plate capacity loss. Electrochemically active PbO_2 contains a proton species lacking in the

inactive form, as revealed by NMR results at the Naval Research Laboratory (NRL), and a neutron/x-ray diffraction structure determination was undertaken to establish the proton lattice location. This proved difficult. Although the first two steps--the high-resolution structure determinations of chemically prepared (inactive, non-proton bearing) β-PbO$_2$ and of α-PbO$_2$--were essentially completed (the α-PbO$_2$ data is being interpreted and the structure is expected to be published), the third step, comparison with the structure of electrochemically produced (and active) PbO$_2$, could not be completed in the contract period. The two "base line" structures and the computational and experimental procedures, however, were established, and future research, at NRL or elsewhere, may build on these results.

In a second major effort, the potential effects of high discharge rates in electric vehicles were investigated by comparing changes in the active material microstructure and plate capacity for positive and negative lead-acid plates cycled at discharge rates ranging from 18 to 2000 A/m^2. Comparisons were also made between pulsed (used in electric vehicles) and unpulsed discharge modes. The negative plate capacity decreased significantly with discharge rate, being about 2 times less for 2000 A/m^2 than 18 A/m^2 rates. Capacity also decreased with cycling, apparently because of development of reduced contact between the lead particles in the charged plate and/or formation of PbSO$_4$ passivating layers on the Pb particles during discharge, especially at high rates. The positive plate capacity was strongly affected by discharge rate, decreasing by 4 times in going from 18 A/m^2 to 2000 A/m^2 rates. Capacity losses with cycling were greater than with negative plates, and appeared to result largely from progressive formation of electrochemically inactive PbO$_2$ during cycling. Pulsed discharge was detrimental to plate capacity, but less for the negative plate than the positive plate. Careful analysis was made of the active material particle size, surface area, composition, and porosity to help explain plate performance under the different discharge rates.

The positive-plate active material has been shown in this laboratory, with both test plates and in-service batteries, to develop a characteristic coral-like, or coralloid, structure with cycling. This structure is densely packed, and PbO$_2$ in its interior is difficult to reduce on discharge, resulting in capacity loss. Limited experiments were undertaken to determine if coralloid formation could be prevented, or its dimensions reduced, by different methods or materials of plate preparation. Procedures were found that delayed coralloid formation, e.g., the use of tetrabasic lead sulfate as the initial plate material, but in each case, the coralloid ultimately formed as cycling continued.

The performance and microstructure of tubular battery plates were also studied, since this construction, although little used in the U.S., offers long cycle life. Results from this research indicate that prolonged preliminary soaking of tubular plates, as normally practiced by manufacturers, may be unnecessary. Also, bursting of tubes, a major cause of tubular plate failure, was shown to be primarily caused by corrosion of the current-collecting lead spline, with the corrosion products of higher volume than the original metal, and not by the normal volume change in active material that accompanies plate formation or cycling.

E. BASIC DEVELOPMENT OF NICKEL/ZINC BATTERIES

DOE Program Manager • A. R. Landgrebe

LBL Project Manager • F. R. McLarnon

LBL Subcontractor • Lockheed Missiles & Space Company (T. Katan)

B&R Number • AL-05-05-05

Contract Value • 93K

Contract Number • 4503610

Contract Term • April 1, 1980 - July 31, 1981

Reporting Period • April 1, 1980 - July 31, 1981

Objectives • Employ microscopy to evaluate the characteristic modes of failure and effects on electrode performance when model zinc/nickel oxide cells are cycled

• Provide fundamental data useful to zinc/nickel oxide battery developers

A series of experiments was conducted to establish governing processes in alkaline-nickel/zinc batteries. Specially designed microcells, acting as simulated pores, enabled in situ access to the dimensional domain and internal area of pores in porous nickel and zinc electrodes. These pore analogs were made with Lucite windows for optical microscopic viewing and with multiple, microreference electrodes for potential, position, and time measurements.

The primary current distribution was determined at 1 to 8 mA, indicating a penetration depth of 0.08 cm in a 1.0 x 0.0020 cm pore, 0.6 cm long.

The evolution of the secondary-current distribution was characterized by a reaction front that moved into the pore, followed by a zone of relatively lower reaction rate. This lower-rate region corresponded, optically, to the appearance and movement of a white, ZnO front. Precipitated ZnO caused blockage of the second kind, masking the pore surface and forcing the front inwards.

Concentration profiles could be obtained from the potentials of the micro-reference electrodes at open circuit, as shown in Fig. 1. The ZnO front extended about 2 mm into the pore, for the time and current of Fig. 1. Here, the OH^- concentration is increased above its initial concentration, from 7.7$\underline{M}$ to values up to 9.5$\underline{M}$. The release of OH^- from $Zn(OH)_2^{2-}$ during ZnO
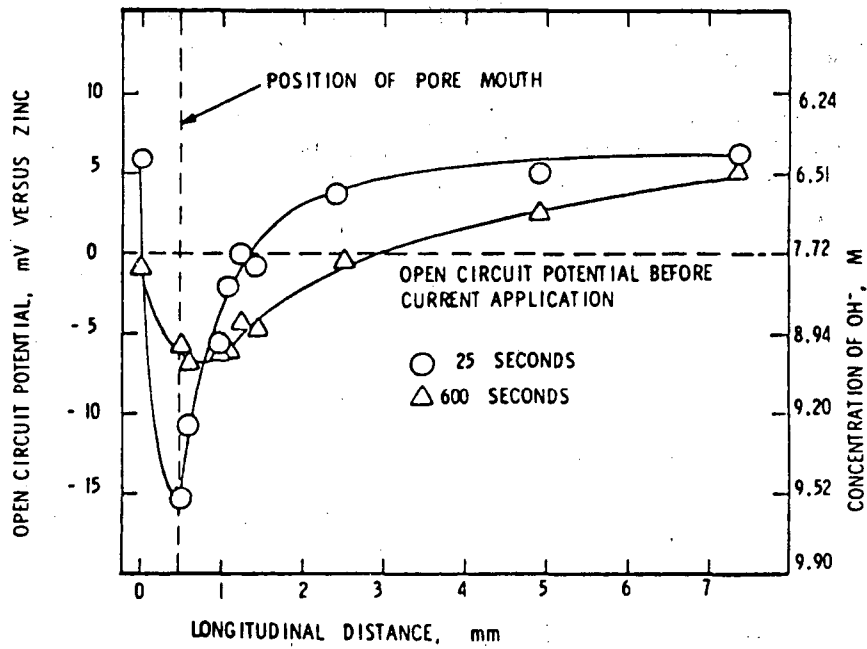
Fig. 1. Open circuit potentials after 86 sec at 1 mA. Corresponding concentrations are indicated at the right.

precipitation is evidently responsible for this perturbation in concentration. Relaxation of the (OH⁻) profile is shown after 600 seconds at open-circuit potential, Fig. 1.

Concentration cells were prepared to show that (OH⁻) changes on the order of those generated in the pores (Fig. 1), could generate corrosion currents and potential differences of up to 1.9 mA cm^{-2} and 40 mV. Simultaneous Zn deposition and dissolution and hydrogen evolution sustain the corrosion current.

Capillary cells were also prepared. These served several purposes: to observe the motion, by electrochemical displacement, of zinc fragments in the pores of separator material; to determine the current and potential domains of zinc morphological changes during deposition; and to obtain the law representing overall zinc dendrite growth. Typically, velocities of up to 5 μm sec^{-1} were obtained at 1200 mA cm^{-2}, and conversion from mossy to dendritic deposition occurred at 250 mA cm^{-2}. Mossy zinc has less overall porosity than dendritic zinc, 60% versus 90%, respectively.

For nickel electrodes, an optimum current density was found with reference to acquired charge when charge/discharge cycle times were fixed. A maximum of 38 mC cm^{-2} was obtained for twelve 1-minute cycles at 0.6 mA for a 1 cm x 0.6 cm electrode.

F. DEVELOPMENT OF A HIGH-RATE, INSOLUBLE ZINC ELECTRODE FOR ALKALINE BATTERIES

DOE Program Manager ● A. R. Landgrebe

LBL Project Manager ● F. R. McLarnon

LBL Subcontractor ● Energy Research Corporation (A. Charkey)

B&R Number ● AL-05-10-10

Contract Value ● 102K

Contract Number ● 4506710

Contract Term ● February 28, 1981 – February 28, 1982

Reporting Period ● November 1, 1980 – November 1, 1981

Objectives ● Determine the effect of electrolyte and electrode additives in lowering zinc solubility

● Characterize electrode/electrolyte combinations which exhibit lowered zinc solubility

● Evaluate insoluble zinc electrodes as a means to improve zinc/nickel oxide battery lifetime

The objective of this project is to investigate the insoluble zinc electrode as an approach to solving shape change problems in zinc-alkaline batteries. The program concentrates on the development of (1) zinc electrode and electrolyte formulations that result in insoluble discharge products, and (2) doped zinc oxides that prevent the formation of passive films in low KOH concentrations or that form more conductive anodic films during cycling.

Zinc oxide samples doped with 0.6 atom-% Sn, Co, La, Bi, Al, Pb, Cd, Ce, and Fe have been prepared, evaluated for solubility in 0-45% KOH, and electro-chemically evaluated as electrodes using cyclic voltammetry. Electrolyte formulations which contain K_3BO_3 and KF have also been screened for their effect on zinc solubility. Table 1 gives the solubility of several of these materials compared to pure ZnO and $CaZnO_2$. In 20% KOH, the solubility of the doped ZnO samples (with the exception of ZnO + Pb) were 37-45% lower than for pure ZnO and only 12-25% higher than for the relatively insoluble calcium zincate.

Table 1. Effect of KOH Concentration on the Solubility of Doped ZnO.

Solubility, in mg/ml (as ZnO)

Wt.% KOH	Pure ZnO	ZnO+Sn (003)	ZnO+Co (009)	ZnO+La (014)	ZnO+Pb (017)	CaZnO$_2$
45	135	129	125	101	98	107
35	85	73	61	59	71	66
30	66	43	47	–	–	53
20	33	18	20	21	57	16
15	16	9	9	–	–	–
10	7	5	8	9	5	–

A preliminary investigation has also been carried out, to determine the solubilities of other zinc compounds in 35% KOH as a precursor to evaluating their electrochemical bahavior as zinc electrodes. Compounds identified as possessing an extremely low solubility include ZnF$_2$ (2 mg ZnO/ml), Zn$_2$B$_5$O$_{11}$ (11 mg ZnO/ml) and ZnTiO$_3$ (5 mg ZnO/ml). An electrolyte composition, in which pure ZnO has a solubility of about 20 mg/ml, has also been found (26 wt% KOH + 8 wt% H$_3$BO$_3$ + 16 wt% KF).

The general current-potential behavior of sparingly soluble zinc oxide samples and doped zinc oxides is being studied for its dependence on repetitive potential sweeps, while electrolyte composition is being analyzed by cyclic voltammetry. The objective is to characterize the charge transfer and diffusion in the films formed during anodic polarization. The doped electrodes were repeatedly cycled using continuous potential scans in the range of -1.49 to -1.0 volts at the rate of 1 mV/sec. The variation of the current (Ip,a) with cycling was determined along with the coulombic efficiency for each sample. Figures 1 and 2 show cyclic voltammograms of the doped ZnO samples in 8.8$\underline{M}$ (35%) and 1.95$\underline{M}$ (10%) KOH at cycle 25. The most favorable performance has been achieved with the Sn-doped electrodes. An increase of both the Ip,c and Ip,a occurred up to 27 cycles. By the 80th cycle, the Ip,c and Ip,a declined 11% and 13%, respectively. The decline in peak current was less pronounced for the ZnO-Sn electrode than for the pure ZnO electrode. For pure ZnO, the Ip,c and Ip,a declined 30% and 33%, respectively, after 53 cycles. Performance of all other doped material tested was substantially poorer than for undoped ZnO. This in part may be due to the formation of a highly resistive oxide film on the electrode surface via a corrosion reaction. This speculation is supported by the presence of small capacitive discharge peaks on some of the cathodic scans in 1.95$\underline{M}$ and 4.2$\underline{M}$ KOH.
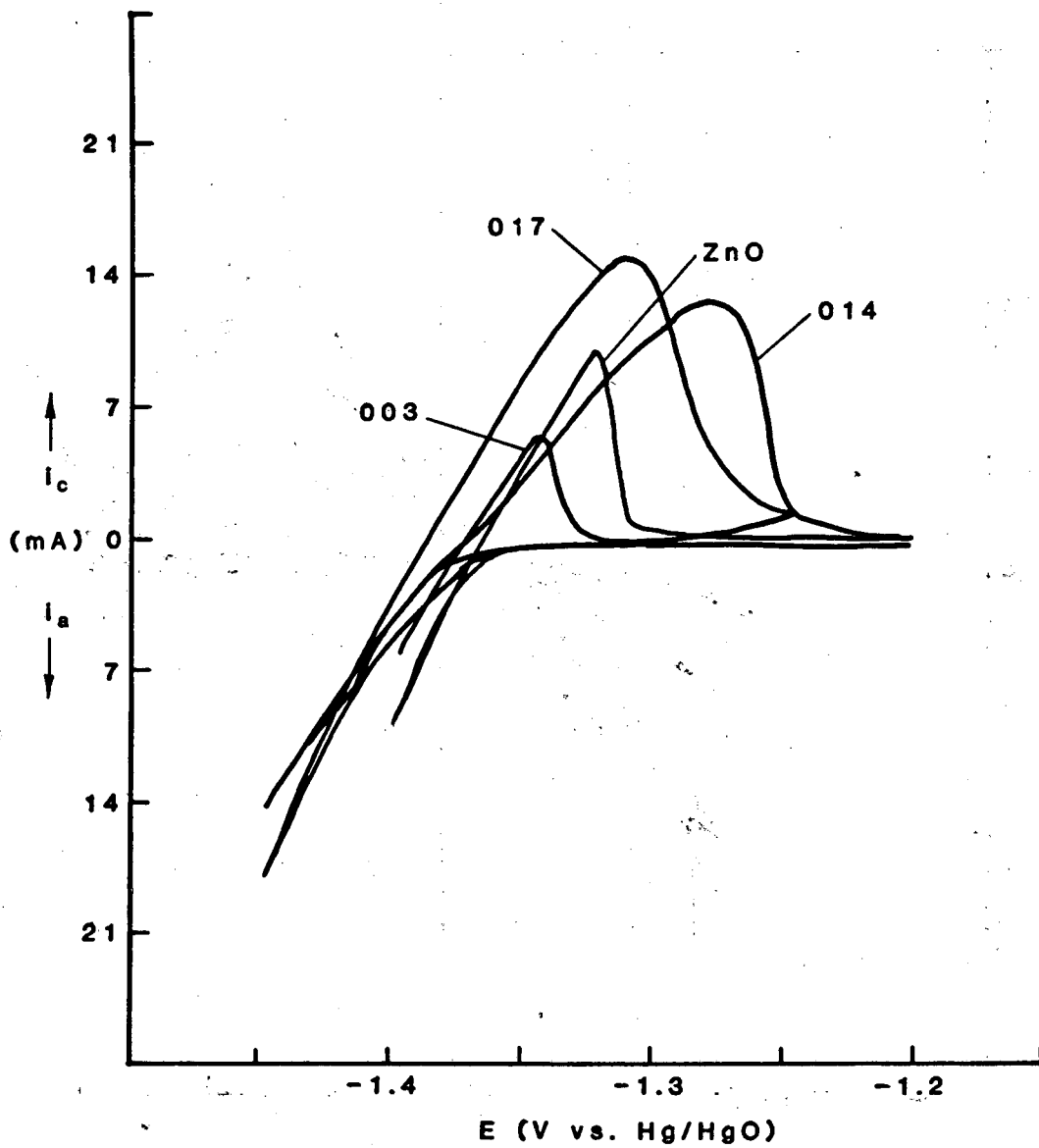
Fig. 1. Cyclic voltammogram in 8.8M KOH, cycle no. 25.
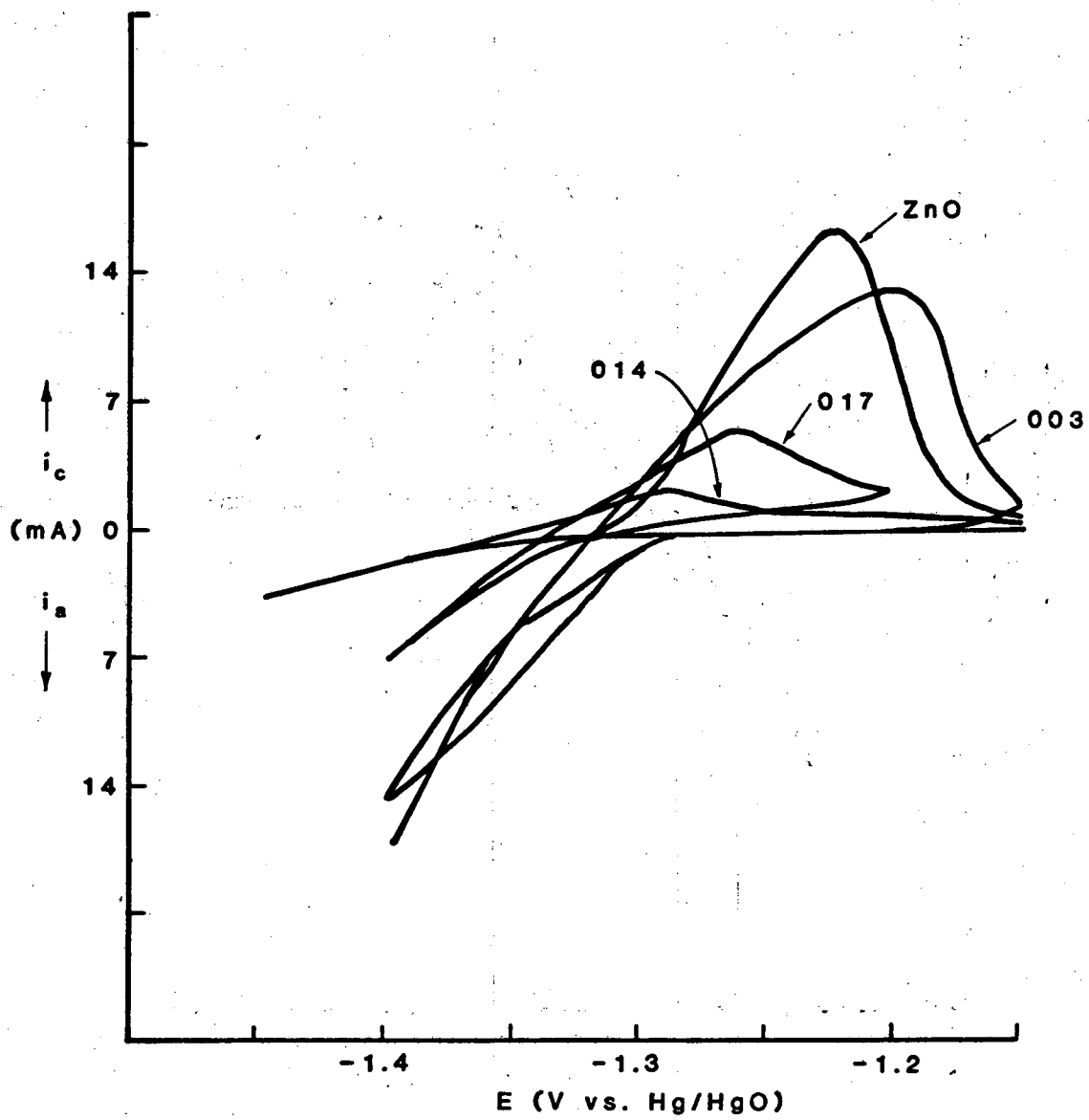
Fig. 2. Cyclic voltammogram in 1.95$\underline{M}$ KOH + Zn^{2+}, cycle no. 25.

On the basis of results obtained thus far, Sn-doped zinc-oxide electrodes are being prepared for evaluation under cyclic conditions in Ni-Zn cells. The evaluation will also include the $KOH/BO_3^{3-}/F^-$ ternary electrolyte composition.

G. SUPPORTED LIQUID-MEMBRANE BATTERY SEPARATORS

DOE Program Manager • A. R. Landgrebe

LBL Subcontractor • Castle Technology (J. P. Pemsler)

B&R Number • AL-05-10-10

Contract Value • 70K

Contract Number • 4512210

Contract Term • March 1, 1981 - February 28, 1982

Reporting Period • March 1, 1981 - November 1, 1981

Objectives • Screen liquid ion exchange reagents for optimal hydroxyl-ion exchange capacity, long-term stability, and hydroxyl-ion transport rates

• Investigate the behavior of zinc electrodes when used in conjunction with supported liquid membrane battery separators

• Evaluate supported liquid membranes as a means to suppress zinc dendrite penetration and improve the lifetime of zinc/nickel-oxide batteries

The objective of this project is to investigate the feasibility of developing a supported liquid membrane as an improved battery separator in the Ni/Zn secondary battery. The concept also has applications to other battery systems.

Supported liquid membrane separators consist of active hydroxyl-ion transport agents dissolved in a suitable organic solvent and absorbed into the pores of a microporous membrane. The transport-agent/solvent combination should ideally be highly specific for rapid transport of hydroxyl ions while preventing zincate diffusion. The inability of zinc to enter the membrane should prevent dendrites from growing further than the membrane/electrolyte interface on the zinc side of the cell.

In order to determine promising transport-agent/solvent combinations, screening tests were performed using shake-out experments with 35% KOH solutions and measuring hydroxyl-ion transport to the organic phase. Several possible transport agents were identified, and two of these have undergone

successful stability tests for 8 weeks at 50°C with no deterioration of transport properties. Many solvent systems for the transport agents have been studied for their stability in KOH solutions, solubility for transport agents, and ability to be retained within the membrane. A number of microporous membranes and similar structures have been examined as support hosts for the liquid membranes.

Hydroxyl-ion and zincate-ion transport rates were measured for a series of supported liquid membranes by measuring the change in pH with time in a two-compartment cell divided by the membrane separator. The hydroxyl-ion transport rates, or fluxes, were on the order of 10^{-9} mole cm^{-2} sec^{-1}. For comparison, Celgard 2500 alone transports hydroxyl ion at a rate of 3 x 10^{-8} mole cm^{-2} sec^{-1}. Zincate-ion transport through the same cells with a zincate-saturated 35% KOH solution on one side of the membrane was below our detectability limit, indicating a transport rate of less than 5 x 10^{-13} mole cm^{-2} sec^{-1}.

Resistivity measurements on the membranes were carried out in a small compression cell using the direct-current method. The separator resistance for one supported liquid membrane separator system was 187 ohm-cm^2. The separator resistance for the membrane loaded with solvent alone (without transport agent) was ~10^4 ohm-cm^2, while the Celgard 2500 alone was measured at 660 ohm-cm^2. These tests demonstrate the ability of the supported liquid membrane separators to transport hydroxyl ions at a moderate rate.

Nickel-zinc test cells built using supported liquid-membrane battery separators have been assembled and tested. Current densities have far exceeded 1 mA/cm^2. Work is now being directed at decreasing the membrane resistance so that the cell can be operated at 10 mA/cm^2.

H. TEMPERATURE LIMITATIONS OF SECONDARY ALKALINE BATTERY ELECTRODES

DOE Program Manager	●	A. R. Landgrebe
LBL Project Manager	●	F. R. McLarnon
LBL Subcontractor	●	SRI International (M. McKubre)
B&R Number	●	AL-05-10-10
Contract Value	●	46K
Contract Number	●	4505610
Contract Term	●	March 1, 1981 - February 28, 1982
Reporting Period	●	November 1, 1980 - November 1, 1981
Objectives	●	Determine the mechanisms of increased irreversibility of Ni associated with deep discharge at elevated temperatures
	●	Quantify the extent of Fe(II) and Fe(III) dissolution at elevated temperature
	●	Quantify dissolution and conduct further studies of passivation and current oscillation phenomena at Zn electrodes
	●	Provide fundamental data useful for the optimal design and operation of Fe/NiOOH and Zn/NiOOH batteries

Within the reporting period, investigations have continued into the mechanisms and kinetics of charge/discharge processes occurring at Ni, Fe, and Zn electrodes in KOH and LiOH/KOH electrolytes. Particular emphasis has been directed to possible failure modes induced by kinetic or thermodynamic effects at extremes of temperature.

Experiments have been performed at two concentration of KOH (30 and 35 wt%) at varying zincate concentrations and at six concentration ratios of LiOH/KOH designed to maintain a constant hydroxide-ion molality (5.0/23.3%, 3.5/26.8%, 2.5/29.2%, 1.5/31.5%, 0.5/22.8%, and 0.35%, Li/K). Measurements have been performed at five temperatures (0°, 25°, 50°, 75°, and 100°C).

Rotating Disk Electrode (RDE) and Rotating Ring Disk Electrode (RRDE) methods have been used in conjunction with potential step and potential sweep voltammetry, programmed rotation sweep, and ac impedance methods. Some of the more significant results may be summarized as follows.

Nickel

The principal temperature limitations associated with $Ni(OH)_2$ electrodes in KOH and LiOH are essentially the same as those observed previously in NaOH. That is, co-evolution of oxygen at high states of charge causes a substantial decrease in the electrode coulombic efficiency at elevated temperatures. An additional irreversible component is observed following deep or prolonged discharge at the nickel positive. This we attribute to a slow equilibrium between α- and β-$Ni(OH)_2$, with a decreased oxidation rate (and/or decreased oxygen overvoltage) for the α phase.

Iron

As observed previously in NaOH, the principal temperature limitations of iron electrodes in KOH and LiOH/KOH electrolytes are associated with oxidative and reductive dissolution in defined regions of potential, both during charge and discharge. Using RRDE methods we have been able to distinguish six dissolution processes in KOH. The temperature dependence at these dissolution processes is complex: some increasing, some decreasing, and others not changing significantly with temperature. The predominant dissolution processes occur outside the normal potential operating range of an alkaline iron negative electrode. Of the processes that occur at more negative potentials, dissolution associated with reactions $Fe \rightarrow Fe(OH)_2$, and $Fe \rightarrow Fe_3O_4$ are effectively uninfluenced by temperature in the range 25° to 75°C, while dissolution associated with $Fe(OH)_2 \rightarrow Fe_3O_4$ increased sixfold in the same temperature range.

By combining cyclic voltammetry with RRDE, ac impedance, and thermodynamic data, we have been able to deduce a detailed reaction sequence for iron in concentrated alkali. The high-temperature and low-temperature reaction sequences are found to be significantly different.

Zinc

The influences of hydrodynamic conditions and zincate concentrations on the dissolution of zinc have been examined extensively, in addition to the effects of KOH concentration and temperature.

The initial discharge of zinc is controlled by two terms: one convection-dependent, and the other convection-independent. We associate the convection-dependent term with a porous pre-passive film, the thickness of which is determined by a dynamic equilibrium between the film formation rate ($\propto$ discharge current) and dissolution rate ($\propto$ diffusion layer thickness). At a constant rotation speed, the film resistance decreases monotonically with increasing temperature.

The convection-independent term is associated with the charge-transfer process. This resistance decreases with increasing dissolved zinc concentration, suggesting that the product (zincate) catalyzes the discharge. The presence of an inductive loop in the measured impedance spectrum also provides evidence that the reaction is auto-catalytic. The dissolution of zinc thus proceeds in two one-electron steps, the first step involving a reaction between Zn metal and a Zn(II) dissolved species to produce an adsorbed Zn(I) intermediate.

PUBLICATION

M.C.H. McKubre and D. D. Macdonald, "The Dissolution and Passivation of Zinc in Concentrated Aqueous Hydroxide," J. Electrochem. Soc., 3, 524 (1981).

I. THERMODYNAMIC FRAMEWORK FOR ESTIMATING THE EFFICIENCIES OF ALKALINE
   BATTERIES

DOE Program Manager	●	A. R. Landgrebe
LBL Project Manager	●	F. R. McLarnon
LBL Subcontractor	●	Ohio State University (D. Macdonald)
B&R Number	●	AL-05-10-10
Contract Value	●	65K
Contract Number	●	4505110
Contract Term	●	March 1, 1980 - February 28, 1982
Reporting Period	●	November 1, 1980 - November 1, 1981
Objectives	●	Develop the thermodynamic framework required for the the proper evaluation of overall thermal, coulombic, and voltage efficiencies of alkaline batteries as a function of concentration and temperature
	●	Provide fundamental data useful for the optimal design and operation of Fe/NiOOH, Zn/NiOOH, and metal/air batteries

The important thermodynamic parameters that characterize the limiting
theoretical performance of a battery system are the change in Gibbs free
energy, change in entropy, and the change in enthalpy of the electrode and cell
reactions. These quantities are directly related to the voltage and the
coulombic and thermal efficiencies of the battery system. Therefore, quanti-
tative assessment of the efficiencies of various alkaline battery systems
requires a detailed knowledge of the thermodynamic properties of the electrode
materials in concentrated hydroxide solutions over a wide range of concentra-
tions and temperatures. Concentrated solutions of alkali hydroxides exhibit
non-ideal behavior, i.e., the activity of the solvent (water) cannot be assumed
to be unity (Raoult's law standard state). Also, the activity of the solute
(alkali-metal hydroxide) varies with solute concentration and temperature in a
non-ideal manner because short-range interactions become significant when the
mean distance between the solute particles is small (i.e., when the concentra-
tion of solute is high). Furthermore, the activity of water in concentrated
solutions depends upon the identity of the cation (Li^+, Na^+, K^+),
contrary to the behavior in dilute systems. The cation also affects the
activity coefficient of the hydroxide ion (or $\gamma_\pm$) in solution because of ion-
pair formation, and ion pairing increases along the series $K^+ < Na^+ < Li^+$.
Therefore, consideration of the non-ideal behavior of concentrated hydroxide
solutions is essential for determining the thermodynamic stability and electro-
chemical performance of battery electrodes in concentrated hydroxide solution.

In this study, we are computing the thermodynamic properties of iron, nickel, zinc, aluminum, and lithium in concentrated (1-12 molal) lithium hydroxide, sodium hydroxide, and potassium hydroxide solutions over the temperature range -20°C to 120°C.

We have reviewed and assessed the data in the literature for vapor pressure, activity coefficient, and other thermodynamic functions for concentrated LiOH, NaOH, and KOH solutions at temperatures over the range -20°C to 120°C. Sufficient vapor pressure data are available over the desired concentrations (1-12 molal) and temperatures (-10°C to 120°C) for NaOH and KOH. However, insufficient vapor pressure data are available for LiOH to generate the required thermodynamic function. Therefore, an experimental apparatus has been constructed to determine vapor pressure data for concentrated LiOH solutions (1-10 mol kg^{-1}) at various temperatures between -20°C and 120°C.

THERMODYNAMIC FUNCTIONS FOR CONCENTRATED HYDROXIDE SOLUTIONS

The activity of water, a_w, is determined by Eq. (1); some values are listed in Table 1:

$$a_w = \frac{P_{soln}}{p^°} \quad , \tag{1}$$

where p_{soln} and $p^°$ are the vapor pressures of solution and pure solvent, respectively; this is the Gibbs-Duhem formula.[1] The activity of solute is determined by integrating this equation to yield:

$$\ln\gamma_\pm = -(1-\phi) - 2 \int_0^m \left(\frac{1-\phi}{\sqrt{m}}\right) d\sqrt{m} \quad , \tag{2}$$

where $\gamma_\pm$ is the stoichiometric mean molal activity coefficient, and ϕ is the osmotic coefficient for the medium. This latter quantity is related to the activity of water by Eq. (3):

$$\phi = -1000 \ln a_w/M\nu m \quad , \tag{3}$$

where M is the molecular weight of water and ν is the number of ions into which the electrolyte dissociates in solution.

At low concentrations, ϕ was calculated from Debye-Hückel theory using Eq. (4):

$$(1-\phi)\ \sqrt{m}\ = 0.767\ A\ \sqrt{d_0}\ \cdot \sqrt{m}\ \ , \qquad\qquad (4)$$

where d_0 is the density of the solvent, and

$$\sigma_m = \sum_{n=1}^{\infty}\ \frac{3n}{n+2}\ (-A_m' \cdot \sqrt{m})^{n-1}\ \ . \qquad\qquad (5)$$

Debye-Hückel coefficients are given by

$$A = 1.814 \times 10^6/(DT)^{3/2};$$

$$A'_m = 153 \cdot \sqrt{DT}\ \ ,$$

where D is the dielectric constant of water at the temperature of interest.

The mean ionic activity coefficient $(\gamma_{\pm}^{*})$ is determined by Eq. (6) as reported by Helgeson.[2]

$$\gamma_{\pm}^{*} = \frac{\gamma_{\pm}}{(1-\alpha_{MOH})}\ \ , \qquad\qquad (6)$$

where α_{MOH} is the degree of association of the solute, defined by

$$\alpha_{MOH} = \frac{m_{comp}}{m_{MOH}}\ \ , \qquad\qquad (7)$$

where m_{MOH} and m_{comp} are the stoichiometric concentration and concentration of associated metal hydroxide, respectively. Values for $\gamma_{\pm}$ and $\gamma_{\pm}^{*}$ as a function of concentration and temperature for NaOH and KOH are reported in Table 1.

The pH values for concentrated hydroxide solutions as a function of temperature have been calculated using Eq. (8), the detailed derivation of which has been given elsewhere[3]:

Table 1. Activity of water and stoichiometric ($\gamma_\pm$) and mean ionic ($\gamma_\pm^*$) activity coefficients of metal hydroxides as a function of concentration and temperature.

NaOH

MOH Conc. Mole kg^{-1}	-10.0°C			40.0°C			80.0°C			120.0°C		
	a_w	Log $\gamma_\pm$	Log $\gamma_\pm^*$	a_w	Log $\gamma_\pm$	Log $\gamma_\pm^*$	a_w	Log $\gamma_\pm$	Log $\gamma_\pm^*$	a_w	Log $\gamma_\pm$	Log $\gamma_\pm^*$
1.0	0.9628	-0.1381	-0.1369	0.9657	-0.1887	-0.1868	0.9665	-0.2055	-0.2042	0.9673	-0.2215	-0.2204
2.0	0.9304	-0.1581	-0.1548	0.9327	-0.2032	-0.1988	0.9339	-0.2228	-0.2198	0.9350	-0.2415	-0.2387
4.0	0.8387	-0.0370	-0.0366	0.8417	-0.1132	-0.1104	0.8554	-0.1631	-0.1599	0.8630	-0.2117	-0.2075
6.0	0.7214	0.1510	0.1599	0.7441	0.0261	-0.0263	0.7640	-0.0652	-0.0644	0.7838	-0.1537	-0.1502
8.0	0.5905	0.3711	0.4311	0.6303	0.1874	0.2018	0.6655	0.0482	0.0488	0.7006	-0.0847	-0.0833
10.0	0.4578	0.6149	0.7650	0.5143	0.3630	0.4209	0.5656	0.1693	0.1778	0.6168	-0.0107	-0.067
12.0	0.3354	0.8766	1.1301	0.4044	0.5475	0.6725	0.4702	0.2929	0.3213	0.5358	0.0646	0.0658

KOH

MOH Conc. Mole kg^{-1}	-10.0°C			40.0°C			80.0°C			120.0°C		
	a_w	Log $\gamma_\pm$	Log $\gamma_\pm^*$	a_w	Log $\gamma_\pm$	Log $\gamma_\pm^*$	a_w	Log $\gamma_\pm$	Log $\gamma_\pm^*$	a_w	Log $\gamma_\pm$	Log $\gamma_\pm^*$
1.0	0.9236	0.4764	0.4765	0.9623	-0.1447	-0.1447	0.9645	-0.1827	-0.1827	0.9627	-0.1571	-0.1571
2.0	0.8651	0.7205	0.7208	0.9078	0.0398	0.0398	0.9120	-0.0178	-0.0178	0.9135	-0.0209	-0.0209
4.0	0.7480	1.0219	1.0233	0.7988	0.2693	0.2694	0.8071	0.1883	0.1883	0.8150	0.1515	0.1515
6.0	0.6309	1.2594	1.2627	0.6898	0.4500	0.4502	0.7021	0.3510	0.3510	0.7165	0.2887	0.2887
8.0	0.5138	1.4885	1.4945	0.5808	0.6220	0.6226	0.5972	0.5057	0.5057	0.6180	0.4192	0.4192
10.0	0.3967	1.7374	1.7474	0.4717	0.8036	0.8048	0.4922	0.6677	0.6679	0.5196	0.5549	0.5549
12.0	0.2796	2.0401	2.0564	0.3627	1.0119	1.0143	0.3872	0.8510	0.8513	0.4211	0.7058	0.7059

$$pH_T = \log \frac{\gamma}{2K\gamma_{\pm}^{*2}} + \log \left[\left(1 + \frac{4K\ \gamma_{\pm}^{*2}}{\gamma}\ m_{MOH}\right)^{1/2} -1 \right]$$

$$-\log a_w - \log \gamma_{\pm}^{*} \quad , \tag{8}$$

where K is the association constant at temperature T and at the saturated vapor pressure of the solution, γ is the activity coefficient of the associated species, and Q_w is the ionic product of water.

Association constants for NaOH and LiOH as a function of concentration and temperature have been estimated by extrapolating the data of Gimblet and Monk.[4] Precise association constants for KOH are not available in the literature. The kinetic studies of Bell and Prue[5] and the conductivity data of Darken and Meier[6] indicate that KOH dissociates completely. On the other hand, we have computed association constants for KOH from the corresponding data for LiOH and NaOH by considering the variation of the association constant with ion size.[7] The value of activity coefficient (γ) of the neutral complex has been taken as equal to one, as indicated by Debye-Hückel theory[1] and experiment.[8]

An important feature of these calculations is that the pH is predicted to vary nonlinearly with composition and to pass through a maximum at $m = 4-6$ mole kg^{-1} in the case of NaOH and at $m = 3-5$ mole kg^{-1} in the case of KOH (Fig. 1). This demonstrates that, at high concentrations, the pH of the medium falls, even though the stoichiometric concentration of the hydroxide increases.

THERMODYNAMIC FUNCTIONS FOR METAL/HYDROXIDE SYSTEMS

The thermodynamic properties of metals in concentrated hydroxide systems have been determined by considering reactions in the general form

$$aA + (x-Z)\ H^+ + (Z/2)\ H_2 = bB + cH_2O \quad . \tag{9}$$
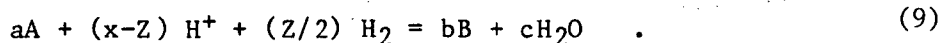
The equilibrium expression for this reaction is

$$E_e = E_e^o + \frac{2.30\ RT}{zF}\ (a \cdot \log a_A - b \cdot \log a_B - c \cdot \log a_w)$$

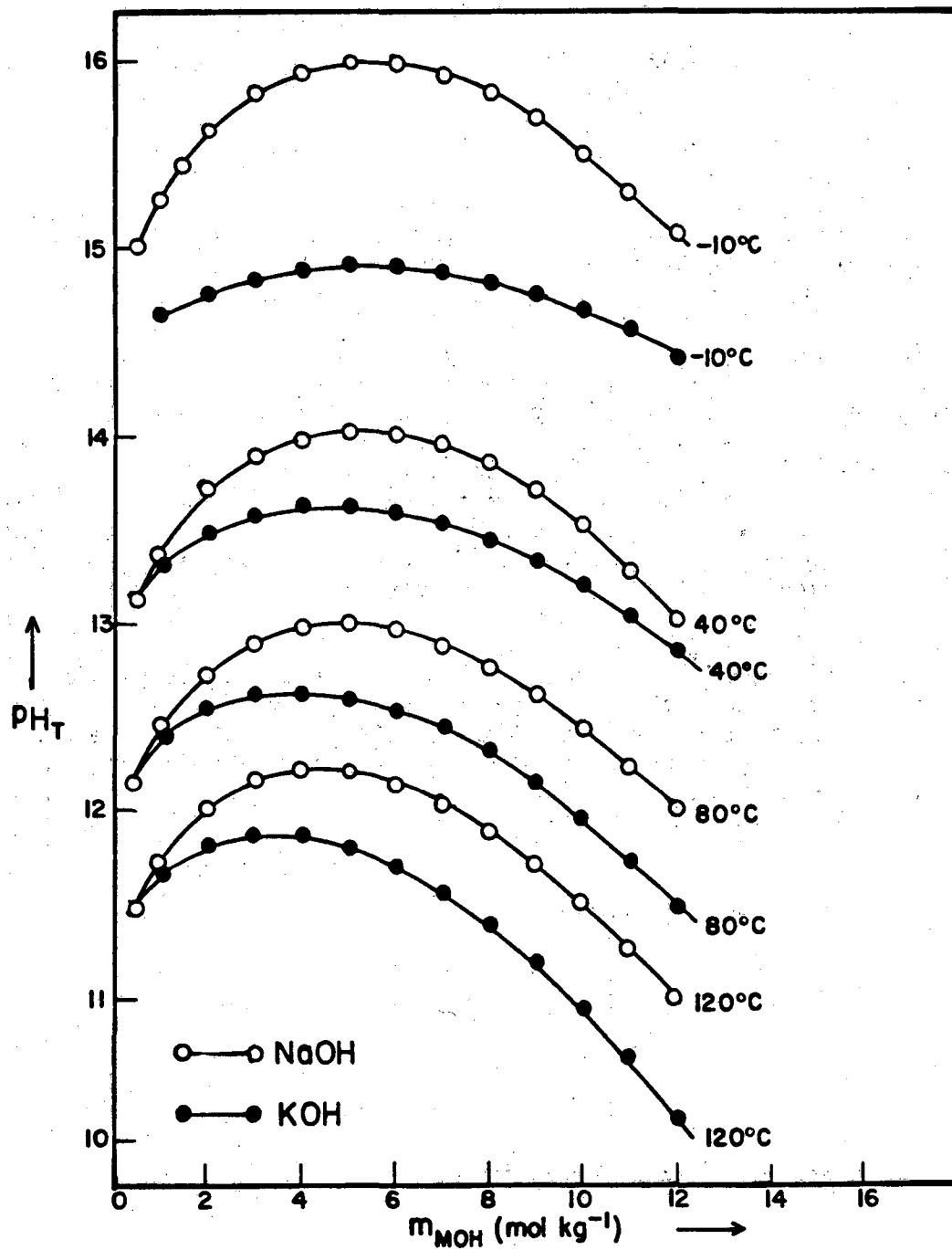$$- \frac{2.30\ RT}{zF} \cdot pH_T \quad , \tag{10}$$

Fig. 1. Variation of pH with composition at different temperatures.

where

$$E_e^\circ = - \Delta_R G^\circ / zF \qquad , \qquad (11)$$

and a_w and pH_T are given by Eqs. (1) and (8), respectively. Details of these calculations are reported elsewhere.[9]

The various reactions to be considered in describing the equilibrium properties of Ni, Fe, Zn, Al, and Li in concentrated hydroxide solutions have been formulated. Our previous studies[9] indicate that the thermodynamic equilibrium relationships for the metals in the concentrated hydroxide media are expressed better in the form of E versus log m_{MOH}, rather than as the more traditional E versus pH equations. An example of this format is shown in Fig. 2, in which the equilibrium potential for the $Zn(OH)_2/Zn$ couple is plotted as a function of the stoichiometric concentration of NaOH and KOH. These plots demonstrate that the equilibrium potential passes through a minimum at a stoichiometric hydroxide concentration of 4–6.5 mole kg^{-1}. Data of this type will therefore permit selection of the most appropriate stoichiometric hydroxide concentration at any given temperature for the maximum voltage output of an alkaline battery electrode.

REFERENCES

1. R. A. Robinson and R. H. Stokes, Electrolyte Solutions, 2nd ed., Butterworths, London (1959).

2. Harold C. Helgeson, Amer. J. Sci. 267, 729 (1969).

3. D. D. Macdonald, R. P. Singh, and B. Sundararaj, "Thermodynamics of Alkaline Battery Electrodes," FCC 2822-4, LBL Progress Report, April through June 1981.

4. F. G. R. Gimblett and C. B. Monk, Trans. Farad. Soc. 50, 965 (1954).

5. R. P. Bell and J. E. Prue, J. Chem. Soc., 362 (1949).

6. L. S. Darken and H. F. Meier, J. Amer. Chem. Soc. 64, 621 (1942).

7. J. O. Bockris and A. K. N. Reddy, Modern Electrochemistry, vol. 1, Chap. 3, p. 175, Plenum, New York, 1970.

8. D. D. Macdonald, "The Electrochemistry of Metals in Aqueous Systems at Elevated Temperatures," Chap. 4 in Modern Aspects of Electrochemistry, J. O. Bockris and B. E. Conway, eds., vol. 11, p. 141, Plenum, New York, 1974.

9. D. D. Macdonald and M. C. H. McKubre, "Temperature Limitations of Alkaline Battery Electrodes, Part II. The Thermodynamic Properties of Iron, Nickel, and Zinc in Concentrated Sodium Hydroxide Solutions," final report to DOE, Contract No. EM-78-C-01-5159 (1979).
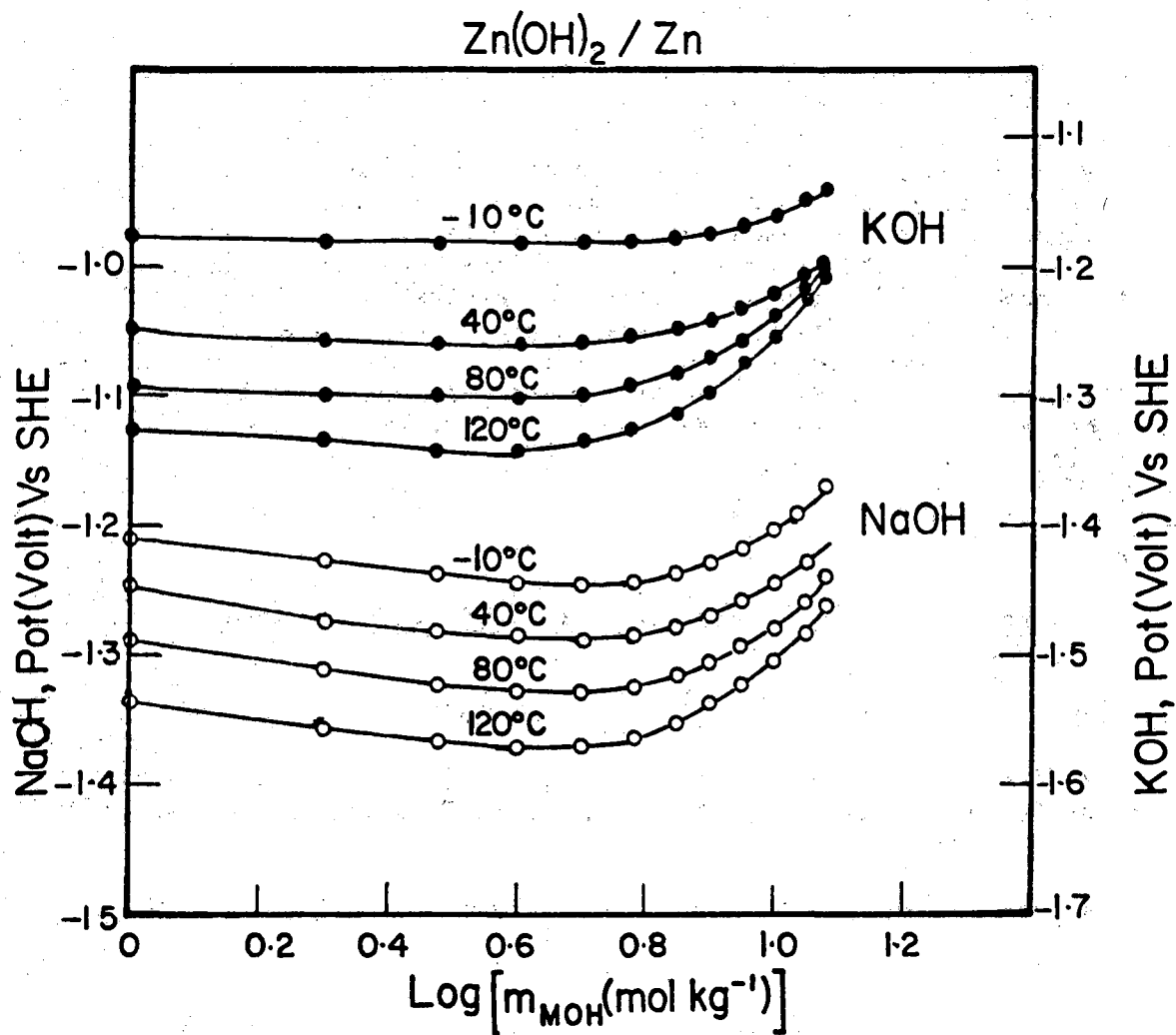
Fig. 2. Equilibrium potentials for the couple $Zn(OH)_2/Zn$ as a function of concentration.

PUBLICATION

B. Sundararaj, R. Singh, and D. D. Macdonald, "The Thermodynamics of Alkaline Battery systems," Proceedings of the 16th Intersociety Energy Conversion Engineering Conference, Paper No. 819324, American Society of Mechanical Engineers, New York, August, 1981.

J. AN ELECTROCHEMICAL AND MORPHOLOGICAL STUDY OF THE EFFECT OF TEMPERATURE
    ON THE RESTRUCTURING AND LOSS OF CAPACITY OF ALKALINE BATTERY ELECTRODES

DOE Program Manager ● A. R. Landgrebe

LBL Project Manager ● F. R. McLarnon

LBL Subcontractor ● Ohio State University (D. Macdonald)

B&R Number ● AL-05-10-10

Contract Value ● 53K

Contract Number ● 4506610

Contract Term ● May 1, 1980 - April 30, 1981

Reporting Period ● November 1, 1980 - November 1, 1981

Objectives ● Investigate the effect of temperature on
the restructuring of porous iron and
nickel electrodes

● Determine the mechanisms of capacity
degradation of the electrodes on
repetitive cycling

● Provide improved understanding of
capacity loss in Fe/NiOOH and Zn/NiOOH
batteries

Restructuring of porous battery electrodes during cyclic charging and
discharging is the principal mechanism of electrode degradation that limits the
capacities and performance of many alkaline battery systems. Our research is
directed at developing an understanding of the restructuring mechanisms for
porous iron and nickel electrodes over a temperature range of 0°C to 100°C.
Our approach and progress are briefly summarized in this report.

We are studying the restructuring phenomenon, using low-frequency ac
impedance techniques, to define the electrical and electrochemical properties
of the porous electrodes. Optical microscopy, scanning electron microscopy
with EDAX, x-ray diffraction, and Auger electron spectroscopy are being used
to investigate the morphological, structural, and chemical properties of each
system. Also, we are carrying out fundamental studies on the growth of oxide
films on massive iron and nickel as a function of temperature for information
on the mechanisms involved. These studies will use both electrochemical and
optical techniques, including measurement of the frequency dispersion of the
interfacial impedance, potentiostatic transient studies, cyclic voltammetry,
and ellipsometry/reflectance studies of film-growth phenomena.

THEORETICAL MODEL FOR A POROUS ELECTRODE

In this study, we have adopted a transmission-line model to represent the porous electrode. The model recognizes the finite thckness of a real battery electrode, and accordingly the electrochemical response will be partly determined by processes occurring at the base of the pore between the current collector (backing plate) and the solution (impedance Z', Fig. 1). Also, the model assumes a finite resistance for the "metal" phase to take into account the resistive degradation of metal particle-particle contacts caused by internal stresses generated on cyclic charging and discharging. The charge storage processes are represented by the interfacial impedance Z, which is expected to involve a large pseudocapacitance associated with electrochemical adsorption.

The discretized form of the transmission line is shown in Fig. 1; R_m and R_s represent the resistances in the "metal" phase (due to degradation of particle-particle contacts) and solution phase, respectively. The current potential distributions within the porous system, and the total impedance, were derived by application of circuit analysis equations to a typical discrete unit.

The total impedance of the electrode was found to be a complex function of many variables:

$$Z_t = Z_p/n = \frac{1}{n} \left\{ \frac{R_m R_s \ell}{R_m + R_s} + \frac{2\gamma^{1/2} R_m R_s + \gamma^{1/2} (R_m^2 + R_s^2)C + \delta R_s^2 S}{\gamma^{1/2}(R_m + R_s)(\gamma^{1/2}S + \delta C)} \right\} \quad (\text{ohm})$$

where $\gamma = (R_m + R_s)/Z$, $\delta = (R_m + R_s)/Z'$, $C = \cosh(\gamma^{1/2}\ell)$, $S = \sinh(\gamma^{1/2}\ell)$, and n is the number of the pores per unit area.

In principle, we can derive all electrochemical and physical-property information concerning the porous electrode through curve fitting of small-amplitude ac impedance measurements to the impedance equation. In practice, however, it is virtually impossible to obtain a unique solution to the problem via multivariate analysis of experimental data. Instead, numerical analysis is used to generate impedance spectra that reproduce the trends observed experimentally. In this way, reasonable estimates can be made for many of the parameters contained in the expression for Z_t. A computer program has been written for this purpose, and extensive theoretical impedance spectra are now being generated. The model has been shown to reproduce the essential features of the experimental impedance data.
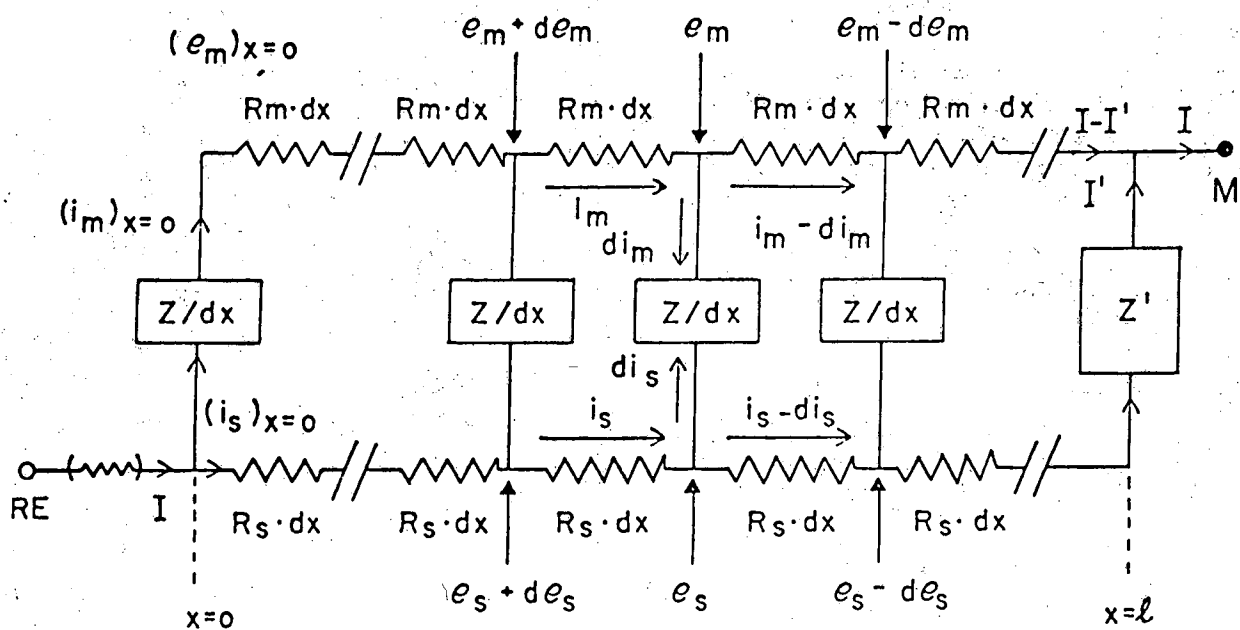
Fig. 1. Discretized form of transmission model for a porous battery electrode of finite thickness: e_m and e_s are potentials in the metal and solution phases, respectively; i_m and i_s are currents in the metal and solution phases, respectively. I and I' are the total current and the current flowing across the electrode backing plate/solution interface at the base of the pore, respectively; and RE and M designate the reference electrode and current collector locations, respectively.

IMPEDANCE STUDIES OF ROLLED AND BONDED NICKEL ELECTRODES
IN CONCENTRATED KOH SOLUTIONS

The frequency dispersion of the impedance for rolled and bonded nickel electrodes has been measured at 0, 25, 45, and 100°C at various cycle numbers in both the charged and discharged conditions. Typical results are shown in Fig. 2. These impedance spectra demonstrate that, at low cycle numbers, at least two electrochemical relaxations can be resolved at high frequencies, whereas at high frequencies a single depressed semicircle is observed. At low frequencies, the system exhibits a pseudo-Warburg response associated with mass transport within the pores. An important feature of these data is that at any given frequency, the impedance increases with cycle number. We believe that this is a direct result of degradation of the porous electrode structure on cyclic charging and discharging.

To date, we have cycled only rolled and bonded electrodes. These electrodes have shown a substantial decrease in cycle time (coulombic efficiency) over a relatively small number of cycles. Because of this sharp reduction in coulombic efficiency, the cycle numbers were limited to 40. After just 40 cycles, some sloughing of the active electrode has been observed, particularly at the higher temperatures. Charge and discharge current densities were 5 mA/cm^2 and 30 mA/cm^2, respectively. These studies will soon be extended to sintered nickel electrodes.

We have also studied the growth of oxide films on planar (metallic) nickel electrodes in 8M KOH at ambient temperature within the potential range -400 to 500 mV (versus $\overline{Hg}$/HgO reference electrode). Reflectance and ellipsometric measurements yielded a time-dependent oxide thickness. Studies at other temperatures are under way. At all potentials studied, the oxide films grow in accordance with the "inverse logarithmic law." That is, the thickness of the oxide film, L (Å), is related to the oxidation time, t (min.), as follows:

$$1/L = A - B \log t \quad ,$$

where A and B are constants. Cabrera and Mott[1] have proposed that films exhibiting the growth kinetics defined by this equation are controlled by field-assisted cation emission from the metal to the film. However, we have found that the point-defect model for film growth,[2,3] recently developed in this laboratory, provides a more satisfactory explanation of the kinetics of film formation on massive nickel in concentrated hydroxide solutions.

In the last half of this research program, we will: (1) continue to measure impedance spectra versus cycle number for rolled, bonded, and sintered nickel electrodes, respectively, and sintered iron electrodes, in concentrated KOH solutions as a function of temperature; (2) conduct numerical analyses to compare measured impedance spectra versus those predicted by the transmission-line model; (3) continue studies of the nucleation and growth of oxide films on planar nickel and iron specimens; and (4) examine the morphology and composition of cycled electrodes.
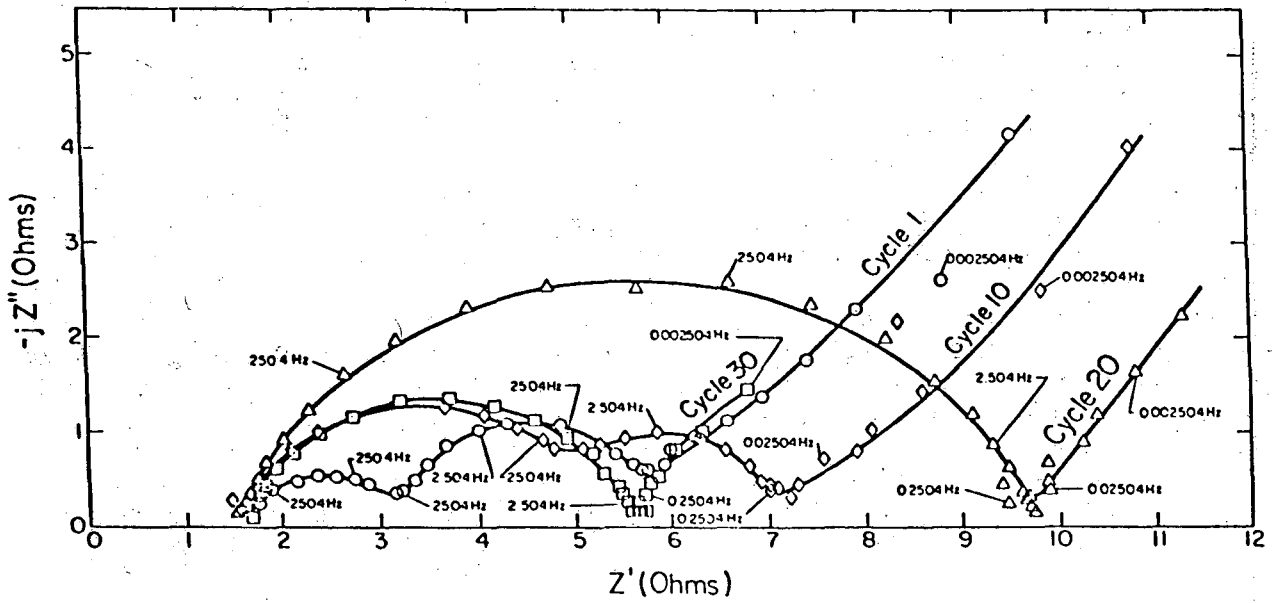
Fig. 2. Impedance spectra (vs. frequency) for discharged Ni(OH)$_2$, rolled and bonded electrode after 1, 10, 20 and 30 cycles, 45°C ± 1°C, -jZ" vs. 2'.

REFERENCES

1. N. Cabrera and N. F. Mott, Rept. Prog. Phys., 12, 163 (1948-1949).

2. C-Y. Chao, L. F. Lin, and D. D. Macdonald, "A Point Defect Model for Anodic Passive Films - (I) Film Growth Kinetics," J. Electrochem. Soc., 128, 1187 (1981).

3. L. F. Lin, C-Y. Chao, and D. D. Macdonald, "A Point Defect Model for Anodic Passive Films - (II) Chemical Breakdown and Pit Initiation," J. Electrochem. Soc., 128, 1194 (1981).

PUBLICATION

S. J. Lenhart, C. Y. Chao, and D. D. Macdonald, "An Electrochemical and Morphological Study of the Effect of Temperature on the Restructuring and Loss of Capacity of Alkaline Battery Electrodes," Proceedings of the 16th Intersociety Energy Conversion Engineering Conference, Paper No. 819325, American Society of Mechanical Engineers, New York, 1981.

K. RESEARCH ON ALKALINE ZINC SECONDARY ELECTRODES

DOE Program Manager ● A. R. Landgrebe

LBL Project Manager ● F. R. McLarnon

LBL Subcontractor ● Linfield Research Institute (D. Hamby)

B&R Number ● AL-05-10-10

Contract Value ● 21K

Contract Number ● 4506910

Contract Term ● May 1, 1980 – August 31, 1981

Reporting Period ● June 1, 1980 – August 31, 1981

Objectives ● Characterize sources of overpotential
and capacity deterioration in zinc
electrodes operated under conditions of
severely limited convective flow

● Evaluate predictions of hydroxyl ion
depletion as a failure mode for porous
electrodes

Failure mechanisms for porous zinc secondary electrodes operated under
conditions of severely limited convective flow have been investigated both
theoretically and experimentally by Bennion and Sunu.[1,2] Their model, for
electrodes of this type, combined with ion-exchange separators such as RAI
P2291, predicts hydroxyl depletion in the zinc electrode chamber to be an
important factor in electrode failure. They have suggested simplified
equations to describe the depletion. Overpotential, cell capacity, and cell
relaxation data have been published to support the theory; however, OH⁻
concentration data, measured by sampling and analysis of the electrolytic
solution from anode compartments of the cells of interest over a range of cell
operating times, have not been reported previously.

The cell used in this work is the simplest compatible with obtaining the
desired information. It consists of a small anode chamber that houses a planar
zinc anode, a supported membrane separator (RAI P2291 40/30), and a zinc
cathode housed in a much larger chamber. Experiments consisted of initiating
electrolysis with a solution of known concentration, allowing electrolysis at
constant current for measured periods of time, followed by sampling and
analysis of the anolyte for OH^-, $Zn(OH)_4^{2-}$, and K^+. Cell design is such
that the catholyte can be removed and the anolyte exposed and sampled within
less than one minute of termination of electrolysis.

In Fig. 1, data are summarized for 17 cells discharged at 0.020 A/cm^2. The regularity, reproducibility, and precision of the data indicate that depletion of K$^+$ and OH$^-$ is being observed under the chosen conditions, i.e., transfer of these species into and out of the anode compartment occurs only through the membrane separator.

In Fig. 2, the concentration data are compared with values predicted on the basis of Sunu's simplified theory. The observed depletion rate is considerably less than predicted. On the basis of membrane transport equations reviewed recently by Bennion and Pintaro,[3] it is suggested that the differences between theory and observation may be explained primarily on the basis of a third driving force, a pressure difference that was neglected in the simplified theory.

Although observed K$^+$ and OH$^-$ depletion rates are less than predicted by the simplified theory, drastic OH$^-$ depletion is observed. This supports the contention that such depletion contributes significantly to the decreased capacity of porous zinc electrodes operated under the stated conditions, and also that the rate of depletion is probably highly dependent on the character- istics of the membrane separator. Finally, there is a need for additional theoretical and experimental work on the behavior and properties of separator materials.

These results are to be presented at the spring meeting of the Electro- chemical Society and will be submitted to the Journal of the Electrochemical Society as a technical note.

REFERENCES

1. W. G. Sunu and D. N. Bennion, J. Electrochem. Soc., 127, 2007 (1980).

2. W. G. Sunu and D. N. Bennion, J. Electrochem. Soc., 127, 2017 (1980).

3. D. N. Bennion and P. N. Pintaro, AIChE Journal, 77, 204 (1981).
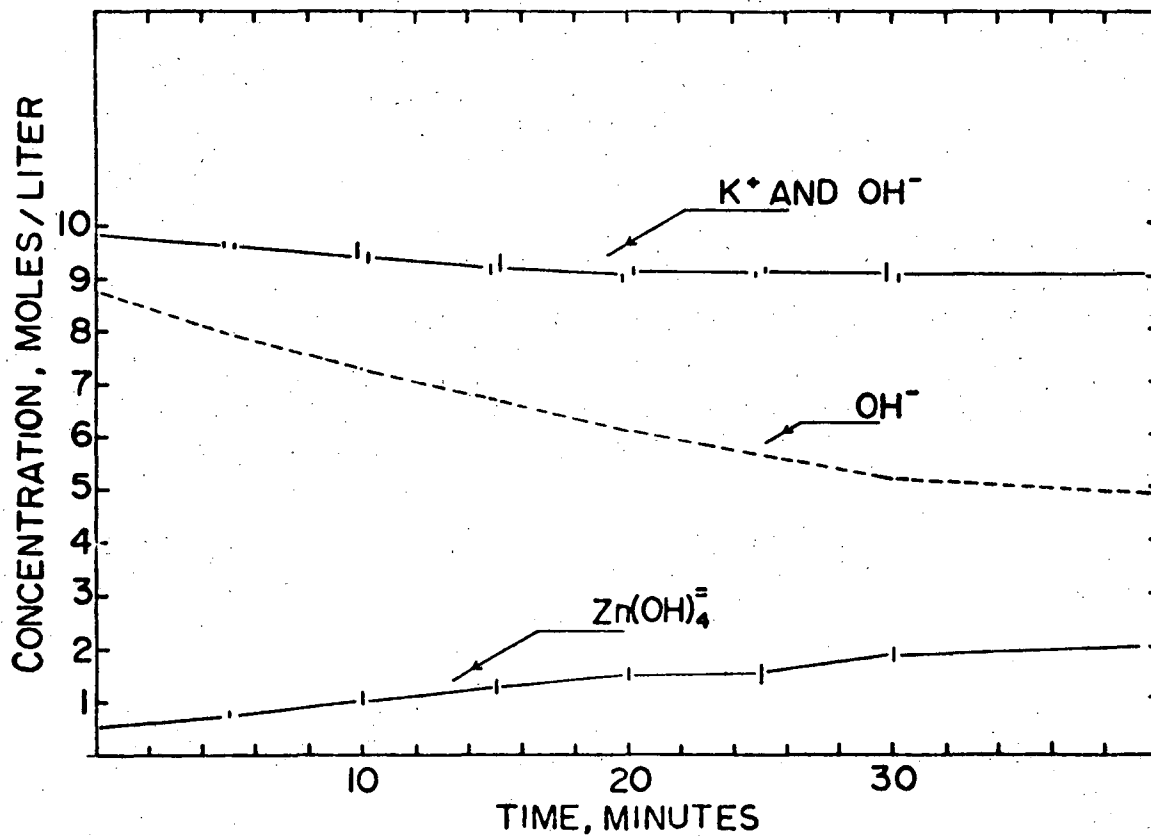
Fig. 1. Graphical summary of analytical data for 17 experiments at constant
cell current of 0.020 A. Bars indicate range of averaged concentra-
tion values determined for the cells operated for the indicated
times. On the line designated "K+ and OH−," the K+ values are
just to the left of the appropriate time and the OH− values just to
the right. $Zn(OH)_4{}^{2-}$ values on the lower line are concentration
values calculated on the basis of zinc found. OH− concentrations
(dotted line) are calculated on the basis of the dissolution equation
and the amount of zinc found.
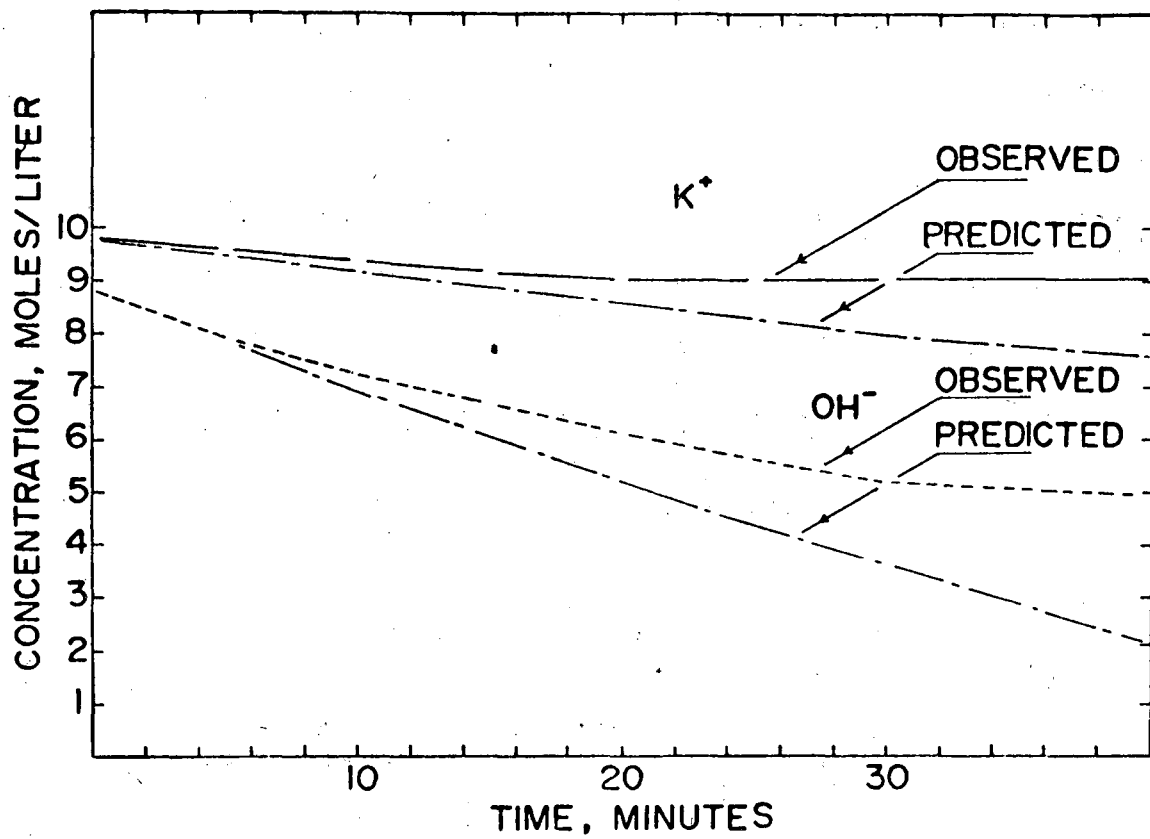
Fig. 2. Graphical comparison of observed and predicted K^+ and OH^- concentrations as functions of time in cells with severely limited convective flow.

L. DENDRITIC ZINC DEPOSITION IN FLOW BATTERIES

DOE Program Manager • A. R. Landgrebe

LBL Project Manager • F. R. McLarnon

LBL Subcontractor • Illinois Institute of Technology
(J. R. Selman)

B&R Number • AL-05-10-10

Contract Value • 94K

Contract Number • 4512010

Contract Term • April 1, 1981 - September 30, 1982

Reporting Period • April 1, 1981 - November 1, 1982

Objectives • Clarify the solution-side transport
processes involved in acidic zinc
deposition, and their effect on electrode
kinetics and deposit morphology

• Investigate the interaction of transport
processes with dendritic microprofiles

• Clarify the role of hydrogen
co-deposition in zinc deposition and
dendrite initiation

• Provide fundamental information needed
to improve the design and performance of
zinc/halogen batteries

The transport properties of unsupported and supported zinc halide
solutions, collected and correlated in an earlier research project,[1] have
been checked for consistency. The correlations for the $ZnCl_2/H_2O$ system
at room temperature cover the molecular diffusivity, the zinc transport number,
the electrical conductivity, and the activity coefficient over a concentration
range of 0.1 to $3\underline{M}$ $ZnCl_2$. These correlations have been used to derive multi-
component binary diffusivities by means of fundamental relationships developed
by Newman.[2] The resulting binary diffusivities reflect basic simplifying
assumptions about complexation in the electrolyte; the following combinations
of species were assumed: $ZnCl^+ - Cl^- - H_2O$, $Zn^{2+} - Cl^- - H_2O$,
$Zn^{2+} - ZnCl_3^- - H_2O$, and $Zn^{2+} - ZnCl_4^{2-} - H_2O$. The solvent-ion
diffusivities are expected to be applicable in supported $ZnCl_2$ solutions,
depending on the degree of complexation.

To estimate the degree of complexation in supported zinc chloride solutions, instability constants reported by Skou and Jacobsen[3] have been applied. The results appear to confirm that $ZnCl_4{}^{2-}$ is the dominant zinc species in typical zinc-halogen battery electrolytes. This, however, does not exclude important association equilibria involving OH as a ligand.

"Effective" (polarographic) ionic diffusivities of zinc in concentrated $ZnCl_2$ + $3\underline{M}$ KCl solutions, reported in previous work,[1] have been checked for reproducibility and accuracy. New data obtained at lower $ZnCl_2$ concentrations tend toward the values reported in the literature. However, the diffusivity rapidly falls off with increase in concentration (Fig. 1). This suggests that limiting current densities on concentrated solutions are far lower than one would estimate with dilute-solution diffusivities.

To obtain some insight into the effect of migration on the effective diffusivitives determined in these concentrated solutions, the migration contribution based on dilute-solution theory was calculated, assuming (1) no zinc complexation and (2) compete complexation to $ZnCl_4{}^{2-}$ (Fig. 2). It is evident from this figure that complexation conditions have a strong effect on the apparent zinc diffusion flux. This explains in part the extreme concentration dependence of the effective diffusivity.

A rotating concentric-cylinder cell has been designed and fabricated. A schematic of the cell is shown in Fig. 3. In the initial version of this cell, only optical observation was provided for; the final version has a vertical knife-edge that can be adjusted to dislodge dendrites. Initial experiments with this cell have started. A vertical flow cell of approximately 3 times the dimensions of Fig. 3 is also being designed.

REFERENCES

1. J. R. Selman et al., "Improved Zinc Electrodes for Load Leveling," final report, Project EPRI-RP 1198-3, Case Western Reserve University and Illinois Institute of Technology, November 1981, Draft.

2. J. Newman, Electrochemical Systems, Chap. 14, Prentice-Hall, 1973.

3. E. Skou, T. Jacobsen, W. van der Hoeven, and S. Atlung, Electrochim. Acta 22, 169 (1977).
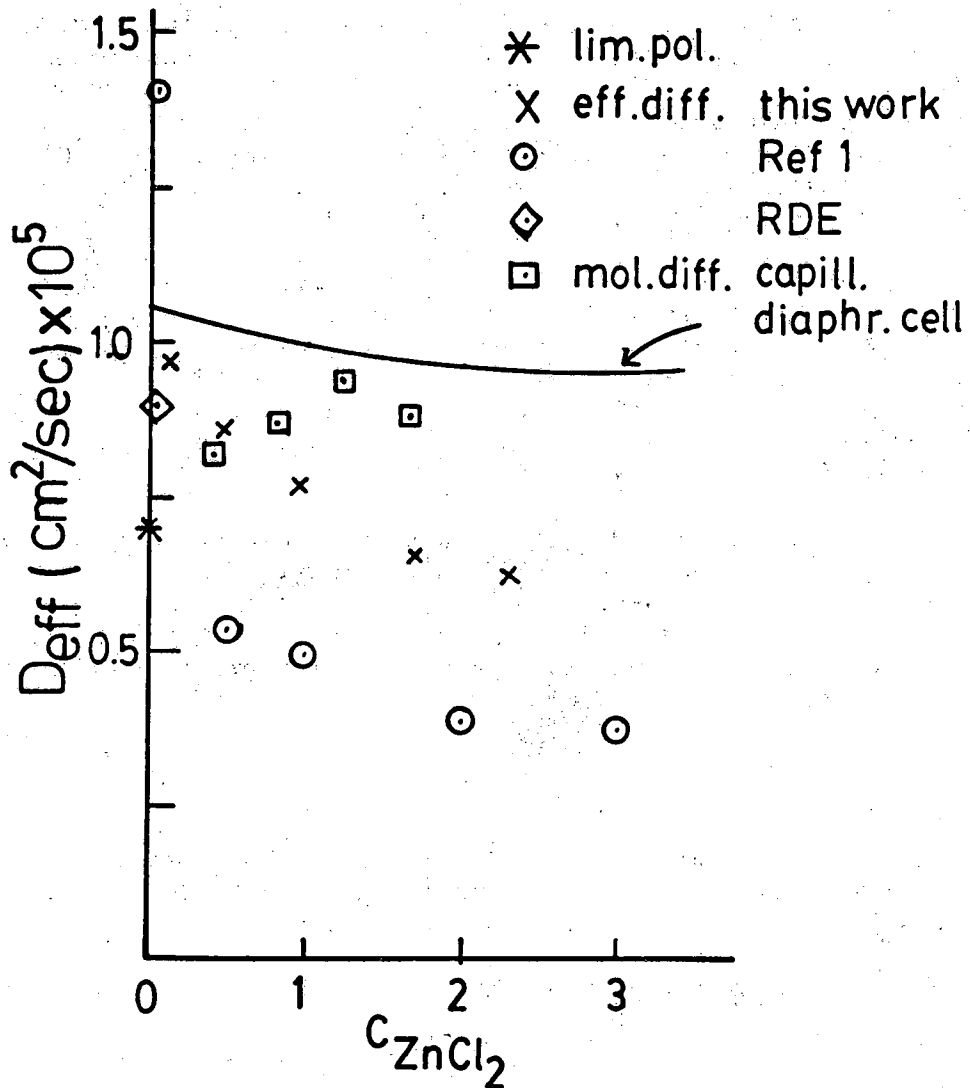
Fig. 1. Effective ionic diffusivities of zinc in $ZnCl_2$ + 3$\underline{M}$ KCl solutions at 25°C. RDE = rotating disk electrode results.
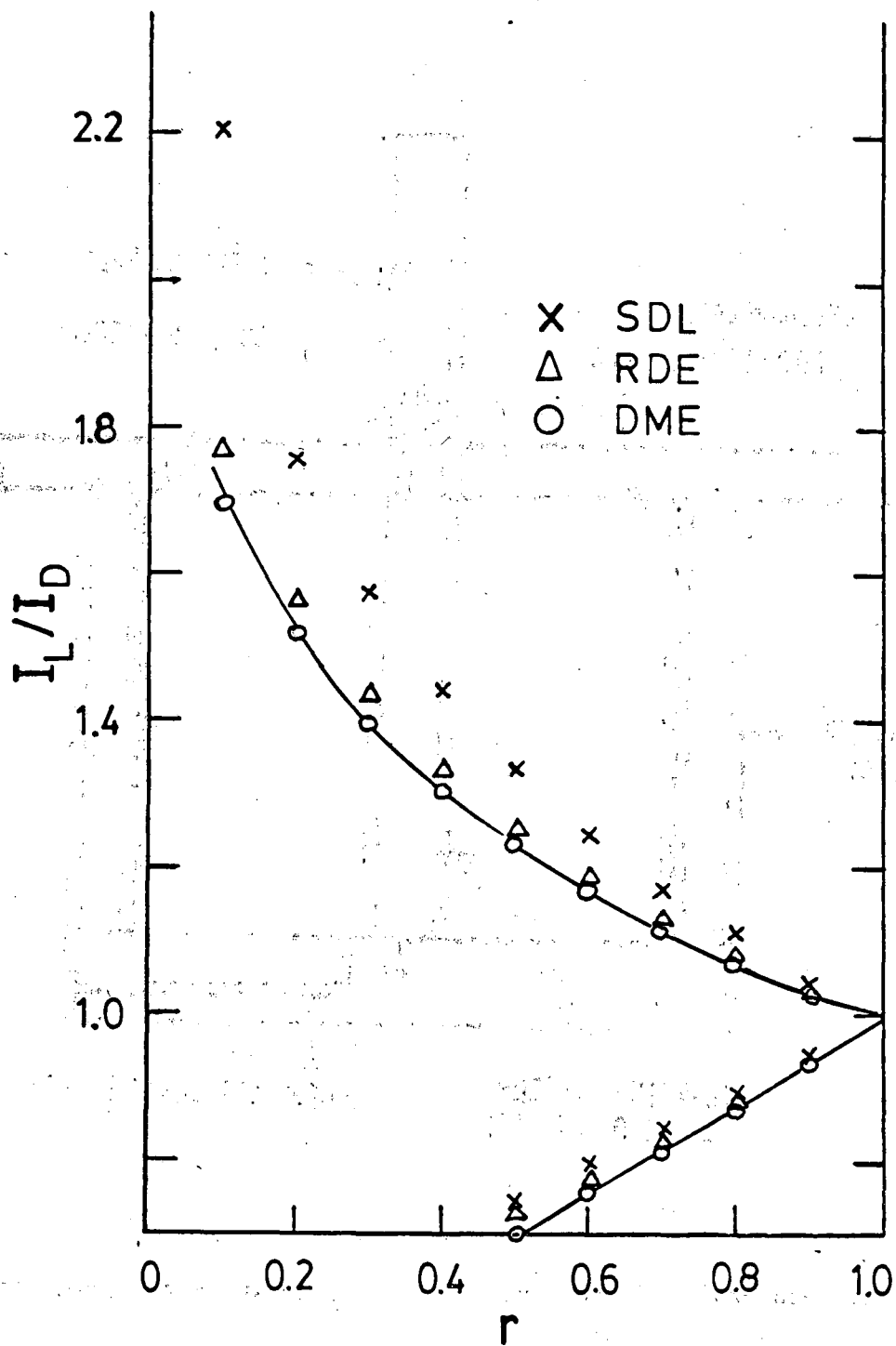
Fig. 2. Migration effect (total flux/diffusion flux) in $ZnCl_2$ - KCl - H_2O at 25°C.
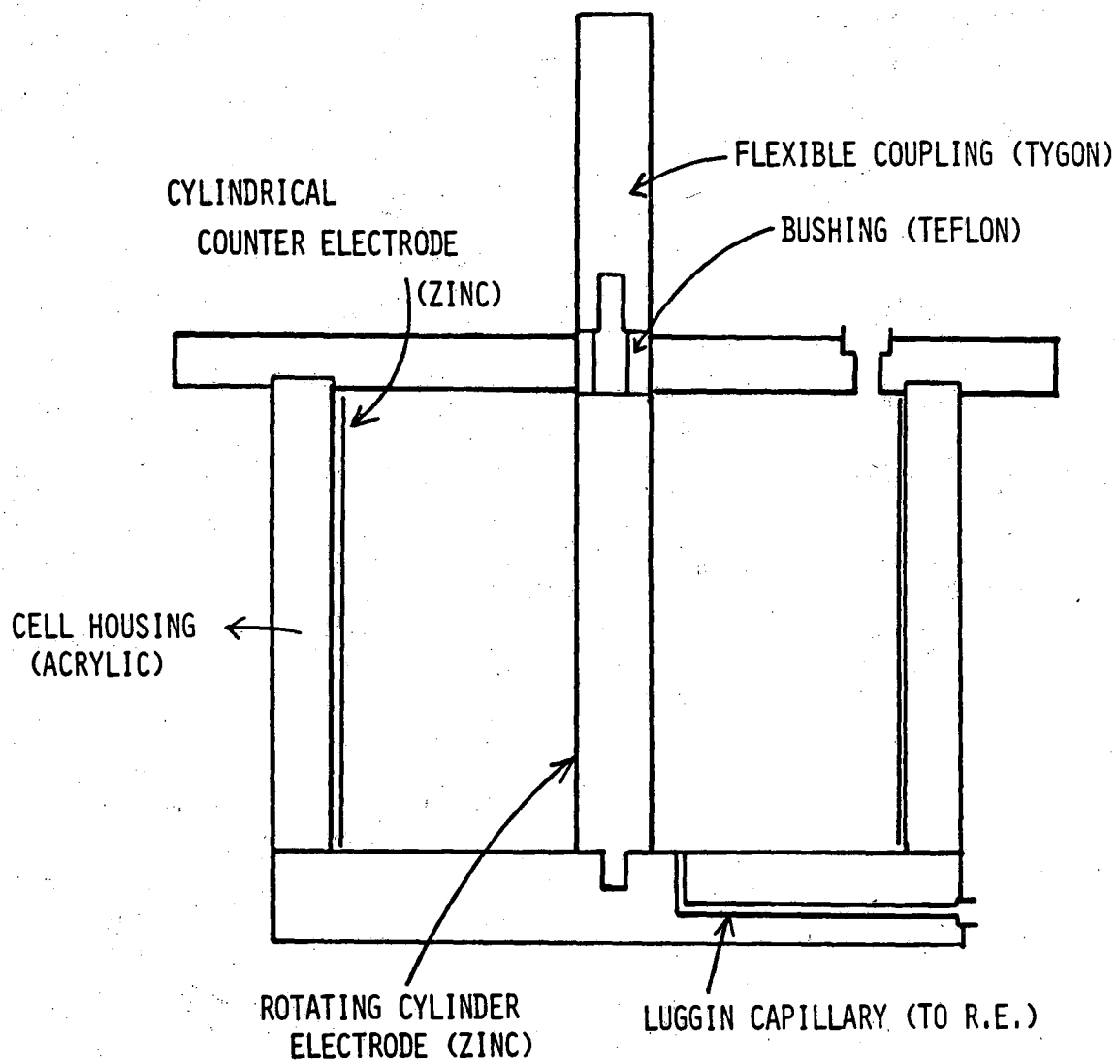
Fig. 3. Schematic of rotating concentric cylinder electrode cell.

M. TRANSPORT IN AQUEOUS BATTERY SYSTEMS

DOE Program Manager	● A. R. Landgrebe
LBL Project Manager	● J. Newman
LBL Subcontractor	● Lawrence Livermore National Laboratory (D. Miller)
B&R Number	● AL-05-10-10
Contract Value	● 49K
Contract Number	● 4512610
Contract Term	● April 15, 1981 - December 31, 1981
Reporting Period	● May 4, 1981 - November 15, 1981
Objective	● Provide experimental data for the four diffusion coefficients of the $ZnCl_2$-KCl-H_2O system at 25°C for three compositions. These data are required for proper analysis and modeling of zinc/halogen batteries

This project is the measurement of the four diffusion coefficients at each of three compositions of the $ZnCl_2$-KCl-H_2O system plus some test measurements of $ZnCl_2$-H_2O, all at 25°C.

To check the $ZnCl_2$-H_2O data of Agnew and Patterson,[1] we have carried out nine measurements at 25°C, using Rayleigh interferometry. The results are in Table 1. As can be seen from Fig. 1, our data are higher than their somewhat scattered results. The largest deviations are at lower concentrations, and agreement is within experimental error at the higher concentrations relevant to batteries. Owing to these differences, which are outside the combined reported experimental uncertainties at lower concentrations, we did five more runs than originally intended. One was a solution with deliberately added acid, since Agnew and Patterson's solutions were prepared differently and probably had different pH's. However, no effect larger than our experimental uncertainty was observed. It would be desirable to extend our measurements to lower and higher concentrations in order to properly characterize the diffusion properties of $ZnCL_2$-H_2O at 25°C.
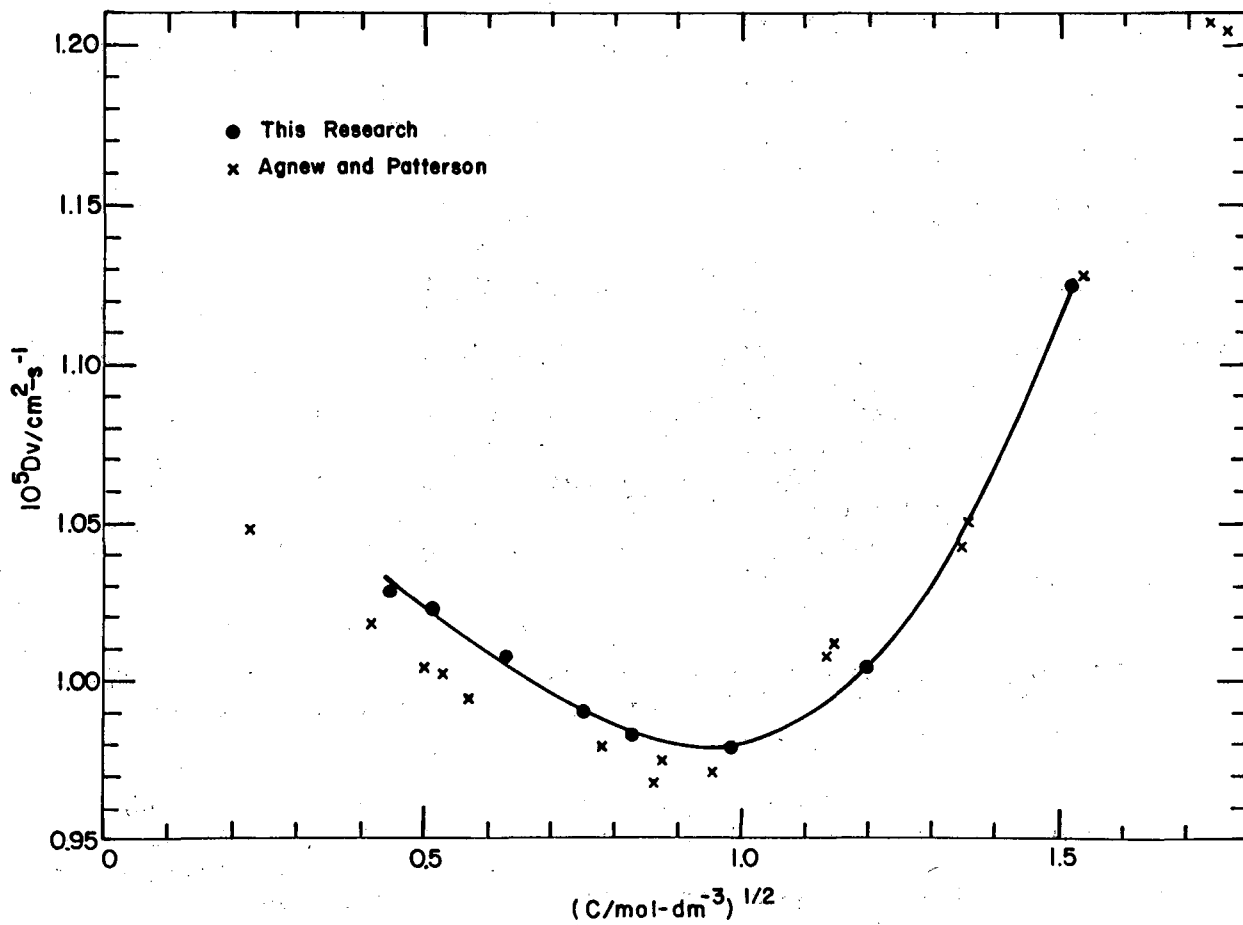
Fig. 1.   Mutual diffusion coefficients of $ZnCl_2$-H_2O at 25°C.

Table 1. Diffusion coefficients of aqueous $ZnCl_2$ at 25°C.[a]

$\bar{c}$	Δc	m	J	$10^5 D_v$
0.19934	0.03778	0.20053	96.10	1.027_6
0.25895	0.04060	0.26076	100.89	1.022_4
0.39418[b]	0.04345	0.39806	101.91	1.006_2
0.39451	0.04335	0.39839	101.51	1.007_1
0.56273	0.05358	0.57067	116.15	0.989_7
0.68965	0.04122	0.70195	84.88	0.982_3
0.97611	0.04994	1.0030	94.47	0.978_4
1.4392	0.0485	1.5051	84.77	1.041_1
2.3118	0.0579	2.5090	95.31	1.125_0

[a] $\bar{c}$ and Δc are average concentration and difference in concentration (mole cm^{-3});

m is molality (mole kg^{-1});

J is total number of fringes (a pure number); and

D_v is volume-fixed diffusion coefficient ($cm^2 s^{-1}$).

[b] This experiment performed on acidified $ZnCl_2$ corresponding to $ZnCl_2 \cdot 0.0014$ HCl.

Densities of all solutions are necessary to convert weight concentrations to mole-dm^{-3}; Since literature data for $ZnCl_2$ densities are discrepant, owing to different preparation methods and different impurities, we have measured densities of all our solutions. All densities have been measured to 3 parts in 10^5 with a 30-ml pycnometer, because $ZnCl_2$ seems to have an adverse effect on our SODEV densitometer.

Ternary diffusion measurements have been started, beginning with the composition $ZnCl_2$ (1.5M) – KCl (2.0M) – H_2O. At least four diffusion runs are required at each composition to get reliable values of the four diffusion coefficients. Preliminary results show surprisingly low values of the cross-term coefficients. These had been expected to be larger, owing to complex ion formation in Zn halide systems. However, this result, if found at other compositions, should simplify the equations for modeling battery systems.

REFERENCE

1. A. Agnew and R. Patterson, J. Chem. Soc., Faraday Trans. I, 74, 2896 (1978).

N. TRANSITION METAL OXIDE COATED POROUS TITANIUM ELECTRODES FOR REDOX BATTERIES

DOE Program Manager • A. R. Landgrebe

LBL Project Manager • F. R. McLarnon

LBL Subcontractor • University of Akron (R. Savinell)

B&R Number • AL-05-10-05

Contract Value • 31K

Contract Number • 4512510

Contract Term • April 15, 1980 - April 14, 1982

Reporting Period • April 15, 1981 - November 1, 1981

Objectives • Investigate the electrocatalytic activity of coated Ti electrodes towards redox reactions

• Provide improved understanding of electrocatalysis in redox batteries

The exploitation of redox batteries for large-scale energy storage will require active electrodes with long-term stability. The purpose of this research is to investigate the electrocatalytic activity of RuO_2, IrO_2 and OsO_2 coatings on a titanium substrate towards redox reactions in concentrated solutions. The efforts during the first six months of this project have been directed at the design and assembly of experimental apparatus in addition to the formulation and characterization of the ruthenized electrode.

Since a primary objective of this study is to evaluate the catalytic activity of several metal oxides, it is desirable to have a measure of true electrode area so that intrinsic activities may be compared. Two techniques of measuring surface area are being employed. The primary technique measures the adsorption of Zn^{2+} ion.[1] A secondary technique records the charge under a cyclic voltammogram (as proposed by Burke[2]); this charge is correlated with the area found by Zn^{2+} adsorption. In this manner, if the true area of a rotating disk electrode (RDE) is too small for accurate Zn adsorption, the area can be conveniently evaluated by measuring the voltammetric charge.

Experience measuring electrode surface areas has been gained using commercial ruthenized titanium electrodes ($Ru_xTi_{1-x}O_2$, where x is believed to be 0.3). Surface-area measurement by the voltammetric charge

correlation* gives a roughness factor (i.e., real area/apparent area) of 247, which is reasonable for these electrodes (O'Leary and Navin[3] report roughness factors of 180-230). Area measurement by Zn^{2+} adsorption (although not of the same samples) reveals a roughness factor of 162-169. Since the voltammetric charge correlation is based on B.E.T. data (which includes contributions to the area from micropores that are not necessarily electrochemically accessible), these results seem consistent.

Ruthenized titanium electrodes were prepared and characterized in our laboratory. Titanium sheets were polished, degreased, etched, coated and fired. The preparation technique was similar to that used by O'Grady[1]; however, hot acid etching of the titanium substrate was necessary to achieve a uniform coating. X-ray diffraction of the final coating revealed the rutile structure of RuO_2. Photomicrographs from a scanning electron microscope displayed a mud-cracked surface characteristic of these electrodes. A range of loadings ($1.05 \times 10^{-5} - 8.3 \times 10^{-7}$ moles Ru/m^2) was prepared to correlate voltammetric charge with Zn^{2+} surface area. Surface-area measurements by Zn^{2+} adsorption did not give reproducible data at the low loadings because of the limited sensitivity of this technique. Electrodes with greater loadings are being prepared, and the Zn^{2+} adsorption method is being refined. Voltammetric charge data from cyclic linear sweep voltammetry is reported in Table 1. These surface-area values are low compared to commercial ruthenized titanium, probably because of less etching of the substrate.

An interesting comparison of a mixed oxide electrode ($Ru_xTi_{1-x}O_2$ with 8.24 g Ru/m^2) and a ruthenized titanium electrode (17.3 g Ru/m^2), both prepared in our lab, revealed an identical roughness factor of 150 for both electrodes, using the voltammetric charge technique. This result appears to support the view that less precious metal may be employed in the mixed oxide form with no decrease in true surface area.

The acquisition of kinetic data for the ferric/ferrous couple by the RDE technique has begun. Initially, data is being taken at low salt concentrations (0.001$\underline{M}$ Fe^{2+}/Fe^{3+}) on smooth platinum in order to compare our results with those of previous researchers. Further work is required to achieve reproducible data that compares well with the literature. Future kinetic studies will be directed toward concentrated solutions (nominally 1 molar).

---

*Burke[2] correlated the charge under the voltammogram with B.E.T. data.

Table 1. Surface areas of ruthenized titanium electrode as measured by voltammetric charge area.

Sample number	Loading (moles Ru/cm^2)	True area / Apparent area
1-5 5-3	1.0×10^{-5}	49
1-5 5-4	4.4×10^{-6}	16
1-5 5-1	1.1×10^{-6}	3.8
1-5 5-2	8.3×10^{-7}	1.7

REFERENCES

1. W. O'Grady, C. Iwakura, J. Huang, and E. Yeager, "Ruthenium Oxide Catalysts for the Oxygen Electrode," in Proceedings of the Symposium on Electrocatalysis, M. W. Breiter, ed., The Electrochemical Society Softbound Symposium Series, Princeton, N. J., 1974, pp. 286-302.

2. L. D. Burke and O. J. Murphy, "Cyclic Voltammetry as a Technique for Determining the Surface Area of RuO_2 Electrodes," J. Electroanal. Chem., 96, 19 (1979).

3. K. J. O'Leary and T. J. Navin, "Morphology of Dimensionally Stable Anodes," reprinted from Chlorine Bicentennial Symposium, pp. 174-186.

O. ELECTROCHEMICAL STORAGE CELL BASED ON POLYCRYSTALLINE SILICON

DOE Program Manager   ● A. R. Landgrebe

LBL Project Manager   ● F. R. McLarnon

LBL Subcontractor   ● SRI International (S. R. Morrison)

B&R Number   ● AL-05-05-15

Contract Value   ● 60K

Contract Number   ● 4510610

Contract Term   ● March 1, 1981 - February 28, 1982

Reporting Period   ● March 1, 1981 - November 15, 1981

Objectives   ● Selection of redox couples and solvents

● Development of corrosion inhibition for silicon

● Construction and evaluation of a test cell

● Evaluation of a novel photoelectro-chemical cell for solar energy conversion and storage

The object of this project is to develop a solar cell with reasonable efficiency and a modest load-leveling capability, such that diurnal and other fluctuations in light intensity would be smoothed over. Thus, the concept is to provide a solar cell/battery combination, with the miniature battery included to load-level the output from each cell.

The requirements on the battery portion of the solar cell are that the cell potential be about 0.8 to 1.0 volts. This requirement arises because the peak power voltage expected from a semiconductor suitable for efficient solar conversion will range from about 0.5 to 0.8 volts, these voltages arising from bandgap optimization. Then, with two solar cells in series, one p-type and one n-type, a battery of the stated voltage could be charged. We chose to aim for the $Sb^{5+}/Sb^{3+}/Sb^0$ antimony redox battery because of its characteristic battery potential and its minimal requirements on the separator. In the final design, the semiconductor must be in contact with these highly corrosive electrolytes. Silicon was chosen as the semiconductor because of its corrosion resistance, its excellent solar characteristics, and its wide use in advanced technology.

In the first 8 months of study, we have concentrated on developing a suitable silicon solar cell. As a pure electrochemical solar cell, silicon has been difficult because of its oxidation, which creates an insulating SiO_2 layer on the electrode. The simple characteristics of the SiO_2, however, have allowed us to make a quantitative analysis of the influence of surface layers on the electrode characteristics of semiconductors. The analysis has shown that such a layer will dominate the fill factor of the solar cell. This analysis will be valuable for many other semiconductor electrodes.

Several approaches have been explored to overcome the limitations of the silicon solar cell. The first approach was to introduce a small amount of fluoride ion into the solution (together with a stabilizing agent to minimize the rate of oxide growth), so that the oxide would be removed as fast as it was formed. Unfortunately, the fluoride ion not only removed SiO_2, but catalyzed its growth. Thus, the stabilizing agent became less effective in the presence of fluoride ions, and this approach had to be ruled out.

The second approach used nonaqueous solutions to avoid oxide formation. The silicon became reasonably stabilized, but only after a thin oxide layer was formed, sufficient to lower the fill factor (and hence the efficiency) of the solar cell. In the case of p-type silicon, this behavior occurred in aqueous solutions, as well. Thus, for both n-type and p-type silicon, systems were found that showed a satisfactory open circuit voltage, but the fill factor was too low for efficient solar cell operation.

At present, two other approaches are being tested. One is the use of a polymeric film to protect the silicon from oxidation. The other is the use of a p-n junction just below a degenerated silicon surface. Others have found that this latter approach provides stability, but unfortunately it also makes the construction of the solar cell somewhat more costly, so we have considered it a last resort.

We will continue studying methods to develop a suitable solar cell, and, in parallel, begin studies of the silicon/antimony cell for the load-leveling function.

P. INVESTIGATION OF INTERCALATION COMPOUNDS FOR PHOTOELECTROCHEMICAL
ENERGY STORAGE

DOE Program Manager   ● A. R. Landgrebe

LBL Project Manager   ● F. R. McLarnon

  LBL Subcontractor   ● EIC Laboratories, Inc. (R. D. Rauh)

      B&R Number   ● AL-05-05-15

    Contract Value   ● 88K

   Contract Number   ● 4507110

    Contract Term   ● February 23, 1981 - February 22, 1982

  Reporting Period   ● February 23, 1981 - November 1, 1981

         Objective   ● Fabrication and evaluation of intercala-
                          tion electrodes for the storage of
                          electrical energy generated in photo-
                          electrochemical storage cells

Layered chalcogenides of general formula MX_2 are being investigated for the storage of electrical energy generated by photoelectrochemical solar cells. These storage materials can be highly economical and have excellent volumetric energy densities, allowing direct incorporation into flat-plate photovoltaic modules. Two approaches are being evaluated: (1) intercalation electrodes, such as Cu_nTiS_2, which can be charged by a separated regenerative photo-electrochemical cell; (2) "active" photointercalation/photodeintercalation cells in which the storage step is effected directly by irradiating a layered semiconducting photoelectrode. Key to the second type of cell is demonstration of photointercalation of transition metals or H in p-type photoelectrodes of structure MX_2 or partially intercalated A_nMX_2, or alternatively, demonstration or photodeintercalation of $n-A_nMX_2$. Electrode systems in which light drives an endoergic electrochemical storage reaction are chosen. Materials to be investigated are selected largely on the basis of previously demonstrated intercalation reversibility (usually with Li), and, in the case of semiconductors, appropriate match of band gap with the solar spectrum. Typical configurations that we envision for such cells are shown in Fig. 1.

We have demonstrated a cell of the first kind, consisting of an n-GaAs photoelectrode and a TiS_2 intercalation electrode. The intercalant was Cu in an acetonitrile-tetrabutylammonium chloride electrolyte. During the charging reaction, $CuCl_2^{-1}$ was oxidized to $CuCl_4^{-2}$ at the n-GaAs photoanode and reduced to TiS_2Cu_n at the cathode. The best results were obtained with TiS_2, which had been pressed onto Ta Exmet. The cell was charged under tungsten-lamp irradiation of 40 mW/cm^2 until the TiS_2 was 36% utilized.

(a)

Contact Tabs

Filling Hole

Back

Celgard Microporous Polypropylene

Intercalation Storage Electrodes

Solid Barrier

Counter Electrode

Spacer

Front

Photoelectrode; Holes for Ion Flow

Spacer

Glass

(b)

Contact Tabs

Filling Hole

Back

Intercalation or Metal Counter Electrode

Celgard Microporous Polypropylene

Intercalation Photoelectrode With Holes for Ion Flow
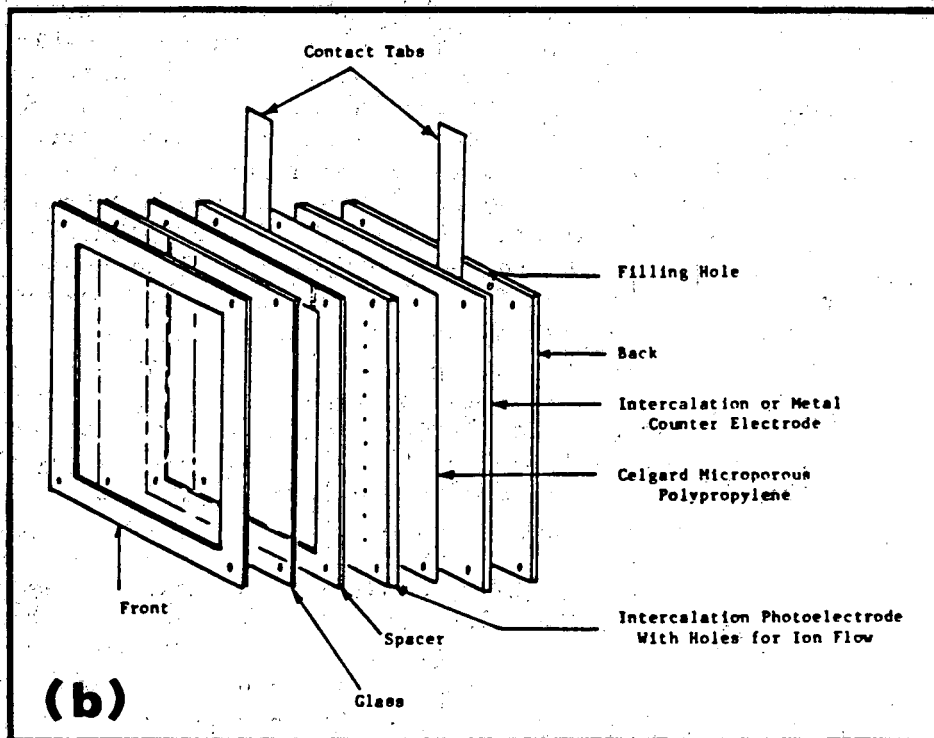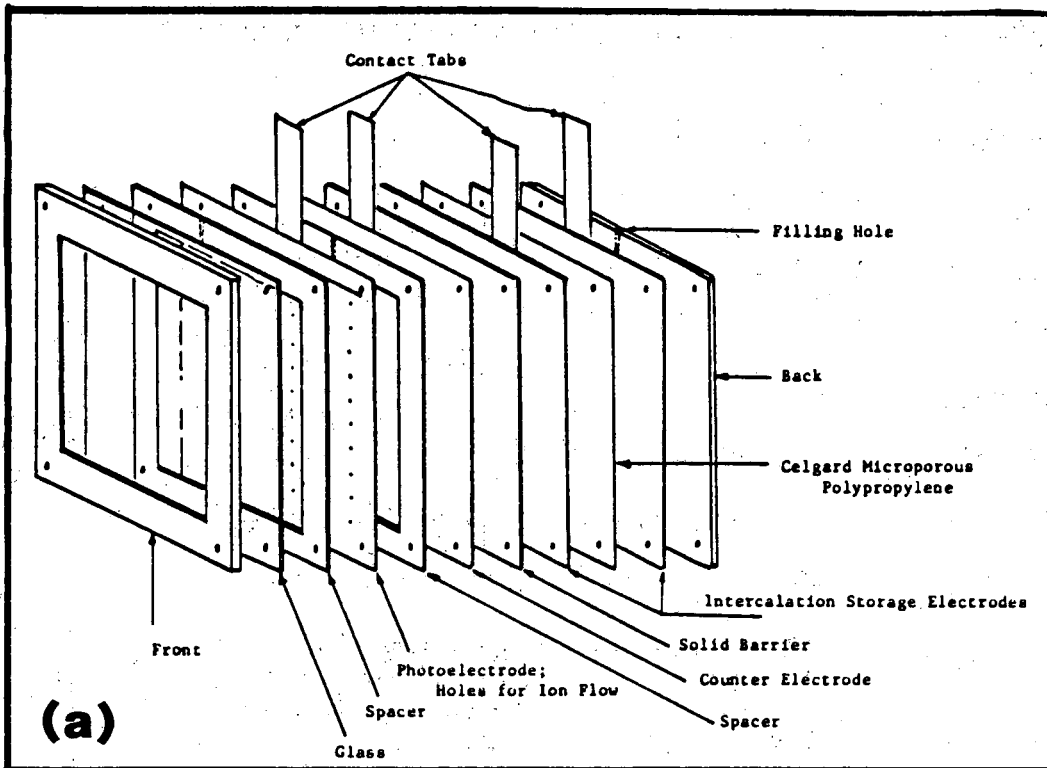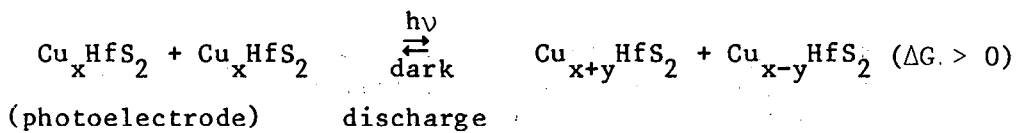
Front

Spacer

Glass

Fig. 1. (a) Prototype laboratory cell for "passive" intercalation storage of electricity generated in an auxiliary regenerative photoelectrochemical device. (b) "Active" photointercalation storage cell.

The spontaneous discharge cycle was continued until 64% of the stored charge was recovered. The major problem encountered in the cycling experiments was deterioration of the physical structure of the TiS_2 electrode, although the system itself appears to be chemically reversible between $0 < n < 0.6$.

Studies of "active" photointercalation devices were made on three single-crystal semiconducting layered dichalcogenides: HfS_2, $ZrSe_2$, and ZrS_2. These were prepared as single crystals by iodine-vapor transport. The photo-electrochemical properties of the three compounds were measured in electrolytes with different redox potentials. HfS_2 and $ZrSe_2$ showed both p- and n-type photoresponse indicative of nearly intrinsic, highly compensated-type material. No photoresponse was observed with the ZrS_2 crystals. Cu was spontaneously intercalation in HfS_2 in aqueous solution. As the intercalation progressed towards 0.5 equivalent/mole passed, the photovoltage and photocurrent increased, and the crystal showed pronounced n-type character. After passage of more current, the crystal became more metallic, with resulting decreases in photoresponse.

The HfS_2 electrode should therefore be coupled with a counterelectrode with a more positive reversible potential than Cu^{2+}/Cu_nHfS_2. The simplest example would be:

$$Cu_xHfS_2 + Cu_xHfS_2 \quad \overset{h\nu}{\underset{dark}{\rightleftarrows}} \quad Cu_{x+y}HfS_2 + Cu_{x-y}HfS_2 \quad (\Delta G > 0)$$

(photoelectrode)   discharge

Experiments to demonstrate such complete photointercalation cells are currently in progress.

Q. STUDY OF AMORPHOUS HYDROGENATED BORON THIN FILMS

DOE Program Manager	● A. R. Landgrebe
LBL Project Manager	● F. R. McLarnon
LBL Subcontractor	● Giner, Incorporated (D. Wong)
B&R Number	● AL-05-05-15
Contract Value	● 97K
Contract Number	● 4511310
Contract Term	● March 1, 1981 - February 28, 1982
Reporting Period	● March 1, 1981 - November 1, 1981
Objectives	● Characterize hydrogenated amorphous boron as a novel material to be employed in photoelectrochemical cells for the conversion and storage of solar energy
	● Screen redox couples and organic electrolytes and test promising combinations in complete photoelectrochemical cells

Amorphous hydrogenated boron (a-B:H) is a new semiconducting material whose optical band gap can be varied from 0.8 to 2.2 eV by controlling its hydrogen content during preparation.[1] Furthermore, it has been demonstrated that both n- and p-type materials can be produced by proper doping.[2] This material is currently of great interest for solid-state photovoltaic cell applications. The objective of this program is to determine the suitability of amorphous hydrogenated boron (a-B:H) as an active electrode material in a photoelectrochemical cell.

Amorphous hydrogenated boron films were prepared on both conductive glass (In-doped SnO_2-coated glass) and metal (Ta, Mo, Invar, etc.) substrates by the glow-discharge decomposition of diborane. Doping was accomplished by introducing a trace amount of silane (less than 0.5 V/o) to the diborane glow. The substrate temperature was carefully maintained at ~350°C to produce a-B:H films with the optimum band gap of ~1.4 eV for the maximum photovoltaic conversion of the solar spectrum. The typical film thickness was found to range from 0.5 to 1.0 µm. Its absorbtivity was determined to be ~5 x 10^4 cm^{-1} at 5000 Å. The dark conductivity of the film was measured as ~10^{-9} Ω^{-1} cm^{-1}. Upon illumination by AM1 sunlight (~10^{17} photons/cm^2/sec), the conductivity was found to increase by a factor of ~50.

The stability of a-B:H films in aprotic solvents (acetonitrile and propylene carbonate) as well as aqueous solutions has also been studied. The results of our visual observations are presented in Table 1. The boron film showed no visible signs of degradation over extended periods in pure acetonitrile and propylene carbonate. In the presence of the Cu^{2+}/Cu^+ redox couple in CH_3CN film, degradation was observed. A more interesting result, perhaps, is that the a-B:H film was left in distilled water for over a week without any visible degradation. No immediate signs of degradation were observed in 3% H_2O_2, 0.1$\underline{M}$ HCl, 1.0$\underline{M}$ KOM, and 0.1$\underline{M}$ $KMnO_4$. These a-B:H films might be kinetically more stable in aqueous environments than the conventional amorphous boron (without hydrogen) reported in the literature.[3]

We have successfully designed and fabricated a Teflon holder that enabled us to conveniently convert an a-B:H film on glass substrate into an electrode for our electrochemical and photoelectrochemical measurements. We have just begun our redox-couple screening test, which covers the range of E_{redox} from +0.76 V (Cu^{2+}/Cu^+ in 0.1$\underline{M}$ TBAP/CH_3CN) to -1.00 V ($PhNO_2/PhNO_2^-$ in 0.1$\underline{M}$ TBAP/CH_3CN) versus SCE.

REFERENCES

1. F. H. Cocks, P. L. Jones, and L. J. Dimmey, Appl. Phys. Lett., 36, 12 (1980).

2. B. L. Zalph, L. J. Dimmey, H. Park, P. L. Jones, and F. H. Cocks, submitted to Solid State Communications, 1980.

3. M. Pourbaix, Atlas of Electrochemical Equilibria in Aqueous Solutions, NACE, 1974.

Table 1. Stability of a-B:H films.

Substrate	Solution Composition	Visual Observation
Glass	Pure CH_3CN	No visible degradation (>1 month).
Glass	Pure propylene carbonate	No visible degradation (>1 month).
Glass	0.1$\underline{M}$ TBAP/CH_3CN	No visible degradation.
Glass	Cu^{2+}/Cu^+ (0.01$\underline{M}$/0.01$\underline{M}$) in 0.1$\underline{M}$ TBAP/CH_3CN	Eventual degradation (days).
Ta	Distilled H_2O	No visible degradation (>1 week).
Ta	3% H_2O_2	No immediate visible degradation, discoloration overnight.
Ta	0.1$\underline{M}$ $KMnO_4$	No immediate visible degradation, discoloration overnight.
Ta	0.1$\underline{M}$ HCl	No immediate visible degradation.
Ta	12$\underline{M}$ HCl	Immediate total dissolution.
Ta	1$\underline{M}$ KOH	Film detached gradually, but but no visible sign of dissolution for weeks.
Glass	1$\underline{M}$ KOH	Film detached gradually, but no visible sign of dissolution for weeks.
Mo	$Fe(Cp)_2^+/Fe(Cp)_2$ (5.8 x $10^{-4}\underline{M}$/0.07$\underline{M}$) in 100% EtOH	No visible degradation for over 1 day.

R. THERMAL MANAGEMENT OF BATTERY SYSTEMS

DOE Program Manager   ● A. R. Landgrebe

LBL Project Manager   ● F. R. McLarnon

LBL Subcontractor   ● Gould, Incorporated (H. F. Gibbard)

B&R Number   ● AL-05-10-10

Contract Value   ● 97K

Contract Number   ● 4505810

Contract Term   ● June 1, 1981 - May 31, 1982

Reporting Period   ● November 1, 1980 - November 30, 1981

Objectives   ● Determine the generation rates in
                        lithium-aluminum/iron sulfide batteries

                      ● Measure temperature distributions and
                        analyze heat transfer within batteries

                      ● Evaluate strategies for thermal
                        management of Li/FeS_2 batteries

    Experiments to study the rate of thermal energy generation in 200-Ah
lithium-aluminum/iron-sulfide cells were performed. Two independent methods
were used to determine the cell heat generation. The first was an indirect
approach, using thermodynamic calculations based on precise measurements of
cell potential as a function of temperature and state of charge, combined with
measurements of the overpotential during discharge at various current
densities. The second method was a direct measurement of heat generation,
using a new, high-temperature battery calorimeter. This device has a
temperature range of 400° to 500°C, a detection sensitivity of 1 mW, and an
upper limit of heat flow of 50 W.

    All cells used in this study were five-plate, prismatic cells containing
three lithium-aluminum negative electrodes and two iron-sulfide positive
electrodes. Three types of cell have been studied. The first had LiCl-KCl-LiF
electrolytes and boron nitride nonwoven separators. The other two had
magnesium oxide powder separators--one with the same electrolyte composition
as the BN-felt-separator cells, and the other with an all-lithium-cation
LiCl-LiBr-LiF electrolyte.

    The results of the two independent methods in determining cell heat
generation are in excellent agreement. The rate of heat generation is 40 to
50 W during the last 30% of discharge at 100 A. For a full-scale, 100-cell
electric vehicle battery, total heat generation may reach 4 kW; this indicates
the need for a cooling system to avoid excessive temperature rise.

We have observed that cells with LiCl-KCl-LiF electrolyte may behave exothermically, then endothermically and back again during discharge at low-current density. This behavior is caused by the formation of intermediate compounds, the so-called J-phase and X-phase materials.

PUBLICATIONS

H. F. Gibbard, D. M. Chen, C. C. Chen, and T. W. Olszanski, "Thermal Properties of LiAl/FeS Batteries," in Proceedings of the 16th Intersociety Energy Conversion Engineering Conference, vol. 1, American Society of Mechanical Engineers, New York, 1981, p. 752.

L. D. Hansen, R. H. Hart, D. M. Chen, and H. F. Gibbard, "A High-Temperature Battery Calorimeter," accepted for publication in Review of Scientific Instruments.

S. PHYSICAL CHEMISTRY OF MOLTEN SALT BATTERIES

DOE Program Manager	● A. R. Landgrebe
LBL Project Manager	● J. Evans
LBL Subcontractor	● Oak Ridge National Laboratory (J. Braunstein)
B&R Number	● AL-05-10-10
Contract Value	● 70K
Contract Number	● 4506210
Contract Term	● October 1, 1980 - September 30, 1981
Reporting Period	● November 1, 1980 - November 1, 1981
Objectives	● Provide experimental measurements of composition profiles in porous LiAl electrodes and molten LiCl-KCl electrolytes
	● Provide experimental data useful for the optimal design and operation of Li/FeS batteries

Basic studies have demonstrated the establishment of current-induced composition gradients in mixed molten salt electrolytes. Composition shifts, if large enough, can produce significant deleterious effects, such as solid-phase precipitation in or near the electrodes of the LiAl/LiCl-KCl/FeS$_x$ battery. Quantitative measurements are needed to determine the extent of the gradients and to find means to reduce them.

A new electrolysis cell (Fig. 1) was designed and constructed for sample preparation and measurement of current-induced composition gradients. The new cell facilitates assembly of electrodes and porous matrix to be filled with electrolyte, provides for improved electrode-electrolyte contact, can accommodate a powdered alloy for porous electrode studies, and simplifies quenching of the electrolyzed salt.

A calibration was carried out for quantitative evaluation of electrolyte compositions from measurements of the K/Cl count ratio (peak areas) by SEM/EDAX. The calibration standards were prepared from mixtures of weighed-in composition introduced into the porous Y$_2$O$_3$ matrix in a cell, quenched, and then cut in a procedure identical, except for electrolysis, with that used for electrolyzed samples.

ELECTRODE LEADS

MACOR INSULATORS

STAINLESS STEEL

TUNGSTEN SPRINGS

MACOR COLLAR

SILICA TUBE

99.8% ALUMINA
TUBE (1 cm ID)

BORON NITRIDE
BUSHING

Li -Al ELECTRODES
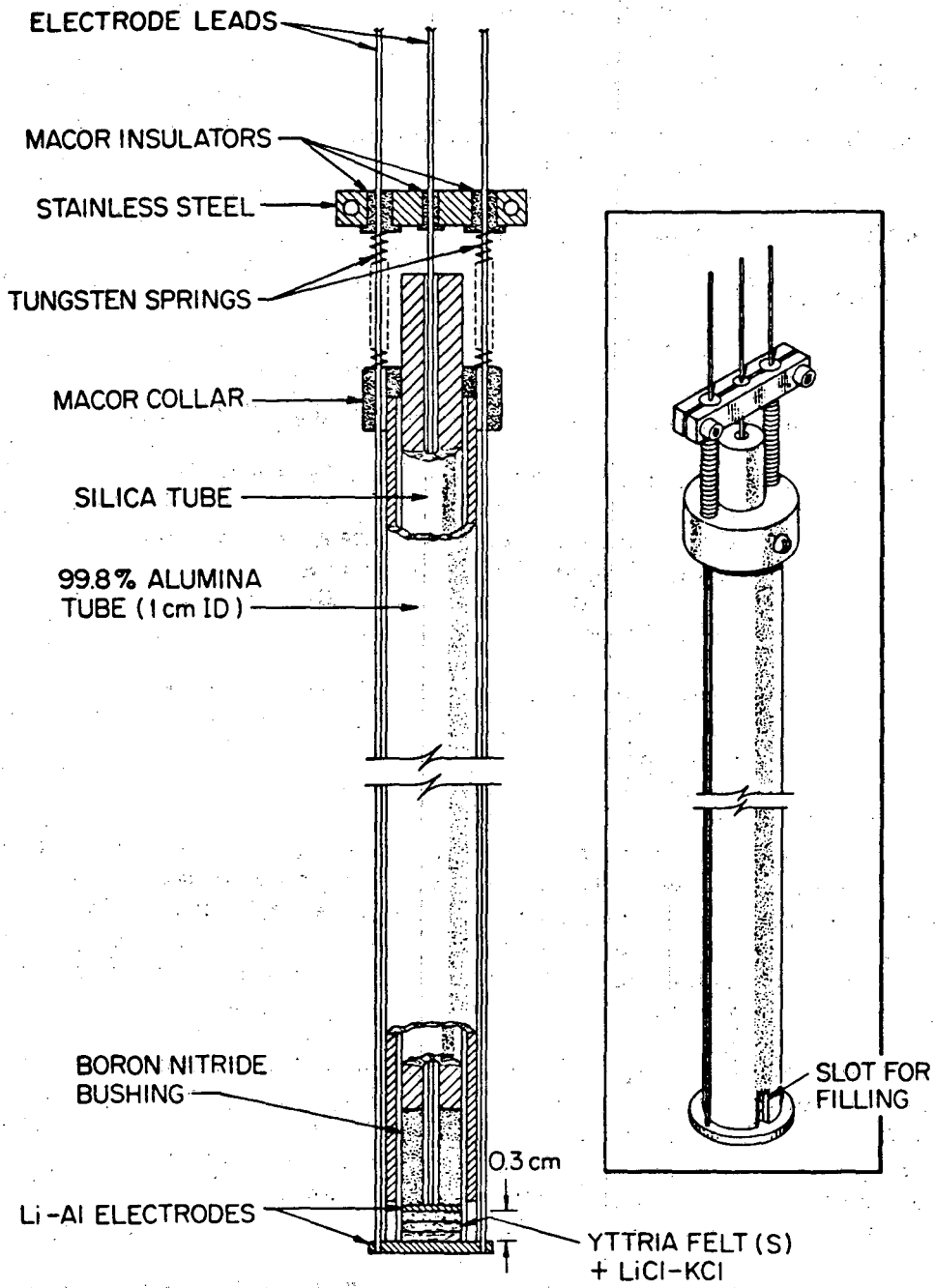
0.3 cm

YTTRIA FELT (S)
+ LiCl-KCl

SLOT FOR
FILLING

Fig. 1.   Electrolysis cell.

Quenched electrolyzed samples of LiCl-KCl eutectic were prepared using either two solid LiAl ($\alpha+\beta$) electrodes or a solid cathode and powdered anode.

Composition profiles have been analyzed by sectioning/atomic-absorption (AA) analysis and by SEM/EDAX scanning; these results are summarized in Fig. 2. The data were analyzed by several methods to ascertain the accuracy with which the shape of the profile can be determined. First, in order to smooth the data without imposing the bias of a function of given form (e.g., a predicted profile), the measurements were averaged in a "moving window" of width ±0.05 times the reduced distance. This smoothing, shown as bars, reduced the fluctuations, but with much smaller loss of distance resolution than that occurring in the AA analysis of sections, about 0.4 mm thick and not contiguous. The dashed line is the predicted profile calculated numerically. The averaging is model-independent and demonstrates the current-induced composition gradients. The bars thus represent overlapping groups of points spanning less than 0.15 mm. Second, in order to obtain a smooth curve to represent the data, again without introducing bias with a theoretical equation, a least-squares fit to the data was done with a simple empirical function (quadratic) that represents a profile passing through the initial composition midway between the electrodes:

$$X_{KCl} - 0.415 = A(y-0.5)^2 \text{ for } y > 0.5 \quad (y = \text{reduced distance}),$$

and

$$X_{KCl} - 0.415 = -B(y-0.5)^2 \text{ for } y < 0.5 \quad .$$

Our previous work had indicated a shift in EDAX count ratios at the electrodes, with qualitative evidence for gradients in LiCl-KCl; the AA analysis is restricted to non-overlapping sections of about 0.4 mm thickness. These new results are the first quantitative measurements of the shape of the concentration profile in electrolyzed LiCl-KCl eutectic.

SEM/EDAX analysis of quenched electrolyzed LiCl-KCl eutectic in a powdered LiAl anode and in the adjacent Y_2O_3 separator was intiated. Preliminary results show a composition gradient across the geometric interface; they also indicate LiCl precipitation in the powdered anode.
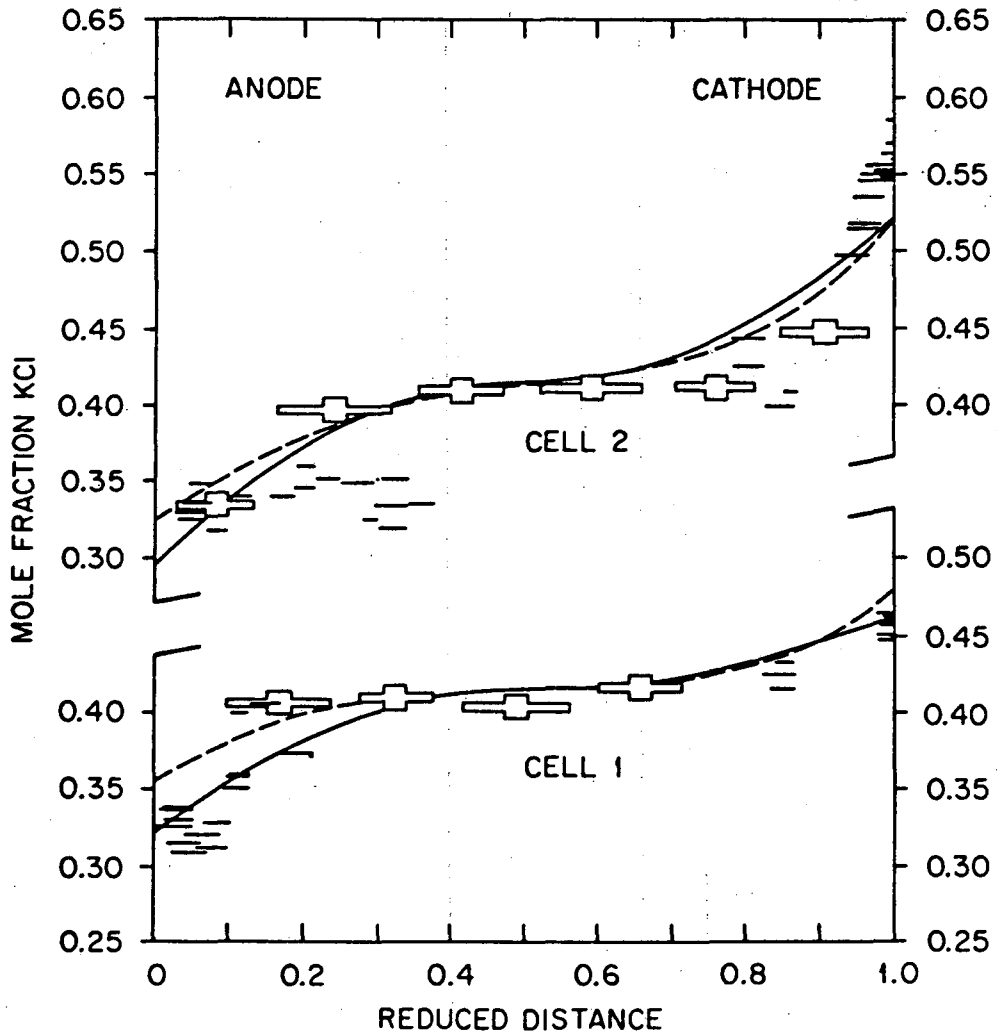
Fig. 2. Measured composition profiles in quenched electrolyzed LiCl-KCl.

⊏⊐ Atomic absorption and width of the analyzed section.
—— SEM/EDAX and width of the moving window.
- - - - - Predicted profile.
———— Least-squares quadratic fit to AA and SEM/EDAX data.

IV.   MATERIALS RESEARCH

A. NEW BATTERY MATERIALS

DOE Program Manager • A. R. Landgrebe

LBL Project Manager • L. C. DeJonghe

LBL Subcontractor • Stanford University (R. Huggins)

B&R Number • AL-05-10-10

Contract Value • 270K

Contract Number • 4503110

Contract Term • October 1, 1980 - September 30, 1981

Reporting Period • November 1, 1980 - November 1, 1981

Objectives • Evaluate the structural, thermodynamic, and kinetic parameters of materials for use as electrode and electrolyte components in high-performance batteries

• Develop new materials based on principles derived from the evaluation

• Provide experimental data and new materials useful to developers of high-temperature batteries

Recent work in this project has introduced several new approaches that may have important practical, as well as scientific, consequences. These represent substantial deviations from the directions followed heretofore in battery-related materials.

We have found that a common and inexpensive molten salt electrolyte can be used in the presence of elemental lithium at intermediate temperatures for both primary and secondary cells. It appears that this salt can be used at temperatures as low as 135°C and with both elemental lithium or high-lithium-activity negative electrodes and positive electrodes with very low lithium activities—thus giving high voltages. This electrolyte, based upon lithium nitrate, is highly oxidizing and causes the formation of a very thin layer of lithium oxide on the surface of the lithium. This layer has the fortunate property of being a good solid electrolyte for lithium ions, and has a very low electronic conductivity. It is also relatively insoluble in the molten salt. As a result, lithium can be passed in either direction through it, making it possible to produce reversible solid lithium electrodes. Although the practical importance of this discovery is still far from demonstrated, it does represent a major new direction in molten salt cells and could have substantial advantages over the higher-temperature approaches.

Recent experiments have confirmed the composition of this layer and made quantitative measurements of its (small) resistance, thickness, and rate of growth as functions of both time and temperature from the melting point of the eutectic composition up to the melting point of lithium. This lithium-oxide layer is very thin, growing parabolically with time in the range of 10 to 100 angstroms. The rate of solution of the layer decreases with time as the salt becomes saturated with lithium oxide. The saturation composition is quite low. We are now quite confident of our understanding of the thermodynamic basis for the operating limits for these nitrate salts.

We have experimented with the use of lithium alloys with higher melting points, so as to avoid the potential danger of lithium melting and rapid heat generation. These experiments have indicated that several such alloys, including Li-Al and Li-Si, also form solid electrolyte protective layers and exhibit the expected potentials and kinetic behavior.

Another interesting development is the introduction of a novel approach to an all-solid electrode structure. This structure may have kinetic properties comparable to the traditional fine-particle, liquid-electrolyte-permeated structures. While work in this new direction is very young, it does lead to the possibility of several major deviations from current practice.

The important feature in this case is the use of a composite microstructure containing finely dispersed reactant phases in a metallic matrix that has a very high chemical diffusion rate for the electrochemical active species, e.g., Li. Work on this program has led to the identification of several candidate matrix materials with the requisite thermodynamic and kinetic properties, and initial experiments have indicated that such an approach behaves as predicted. The use of an all-solid electrode, rather than the more typical powder-containing structures, presents some attractive alternate possibilities for cell design and fabrication. The achievement of a micro-scopically reversible internal morphology might lead to a truly reversible electrode structure, a long sought-after goal. This concept is being evaluated in connection with electrodes to be used with the low-melting molten salt electrolytes.

Recent progress on positive electrode materials has also been substantial. Part of our recent work involved the development of the thermodynamic basis for the quantitative understanding of the reactions and titration curves (and very low rate discharge curves) in ternary lithium-metal-oxide systems. This also leads to the realization that a number of such oxide materials should be very intersting as positive electrode reactants--comparable to the sulfides being pursued elsewhere--yet without the difficult sulfur-related corrosion problems.

Another question that we have been pursuing this year is that of the fundamental factors that determine both the absolute magnitude of the potential of the solid-solution insertion reaction (as distinct from the polyphase dis-placement reaction) positive electrode materials, and its composition dependence. This has turned out to be quite successful, and it has been possible to predict the potentials of a series of binary oxides versus lithium from data such as the electronegativities of the components and the position of the Fermi level from information on the flat band potential.

The shape of the potential-composition relation in single-phase, solid-solution electrodes has also been studied. A model in which the change in the chemical potential of the ions is due primarily to the composition-dependence of the configurational entropy of the lithium solute species, calculated from a model based upon the random filling of identical sites, has been found to fit quite well data on ternary oxide bronze materials in which the electrons can be considered to be degenerate. The composition-dependence of the electrode potential is the sum of this effect and the contribution due to the change in the Fermi level of the electrons. Electrochemical data on such electrode materials have been used to calculate the effective mass of the electrons in the cubic sodium tungsten bronzes, and have been found to agree very well with values obtained from other, entirely different methods.

In an attempt to improve the diffusion kinetics in mixed-conducting electrode materials, the concept of synthesizing materials with "propped structures" has been introduced. As model materials of this type, two different, well-characterized alkali-metal/tungsten-bronze structures have been investigated. It was demonstrated that the diffusion kinetics for the insertion of a small ion, such as lithium, can be dramatically enhanced if the host oxide structure is "propped up" by the presence of another, but relatively immobile, large alkali-metal ion (e.g., sodium or potassium). This has been investigated in the case of the cubic structure containing sodium, in which it was found that the lithium solubility range is quite large (depending upon the amount of sodium present), and that the lithium has a very high chemical diffusion coefficient. In single-alkali bronzes, both all-sodium and all-lithium, on the other hand, diffusion is very slow. Similar results have been observed with lithium in bronzes with the hexagonal structure, stabilized with potassium. Work is underway on the thermodynamic and kinetic features of the poly-alkali bronze structures, in which such parameters as the electronic conductivity and the position of the Fermi level can be systematically varied.

Because of the stability range of the nitrate molten salt, we have been interested in reversible positive electrode materials that would result in lithium cells with voltages in the range of 2.5 to 4.5 volts. Since other electrolytes (e.g., the organics) are not stable over such a wide voltage range, little is known about such very electropositive reactants. From our earlier work on ternary oxide systems, we knew that some of the vanadium, manganese, and chromium oxides should fall into this range. We have performed preliminary experiments on lithium-chromium oxides and have demonstrated lithium-vanadium pentoxide cells with voltages in the range of 3 to 3.5 volts.

However, the concentration range over which some of these materials can be reversibly operated is limited. To look into the possibility of extending this range, as well as to achieve more favorable reaction kinetics, we have also started to investigate the use of "propped structures." An example is a sodium-vanadium-oxide bronze. This material has a "propped" tunnel structure related to the ribbon structure of vanadium pentoxide. Although these experiments are still quite preliminary, several interesting observations can be made. An appreciable amount of lithium can be inserted into this structure, with good kinetics even at room temperature (using a propylene carbonate

electrolyte). Some experiments have been made at about 400°C in the LiCl-KCl eutectic salt, which show very fast kinetics, and work is starting on the behavior of this material in the nitrate salt, where the potential falls within the potential window suitable for use in secondary cells. Similar work will be undertaken with other materials of similar structure and thermodynamic properties in the desired range.

This work demonstrates that these new concepts can provide a potential new family of electrodes for practical battery systems. With our earlier work on ternary lithium-metal-oxide displacement-reaction materials, it is now obvious that a wide spectrum of possible electrode reaction materials might be used in lithium systems that do not contain sulfur, hence avoiding sulfur-related corrosion problems.

In the solid electrolyte work, attention is being given to the question of electrolyte stability as well as conductivity. The experiments have involved a small amount of further work on lithium-conducting materials with tetrahedral anionic groups, so as to elucidate the transport mechanism. We have also shown that one can synthesize solid solutions containing both iodine ions and several different polyatomic anionic groups. This means that one can change the concentration of ionic defects in the lithium iodide lattice. It has already been demonstrated that this can lead to higher values of lithium-ion conductivity than those found in pure LiI at low temperatures.

Work on the thermodynamics of the lithium-aluminum-oxygen ternary system is almost completed. This is leading to a quantitative understanding of the stability of compounds in this system with respect to reduction by lithium. It also confirms the instability of lithium beta-alumina (which has quite high values of ionic conductivity) in the presence of elemental lithium.

B. FABRICATION OF THIN-WALLED SOLID ELECTROLYTE TUBES

DOE Program Manager   ● A. R. Landgrebe

LBL Project Manager   ● L. C. DeJonghe

LBL Subcontractor   ● Johnson Controls (G. Goodman)

B&R Number   ● AL-05-10-10

Contract Value   ● 54K

Contract Number   ● 4505410

Contract Term   ● March 1, 1980 – August 31, 1981

Reporting Period   ● March 1, 1980 – August 31, 1981

Objective   ● Demonstrate the feasibility of fabricating thin-walled β-alumina tubes by a tape-winding technique

Subject to meeting minimum strength requirements, it is advantageous in the sodium-sulfur battery to make the electrolyte tubes as thin as possible to reduce cell impedance and increase its efficiency. We have previously demonstrated that thin-walled tubes could be fabricated by wrapping sheets of cast tape into a tubular configuration. These tubes, however, were handmade. The object of this work was to fabricate and characterize spiral-wound tubes made by a process based on commercial tube-wrapping equipment.

Ceramic slip was prepared and cast into tape 15 cm wide by 0.1 mm thick. The paper-backed material was slit to appropriate winding widths using a slitter of in-house design. Two-ply tubes were fabricated on a commercial spiral winder designed originally for fabricating cardboard tubes. The tubes are formed by wrapping one ply around a stationary mandrel and a then second, displaced over the first by a half-width, ceramic face to ceramic face, in a single winding operation. Application of liquid solvent and an outer wrapping of masking tape assure coherence. The fabrication rate was 3 meters of green tubing per minute.

The substrate paper and masking tape were removed following drying. Two methods of end sealing were tested. Previously-defined firing schedules were employed.

The fired tubes were characterized as to straightness, roundness, breaking strength, end-seal leak tightness, microstructure, and conductivity at 300°C. In-house conductivity measurement was done at 1 kHz using molten salt electrodes. Several samples were sent to Ceramatec Inc., for dc measurement in a sodium-sodium cell.

137

This project has led to a procedure for fabricating β''-alumina electrolyte tubes with 0.25 mm thick walls, using cast ceramic tape. The bulk of the effort was on tubes measuring 1 cm diameter by 10 cm long, although 2 cm diameter by 20 cm long was also demonstrated to be feasible. The problems remaining are associated with the small scale and the lack of automation in parts of the process and are considered to be readily solvable. They have to do with the yield of good seals at one tube end and the extent of deviation from roundness at the other. A cost analysis indicates the process to be economically viable and potentially competitive with conventional manufacturing methods.

C. FABRICATION AND CHARACTERIZATION OF NASICON SOLID ELECTROLYTES

DOE Program Manager • A. R. Landgrebe

LBL Project Manager • L. C. DeJonghe

LBL Subcontractor • Ceramatec, Inc. (R. Gordon)

B&R Number • AL-05-10-10

Contract Value • 172K

Contract Number • 4507310

Contract Term • June 15, 1980 - December 31, 1981

Reporting Period • November 1, 1980 - October 31, 1981

Objectives • Fabrication of NASICON tubes and their quality control evaluation

• Evaluation of NASICON as a superior alternative to β''-Al_2O_3 electrolyte for use in Na/S batteries

Mechanical powder mixtures containing various combinations of $Na_3PO_4 \cdot 12H_2O$, SiO_2, ZrO_2, $NH_4H_2PO_4$, Na_2CO_3, and $ZrSiO_4$ were calcined and milled prior to isostatic pressing and conventional sintering. In all cases, NASICON ceramics that were conventionally sintered contained various amounts of free zirconia (ZrO_2). Gel-processing was investigated as a method for producing homogeneous powders. Calcination and milling operations were necessary to produce powders sufficiently active for sintering. While gel-processed ceramics were significantly more homogeneous than those fabricated from mechanically mixed powders, second phases could be detected by SEM and wet-chemical analyses even though they were undetected by x-ray diffraction.

The densification of NASICON takes place in a narrow range of temperatures between 1175°C and 1275°C. Hot-pressing and hot isostatic pressing, while effective in increasing the kinetics of the densification process, were not effective in producing dense ceramics at lower temperatures. Densification of NASICON occurs at temperatures within 10% of the melting point. At these temperatures, problems are encountered with the decomposition of NASICON in that free ZrO_2 is expelled along with various amounts of Na_2O and P_2O_5 in gaseous form. This decomposition process, which appears to enhance densification, is responsible for the development of large semi-spherical voids. The degree of decomposition is critically dependent upon the sintering temperature. It is probable that the poor mechanical properties and corrosion resistance in liquid sodium of sintered NASICON ceramics are caused, in part, by the partial decomposition of the material during densification.

Although we know that the corrosion resistance of NASICON ceramics in liquid sodium depends on the method of firing, long-term stability, at least at temperatures over 300°C, is difficult to project. However, since NASICON may be relatively insensitive to aqueous environments, the potential use of this material in electrochemical systems such as the chlor-alkali cell was investigated. Several small chlor-alkali cells were fabricated from tubular forms of NASICON and operated for periods of up to a few hours. The anolyte concentration was 25 wt% NaCl, while the catholyte concentration varied from 0 to 20 wt% NaOH. These cells were operated at temperatures between 45°C and 90°C at current densities up to 0.78 A/cm^2. The cell voltages, extrapolated to zero current, were 2.15-2.30 V, depending on the cell temperature and compositions of the anolyte and catholyte. The observed cell resistances were generally between 50 and 100 ohm-cm^2 at 75°C and were strongly dependent on the current density. The NASICON electrolytes all exhibited some signs of minor degradation after testing.

In parallel with the studies on chlor-alkali cells, static leaching studies in aqueous environments were conducted. The amounts of sodium and phosphorous that can be leached depend on the firing conditions during densification. Higher sintering temperatures resulted in more leachable sodium and phosphorous. With the proper choice of composition and the development of active powders that densify at lower temperatures, it is believed that NASICON ceramics suitable for use in chlor-alkai cells can be developed.

PUBLICATION

R. S. Gordon, G. R. Miller, B. J. McEntire, E. D. Beck, and J. R. Rasmussen, "Fabrication and Characterization of NASICON Electrolytes," Solid State Ionics, 3/4, 243-248 (1981).

D. RESEARCH ON THE PRINCIPLES OF SUPERIONIC CONDUCTION

DOE Program Manager · A. R. Landgrebe

LBL Project Manager · L. C. DeJonghe

LBL Subcontractor · Massachusetts Institute of Technology
(B. Wuensch)

B&R Number · AL-05-10-10

Contract Value · 66K

Contract Number · 4507910

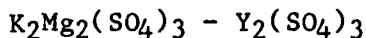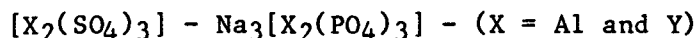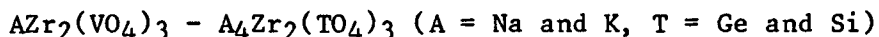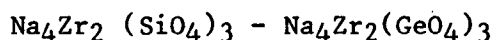Contract Term · July 1, 1980 - June 30, 1981

Reporting Period · July 1, 1980 - June 30, 1981

Objectives · To determine the principles of superionic
conduction by the detailed crystallo-
graphic analysis of various ionic
conductors

· Suggest candidate maerials as superior
alternatives to β''-Al$_2$O$_3$ electrolyte
for use in Na/S cells

The objectives of this project, which has just concluded its first year,
are to perform exploratory syntheses and measurements of the electrical con-
ductivity of potential new fast-ion conducting phases and of crystal-chemical
modifications of known conductors. The ultimate goals are (1) discovery of new
compositions displaying improved alkali ion conduction and (2) identification
of systems with a marked dependence of conductivity on crystal chemistry for
which diffraction analysis will provide insight into the mechanism of
conduction.

NASICON, Na$_2$Zr$_2$PSi$_2$O$_{12}$, is known to possess Na conductivity comparable
to β-Al$_2$O$_3$ and properties that are superior in other respects (e.g., sinter-
ability at lower temperatures). NASICON belongs to a general family of phases
A$_n^{1+}$X$_2^{k+}$(T$^{\ell+}$O$_4$)$_3$ (where A$^+$ is an alkali ion, X is an octahedrally coordinated
cation, and T is a tetrahedrally coordinated cation) in which there is great
scope for modification of the structural framework. We have completed
synthesis, characterization (using optical and diffraction techniques), and ac
conductivity measurements at 1 kHz for more than 50 solid-solution phases in
10 different NASICON-related systems:

$Na_4Zr_2(SiO_4)_3$ - $Na_4Zr_2(GeO_4)_3$

$Na_3Zr_2PSi_2O_{12}$ - $Na_3Zr_2PGe_2O_{12}$

$AZr_2(VO_4)_3$ - $A_4Zr_2(TO_4)_3$ (A = Na and K, T = Ge and Si)

$[X_2(SO_4)_3]$ - $Na_3[X_2(PO_4)_3]$ - (X = Al and Y)

$LiT_2(PO_4)_3$ - $TiTa(PO_4)_3$

$K_2Mg_2(SO_4)_3$ - $Y_2(SO_4)_3$

In the original NASICON system, the hexagonal c axis was found to rise through a maximum as the larger Si ion was substituted for P, and then decrease anomalously. The conductivity rises to a maximum (much larger than that of either end member) at similar composition. The crystal chemistry of the framework and concentration of alkali ions is thus closely connected with the conduction mechanism. The anomalous behavior in lattice constants was assumed to arise from changing site occupancies for the Na ions and repulsive interactions between these ions. In the $Na_4Zr_2(Si_{1-x}Ge_xO_4)_3$ solid-solution system, the c axis has been found to display a similar anomaly, even though the Na content is constant and fixed at its maximum value. The conductivity is not strongly dependent upon composition. Changed interactions between alkali ions therefore cannot be the source of the anomaly. Appreciable but limited solubility has been found between $Na_3Zr_2PSi_2O_{12}$ and $Na_3Zr_2PGe_2O_{12}$. The conductivity at 300°C changes little with composition, but the activation energy displays an apparent decrease with Ge content. The c axis decreases monotonically and anomalously upon substitution of the larger Ge ion. Upon substitution of a smaller octahedral cation in the framework, improved Li conductivity was obtained: $LiTi_2(PO_4)_3$ was found to possess a NASICON-like structure and displayed conductivity superior to Li-β Al_2O_3. These significant changes of properties with crystal chemistry will be examined in detail in diffraction studies.

Attempts to substitute vanadium in the tetrahedral site revealed only limited ranges of solid solubility, a decrease in conductivity, and unstable sintered compacts. Phases in the system $[X_2(SO_4)_3]$-$Na_3[X_2(PO_4)_3]$, with X = Al or Y, are polyphase but exhibit a moderately high conductivity that is probably due to the presence of an unidentified conducting phase.

E. ELECTRICAL CONDUCTION AND CORROSION PROCESSES IN FAST LITHIUM-ION-CONDUCTING GLASSES

DOE Program Manager • A. R. Landgrebe

LBL Project Manager • L. C. DeJonghe

LBL Subcontractor • Massachusetts Institute of Technology
(H. Tuller)

B&R Number • AL-05-10-10

Contract Value • 75K

Contract Number • 4503810

Contract Term • January 1, 1981 - October 31, 1981

Reporting Period • January 1, 1981 - October 31, 1981

Objectives • Relate glass composition and structure
to fast ion transport and chemical
durability

• Identify glasses with optimized alkali-
ion transport rates, chemical durability,
and thermal stability

• Suggest candidate glasses for use as an
electrolyte in Li/S cells

In recent years, we and others have demonstrated that fast ion conduction (FIC) may be found in glasses as well as crystalline materials such as AgI and β-alumina. Because of the relative ease with which glasses may be fabricated and their lack of potentially troublesome grain boundaries, these materials are attractive candidates for solid electrolytes in electrochemical devices.

We have continued to concentrate on achieving an improved understanding of how glass composition and structure correlate with fast ion transport and chemical durability. Specifically, we have studied lithium borate systematically modified by the addition of chlorine and sulfate anionic species. We had previously examined the system $Li_2O-(LiCl)_2-B_2O_3$ with 36.4 mole% $Li_2Z(Z = 0,Cl_2)$, in which the ratio $(LiCl)_2/Li_2Z$ was varied from 0 to 0.5. In this reporting period, we investigated glasses of composition $Li_2Z \cdot 2B_2O_3$ (diborate) and $Li_2Z \cdot B_2O_3$ (metaborate) so as to be able to study glasses in different network regimes as a function of Cl additions.

As previously found, log σ for the diborate and metaborates exhibited a linear dependence of Cl for O substitution due to a complementary decrease in activation energy, E. Conductivities as high as $2 \times 10^{-2} ohm^{-1}$ at 300°C were reached for a glass in the metaborate system, with a corresponding activation energy of 0.46 eV. This falls within a factor of 5 of the lithium-ion conductivity of Li_3N, often cited as the best crystalline lithium-ion conductor.

Corresponding measurements of glass transition and density on these same glasses demonstrated that, in contrast to conclusions based on spectroscopic data, the glass structure is markedly affected by the substitution of $(LiCl)_2$ for Li_2O even while maintaining a constant oxygen-to-boron ratio. Consequently, it is not surprising to find major changes in conductivity with chlorine additions. Detailed discussions of the structural changes and their implications for fast ion transport are included in our recent publications.

In the previous year specimens in the binary $Li_2O-B_2O_3$ were studied, upon exposure to molten Li at various temperatures and for various times. All specimens formed a thin black reaction layer whose thickness varied parabolically with time, supporting a model involving diffusion-controlled chemical attack.

We also extended our studies of corrosion to a large number of additional glasses in the ternary $Li_2O-(LiCl)_2-B_2O_3$. The affect of LiCl additions was found to differ in different composition regimes. For glasses with high B_2O_3 contents (>70 mole%), the durability decreases with increasing chlorine concentration; for low B_2O_3 contents (>50 mole%), the addition of LiCl increases the durability of the glasses at modest temperatures. The last observation is particularly important since it suggests glasses with both enhanced ionic conductivity and durability can be prepared by proper choice of LiCl additive.

Similar glasses have also been tested for their durability in water. All glasses dissolved at constant rate, suggesting a surface-reaction-controlled mechanism of attack. A minimum in dissolution rate found at 25 - 30 mole% Li_2O in the binary $Li_2O-(LiCl)_2-B_2O_3$ system has been correlated with the degree of dimensionality of the glass network. Work to give a clearer understanding of the microscopic mechanisms that control both transport and stability in these related glasses is continuing.

F. POLYMERIC ELECTROLYTES FOR AMBIENT-TEMPERATURE LITHIUM BATTERIES

DOE Program Manager ● A. R. Landgrebe

LBL Project Manager ● L. C. DeJonghe

LBL Subcontractor ● University of Pennsylvania
(G. Farrington)

B&R Number ● AL-05-10-10

Contract Value ● 112K

Contract Number ● 4505210

Contract Term ● April 1, 1981 - January 31, 1982

Reporting Period ● November 1, 1980 - November 1, 1981

Objectives ● Investigate the properties of
intrinsically conductive polyacetylene
materials

● Characterize electrode/polymer interfaces

● Explore the feasibility of new polymers
for use as electrodes and electrolyte in
ambient-temperature rechargeable lithium
batteries

In our study of polymeric materials for lithium battery applications, we
have made progress in two principal areas. First, we have completed our
investigation of the preparation and electrochemical properties of the com-
plexes formed between polyethylene oxide (PEO) and various alkali metals.
Armand[1] has proposed using films formed of these complexes as solid electro-
lytes in lithium batteries. Second, we have begun studying the electrochemical
behavior of various doped polyacetylenes. These compounds have been
proposed[2] as potential anode and cathode materials for nonaqueous battery
applications. Our progress in each of these areas is summarized below.

PEO/ALKALI-SALT SOLID ELECTROLYTES

To evaluate the potential applications of the association complexes of PEO
as ionically conductive membranes in lithium batteries, we prepared PEO
complexes with KSCN, $LiCF_3COO$ (LiTFA), and NaSCN. Using complex ac impedance
analysis, dc coulometric and potential sweep analysis, solid-state NMR, dif-
ferential scanning calorimetry, and thermogravimetric analysis, we have studied
their preparation, thermal stability, and conductivity. We paid particular
attention to the influence of stoichiometry, moisture, and molecular weight
upon conductivity in the PEO complexes.

All of our results are consistent with the following conclusions:

1. The PEO-LiTFA complexes are predominantly Li$^+$ conductors.

2. PEO-LiTFA films readily hydrate, and hydration increases their conductivity by as much as three orders of magnitude at 25°C.

3. Above about 100°C, PEO-LiTFA films melt to form extremely viscous liquids. Although the films do not immediately flow, they slowly deform and begin to decompose over a period of several hours.

4. The highest conductivities were observed on [PEO]$_5$LiTFA films and were 3.0×10^{-8} (ohm-cm)$^{-1}$ at 25°C and 1.0×10^{-3} (ohm-cm)$^{-1}$ at 150°C.

DOPED POLYACETYLENES AS ANODE AND CATHODE MATERIALS

We have examined four aspects of the electrochemistry of the polyacetylenes: (1) the chemical and thermal stability of doped and undoped films in contact with dry air, moist air, dry oxygen, and argon; (2) the oxidation of polyacetylene films in a nonaqueous electrolyte consisting of propylene carbonate with dissolved LiAsF$_6$; (3) the reduction of polyacetylene films in a 90% diethyl ether/10% tetrahydrofuran electrolyte; and (4) the reaction between polyacetylene doped with bromine and an undoped film in the absence of a liquid electrolyte.

We find that undoped polyacetylene films must be stored very carefully, typically at liquid nitrogen temperature in an inert gas, in order to prevent spontaneous reaction with oxygen. This reaction is accelerated by the presence of moisture. We also have observed that the oxidation of polyacetylene films is electrochemically far faster than the reduction. Initial results suggest that the polyacetylenes may be interesting cathodes, but it is unclear whether they will be attractive alternatives to the lithium anode. Our results indicate that polyacetylene cathodes may be capable of moderate energy densities and high power densities. Whether they will store charge efficiently is uncertain. We have seen some indications of fairly rapid self-discharge reactions due to the large electrode surface area. Finally, it appears that a liquid electrolyte must be present to achieve rapid doping and undoping.

Our preliminary results confirm that the doped polyacetylenes are promising and completely unconventional materials for nonaqueous lithium cells. However, by no means can we yet conclude that the polyacetylenes are so extraordinary as to revolutionize electrochemical energy storage technology.

REFERENCES

1. M. Armand, J. M. Chabagno, and M. Duclot, in Fast Ion Transport in Solids, P. Vashishta, J. N. Mundy, and G. K. Shenoy, eds., North-Holland, New York, 1979, p. 131.

2. A. J. Heeger and A. G. MacDiarmid, in The Physics and Chemistry of Low Dimensional Solids, L. Alcacer, ed., D. Reidel, 1980, pp. 353-391.

PUBLICATION

F. L. Tanzella, W. Bailey, D. Frydrych, G. C. Farrington, and H. S. Story, "Ion Transport in PEO-Alkali Salt Complex Polymeric Electrolytes," Solid State Ionics $\underline{5}$, 681 (1981).

G. RESEARCH ON NOVEL MEMBRANES FOR LITHIUM BATTERIES

DOE Program Manager • A. R. Landgrebe

LBL Project Manager • L. C. DeJonghe

LBL Subcontractor • Case Western Reserve University (M. Litt)

B&R Number • AL-05-10-10

Contract Value • 166K

Contract Number • 4508010

Contract Term • August 1, 1980 – September 30, 1982

Reporting Period • November 1, 1980 – November 1, 1981

Objective • The synthesis and characterization of polymeric membranes for use in lithium batteries

We started with two approaches. We wanted to make membranes out of block copolymers that had alternating hard (crystallizable, ~100 Å long) and soft (Li^+ chelating) segments. The hard segments would crystalize into planar domains and force the soft segments into similar intercalated planar domains that should have low resistance to ion transport. The crystalline regions would provide the mechanical strengths. We chose to work first with polyethylene glycol as the soft segments and poly (N-p-toluyl ethylene imine) (from 2-tolyl oxazoline) as the hard segment. The polyethylene glycol was reacted to make the toulene sulfonic acid ester, which was then used as the initiator for the 2-tolyl oxazoline. The oxazoline system was chosen because its molecular weight can be controlled exactly.

Several problems were encountered, but have since been solved:

1. We found it very difficult to prepare polyethylene glycol ditoluene sulfonate in 100% purity. Purity ranged from 30% to 75%; 90% is needed to get good mechanical properties. (Very recently, we have been able to get the pure ester).

2. The polymers prepared therefore did not have strength, and films could not be made.

3. Poly(N-p-toluyl ethylene imine), while crystallizing well in the presence of plasticizer, did not crystallize from the mlts. It was therefore not the right material for the purpose. We have shifted to poly(N-isovaleryl ethylene imine), which melts at 210°C and does recrystallize well.

4. Block polymers of alternating segments of polyethylene glycol and poly(N-p-toluyl ethylene imine) were made by polymerizing 2-tolyl oxazoline with glycol ditosylate and reacting the two-active-ended polymer with the disodium salt of polyethylene glycol. Good polymer was made, but it did not crystallize in the desired form. The morphology was inappropriate for films.

5. When the above reaction was applied to poly(N-iso-valyrl ethylene imine), the active ends deprotonated instead of reacting with base. (The addition of several molecules of tolyl oxazoline to the chain ends seems to counteract this.)

The second approach--using a soft segment consisting of a poly(N-methyl or alkyl polyethylene imine or trimethylene imine)--has also proceeded slowly. The first approach--using oxazoline to make poly (N-formyl ethylene imine) and reduce the formyl group the methyl--foundered because that monomer cannot be polymerized quantitatively. It terminates itself. Thus, block copolymers cannot be made with it. We have therefore shifted to polymers from 2-ethyl-oxazoline, which is reasonably non-terminating. The polymer from this can be reduced to poly(N-propyl ethylene imine) or hydrolyzed and methylated. We have tested the hydrolysis; under conditions where the propionyl group is hydrolyzed (the polymer is amorphous and dissolves in water), the crystalline poly)N-isovaleryl ethylene imine) is unaffected.

V. ELECTROLYTIC PROCESSES

A. MULTICOMPONENT TRANSPORT THEORY AND TRANSPORT DATA FOR CONCENTRATED ELECTROLYTES

All measurements at Electrochemical Technology Corporation (ETC) and Brigham Young University (BYU) have been made on Du Pont Nafion 7-1100. D. N. Bennion and P. Pintauro had already made some measurements on this membrane,[1] and material was still available at the University of California, Los Angeles, from the same lot. A Du Pont representative said that there would be no degradation or change of properties due to storage in an air environment for three years. Because of a delay in obtaining this membrane from UCLA, work did not begin at ETC until July, two years after the work of Bennion and Pintauro.

Measurements were made at BYU of the equilibrium parameters, membrane fixed-ion concentration, and membrane anion concentration, in 1, 4, 8, and 12M NaOH at temperatures from 22°C to 70°C. Wet membrane densities were also determined, as they are necessary to correct units for membrane salt and water concentration. Bennion's results are discussed in more depth in Appendix B of a manuscript prepared for the January, 1982, American Institute of Chemical Engineers meeting in Orlando, Florida.

At ETC, measurements of hydraulic permeability were made because the apparatus was available and ready for use from another project. A review of the literature of Nafion membranes showed that little such data were available. Tests were conducted at pressures from 80 to 800 psig. Three separate pieces of Nafion gave reproducible results. Permeability coefficients were obtained in different NaCl solutions at two temperatures. The data are summarized in Table 1 and Figs. 1 and 2. The data for 50°C are represented by bars in the

Table 1. Hydraulic permeability coefficients.

Nafion sample number	NaCl concentration ($\underline{N}$)	Temp. (°C)	Pressure (MPa)	Average permeability coefficient (m^2/Pa s)
A	0.3	25	0.69	1.78×10^{-17} (3)[a]
			1.38	1.73×10^{-17} (2)
			2.07	1.38×10^{-17} (2)
			2.76	1.19×10^{-17} (3)
			3.45	1.24×10^{-17} (2)
B	1.0	25	0.69	7.54×10^{-18} (2)
				6.43×10^{-18} (2)
			1.38	8.13×10^{-18} (2)
				6.32×10^{-18} (2)
			2.07	6.63×10^{-18} (2)
				5.86×10^{-18}
			2.76	6.58×10^{-18} (2)
				6.53×10^{-18} (2)
			3.10	5.28×10^{-18}
			3.45	6.38×10^{-18} (3)
			4.14	5.76×10^{-18} (4)
			4.83	6.34×10^{-18} (3)
			5.52	5.98×10^{-18} (3)
C	1.0	50[b]	0.69	5.75×10^{-17}
			1.31	2.37×10^{-17}
			1.45	2.95×10^{-17}
			1.52	2.39×10^{-17}
			2.07	1.76×10^{-17} (2)
			2.10	2.16×10^{-17}
			2.62	1.73×10^{-17}
			2.76	3.29×10^{-17}
				1.60×10^{-17}
				1.83×10^{-17}
D	3.0	25	0.49	3.94×10^{-18}
			0.69	3.43×10^{-18} (2)
			1.38	4.10×10^{-18} (2)
			2.07	3.84×10^{-18} (2)
			2.76	3.79×10^{-18} (2)
			3.45	3.16×10^{-18} (3)
			4.14	2.90×10^{-18} (2)
			4.69	2.71×10^{-18}
		50[b]	0.76	1.78×10^{-17} (2)
			1.38	1.38×10^{-17} (2)
			2.76	7.03×10^{-18} (2)
			3.45	8.91×10^{-18} (3)
			4.14	7.65×10^{-18} (2)

[a] Number of determinations in the average, if greater than 1.

[b] Tabulated data at 50°C are maximum values.
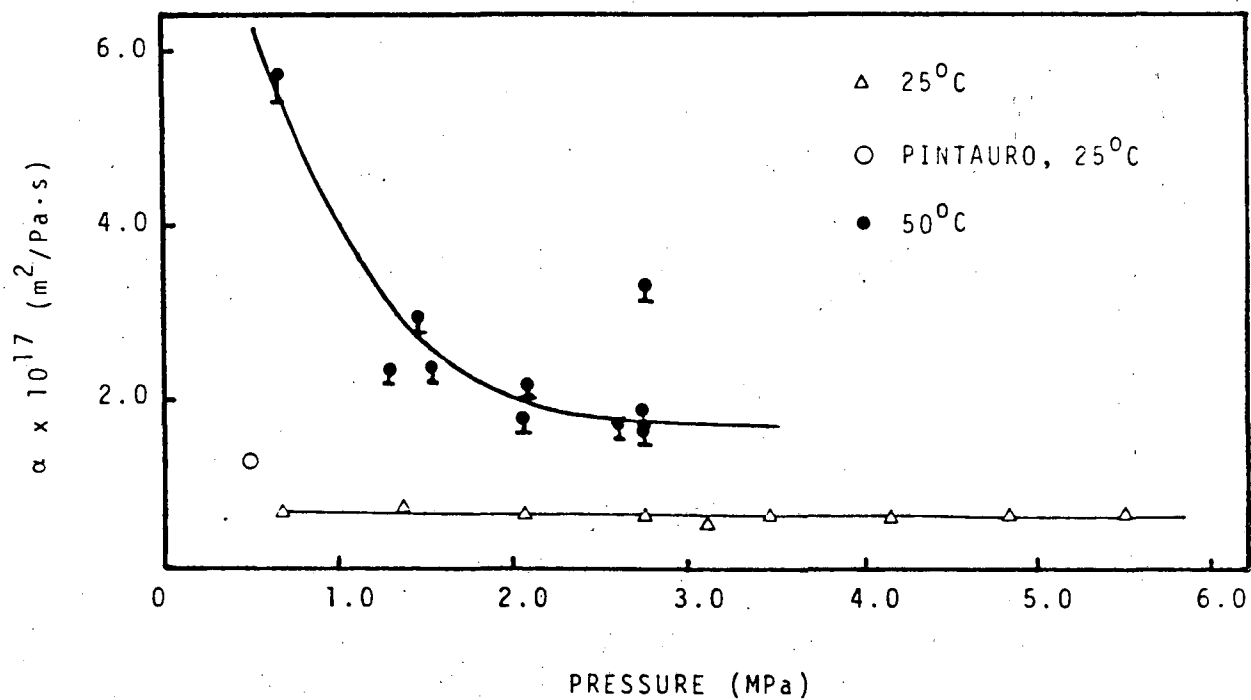   Theoretical minima are 95% of the tabulated value.

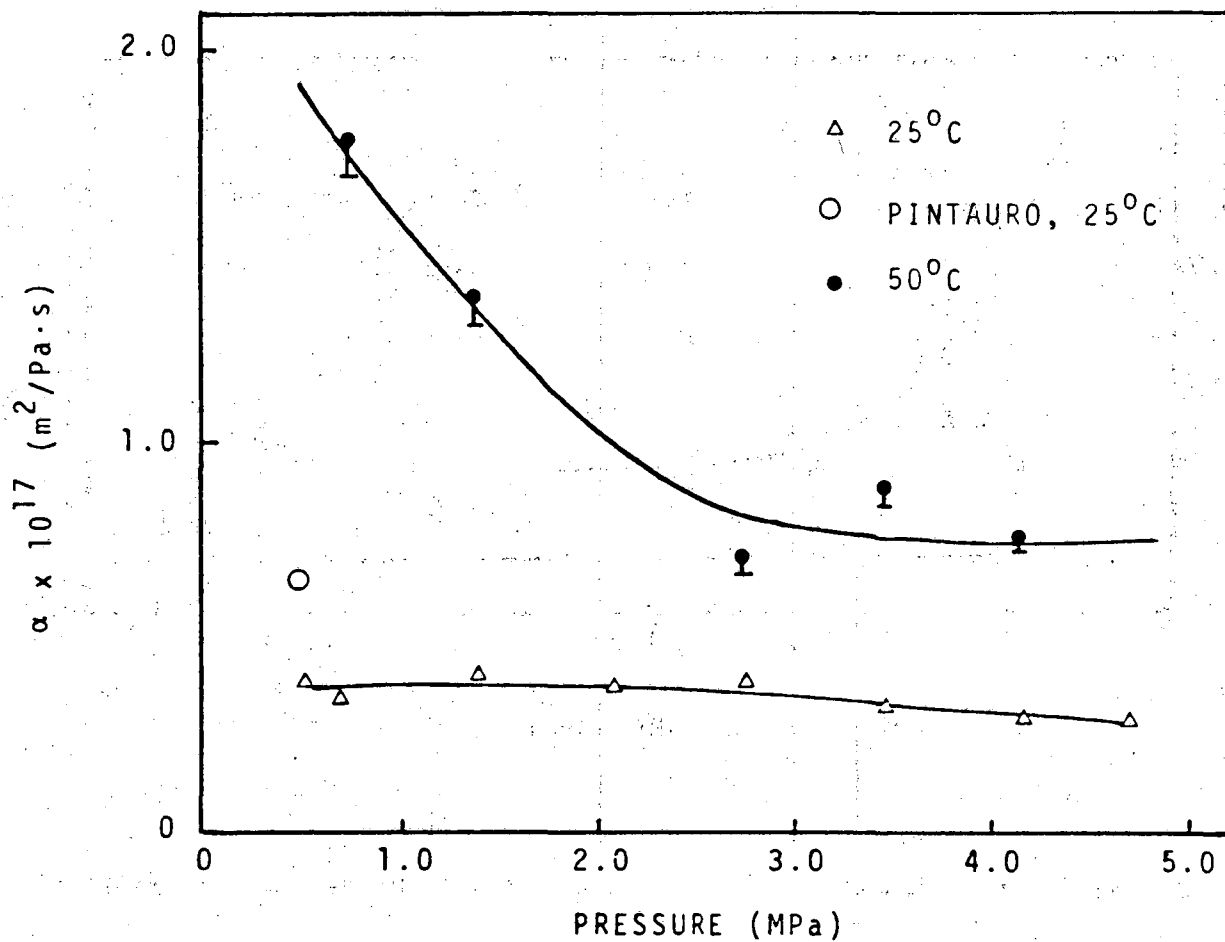Fig. 1. Permeability coefficient (α) of 1<u>N</u> NaCl flowing through Nafion 7-1100.

Fig. 2. Permeability coefficient (α) of 3N NaCl flowing through Nafion 7-1100.

figures. The upper edge of each bar is based on the observed flow rate, but gas bubbles formed in the filtrate solution. The bubbles were assumed to be air, and calculations were made to estimate their volume. The lower edge of each bar is based on the flow rate of filtrate without bubbles. These data clearly indicate that the hydraulic permeability coefficients are a complex function of three variables: temperature, concentration, and pressure. The results also show a difference in permeability coefficient, α, compared to Bennion and Pintauro's work. This difference indicates that the Nafion sample may have aged in some manner in the two years since their measurements.

Attempts were made to determine the salt-rejection coefficient in the hydraulic permeability experiments, but they were unsuccessful. The filtrate concentration did not reach steady state because of the large void volume in the porous stainless-steel disc supporting the membrane. A modified membrane-support disc with reduced void volume was designed and constructed, but corrosion and plugging problems precluded its use.

Apparatus to be used in Hittorf experiments were constructed and tested. Porous silver electrodes were obtained, and they performed satisfactorily. Titration methods for determining chloride concentration were also investigated. The concentration of a 10 $\mu\ell$ sample of $\sim 1\underline{N}$ NaCl was determined, within $\pm 2\%$, by titration with $AgNO_3$. Most of the experimental error was attributed to instability in the specific-ion electrodes used to sense the chloride-ion activity. Other analytical methods of measuring chloride concentration are being investigated.

The objective of the Hittorf experiments is to determine the magnitude of the phenomenological cross coefficients that arise when radiotracers are used in Hittorf and dialysis experiments. Pintauro[1] discussed the cross coefficients ($\mathcal{L}_z*$). Classical Hittorf and dialysis experiments will be conducted in NaCl solutions with radiotracers. A number of data points will be collected in combined dialysis and Hittorf experiments on single Nafion specimens. The results will be analyzed to obtain the straight and cross coefficients for the radiotracer, and a statistical analysis will be performed to provide an internal check on the validity of the results.

A quick transference number determination was made for the Nafion 7-1100 membrane in potassium hydroxide solutions. The potassium hydroxide concentration was held constant at 20 wt% on one side of the membrane (reference solution) and varied on the other. The transference number was calculated from the gradient of potential with respect to potassium hydroxide activity. Saturated calomel reference electrodes were used to measure potential. Without correcting for the two liquid-junction potentials between the reference electrodes and the potassium hydroxide solutions, the potassium-ion transference numbers in the membrane varied between $0.98 < t_+ < 0.99$. When the Henderson equation was used to correct for the junction potentials, the value was $0.94 < t_+ < 0.96$. The membrane transference numbers depend slightly on the external solution concentration.

A paper has been prepared for publication on a technical and economic comparison of diaphragm and membrane cells for chlor-alkali production.[2] Information developed for an earlier DOE study[3] is being updated by new membrane data.

REFERENCES

1. P. N. Pintauro, "Mass Transfer of Electrolytes in Membranes," Ph.D. Dissertation, University of California, Los Angeles, 1980.

2. R. E. Means and T. R. Beck, "An Engineering and Economic Comparison of Membrane and Diaphragm Cell Chlor-Alkali Plants," accepted for publication by Chemical Engineering (with updating).

3. ABAM Engineers, "Process Engineering and Economic Evaluations of Diaphragm and Membrane Chlorine Cell Technologies," ANL/OPEM-80-9, prepared for Argonne National Laboratory under Contract No. 31-109-38-5474, with assistance from ETC, December 1980.

B. SYNTHESIS AND DEVELOPMENT OF NOVEL FLUOROCARBON/PHOSPHORIC-ACID POLYMERS FOR ION-EXCHANGE MEMBRANES

DOE Program Manager • A. R. Landgrebe

LBL Project Manager • L. C. DeJonghe

LBL Subcontractor • University of Texas (R. Lagow)

B&R Number • AL-05-10-15

Contract Value • 65K

Contract Number • 4513110

Contract Term • June 1, 1981 - May 31, 1982

Reporting Period • June 1, 1981 - November 1, 1981

Objectives • Investigate the synthesis of new phosphous monomers and study the cross-linking of copolymer systems

• Suggest candidate materials for use as cost-effective ion-selective membranes

Fluorocarbon ion-exchange membranes incorporating sulfonic acid groups, such as the Du Pont product Nafion, constitute a new generation of high-performance materials that make possible new, energy-efficient processes in very aggressive environments, e.g., chlor-alkali cells, fuel cells, and batteries. This development has stimulated interest and imitation. Asahi Glass Co. of Japan has announced the preparation of an analagous fluorocarbon polymer bearing carboxylic acid functions. Phosphonic functions on a fluorocarbon backbone have not yet been reported.

It is clear that the carboxylate, sulfonate, and doubly-ionized phosphonic acid functionalities will have different ion-transport properties that may be advantageous in specific electrochemical devices.

The nature of the ionizing group is one important determinant of transport properties, others being the distribution of functional group, the concentration, nature, and distribution of chemical or physical cross-links, and the nature and physical state of the fluorocarbon matrix.

A severe limitation in the microstructure of Nafion (Du Pont) and Flemion (Asahi Glass) is the lack of a chemical cross-linking mechanism that would be capable of (1) preserving the morphology of the swollen membrane with time, temperature, and chemical environment, and (2) limiting the swelling of the membrane independently of the concentration of ionizable groups. The consequences of (1) and (2) are excessive swelling and dimensional changes resulting in undesirable electrochemical and mechanical performance. Crystallites having high melting temperatures could serve as physical cross-links.

Conventional methods of synthesis of fluoropolymer ion exchange membranes such as Nafion are severely restricted in scope, technically challenging to control, and expensive, accounting for the present $15-$20/sq. ft. price for 0.005-inch thick membranes.

The new synthetic method of preparing fluorocarbon membranes, developed at the University of Texas, consists of first synthesizing a hydrocarbon precursor, introducing cross-links, and then fluorinating with elemental fluorine; this permits wide flexibility in the structure of the membrane. For example, we have incorporated both isolated and vicinal carboxylic acid functions in a polyethylene matrix, cross-linked with radiation, and fluorinated to convert C-H bonds to C-F bonds. The anhydride and ester functions survive fluorination (as the acid fluoride) and, on hydrolysis, yield functional fluoropolymers. The system has been applied to polymers as thin films, and the resulting membranes are highly conductive (after hydrolysis in boiling aqueous acid).

APPENDIX.   AGENDA FOR APPLIED BATTERY AND ELECTROCHEMICAL
RESEARCH PROGRAM REVIEW MEETING, DECEMBER 1981

TUESDAY, DECEMBER 15

9:00   Introductory remarks

9:30   R. Gordon, Ceramatec

     NASICON

9:55   B. Wuensch, MIT

     Superionic Conduction

10:20   BREAK

10:40   H. Tuller, MIT

     Li-Conducting Glasses

11:05   G. Goodman, Globe Division Johnson Controls

     β''-Al$_2$O$_3$ Fabrication

11:25   S. Caulder, NRL

     PbO$_2$ Atomic Structure

11:50   LUNCH

1:00   M. McKubre, SRI

     Alkaline Battery Electrode Kinetics

1:20   D. Macdonald, Ohio State

     Alkaline Battery Electrode Thermodynamics
     Alkaline Battery Electrode Restructuring

2:00   J. R. Selman, IIT

     Dendritic Zinc Deposition

2:25   D. Miller, LLNL

     Transport in Zinc Halide Electrolytes

2:50   BREAK

3:10   R. Savinell, University of Akron

     Ti Electrodes for Redox Cells

3:30   S. R. Morrison, SRI
       Photoelectrochemical Cell with Si Electrodes

3:55   R. D. Rauh, EIC
       Photointercalation Electrodes

4:20   D. Wong, Giner
       Photoelectrochemical Cell with B Electrodes

4:45   ADJOURN

WEDNESDAY, DECEMBER 16

8:30   R. Huggins, Stanford
       New Battery Materials

9:05   J. Braunstein, ORNL
       Li/FeS Composition Profiles

9:30   D. M. Chen, Gould
       Li/FeS Thermal Management

9:50   BREAK

10:10 A. Dey, Duracell
       $LiSO_2$ R & D

10:40 M. Litt, CWRU
       Polymeric Membranes

11:05 R. Lagow, University of Texas
       Polymeric Membranes

11:30 T. Beck, ETC
       Transport in Membranes

11:55 Wrap-up

12:00 ADJOURN